**Millar Western Forest Products Ltd.**

# Cumulative Impacts Modeling On the DFA

**Report from the Landscape Projection Group**

**Stephen Yamasaki, IQAFF**

**In collaboration with Frédérik Doyon and Robin Duchesneau**

**2007-2016 Detailed Forest Management Plan**

October 26, 2007

# EXECUTIVE SUMMARY

The cumulative impacts of human and natural activity on forest landscapes in Alberta are obvious.  Human activity, such as forestry and oil & gas, and natural processes such as wildfire leave a clear mark on the composition, age class structure and spatial arrangement of forests.  As well, other processes such as climate change may be slowly and subtly modifying forest dynamics and may lead to important changes over time.  Given the importance and ubiquitous nature of these cumulative impacts, a forest management plan that does not take such impacts into account cannot be expected to adequately manage the forest, neither its components nor its processes.  If forest management planning is to successfully manage for timber supply as well as for biodiversity and the host of other benefits that are derived from the forest, it must broaden its scope and consider the sum of all dynamic processes within, and in some cases without, its bounds.

The work presented herein addresses the question of sustainability within the context of ecological complexity, and the cumulative impacts of forestry, oil & gas, climate change, wildfire (the term fire and wildfire are used interchangeably in this text), and demographic change for the Whitecourt forest management area.  The work forecasts forest landscape states under the combined influences of these processes over a long time horizon (200 years), and evaluates the fate of some key indicators of biodiversity and forest productivity.

A summary table of results is presented in Table 1.  The 9 scenarios tested are presented, along with the values of some of the key indicators evaluated by the model and by analysis run following simulation.  Simulations of harvesting as the only disturbance yield results that differ greatly, in every respect, from the results of simulations of harvesting with fire, and fire and oil & gas.  There is an important interaction between fire and oil & gas, which suggests that modeling of the impact of harvesting, fire and oil & gas, could not be deduced from the impacts of harvesting and fire and harvesting and oil & gas.  Results also show that climate and demographic change will intensify the impact of fire on the supply of timber and other values.

Also, the continued exploitation of petroleum resources and encroachment by aspen parkland may lead to an important erosion of the forest landbase. Overall, this report makes a strong case for the importance of spatial and temporal stochastic modeling for forest management.

**Table 1. Summary of scenarios tested, presenting means over the 200 yrs of simulation for the timber supply indicators, and the end point (after 200 yrs) for biodiversity indicators.**

| Scenario | Abbrev. | Timber supply indicators | | | Biodiversity indicators | | | | |
| | | Mean volume harvested (m3) | Volume harvested (% of H only) (%) | Mean fire return interval[1] (years) | Sum forest core area (ha) | Sum forest patch area (ha) | Mean contrast-weighed edge length[2] | Mean forest patch size[2] (ha) | Mean edge contrast index[2] |
|---|---|---|---|---|---|---|---|---|---|
| Harvesting | H | 577,746 | 100 | N/A | 238,556 | 48,618 | 19,045 | 9.27 | 0.617 |
| Harvesting, fire | HF | 434,138 | 75 | 89 | 182,662 | 8,130 | 22,059 | 5.11 | 0.620 |
| Harvesting, oil & gas | HO | 564,431 | 98 | N/A | 222,166 | 48,013 | 20,953 | 8.81 | 0.650 |
| Harvesting, fire, oil & gas | HFO | 419,717 | 73 | 91 | 168,843 | 6,709 | 24,057 | 4.94 | 0.628 |
| Fire | F | N/A | N/A | 90 | 205,610 | 21,053 | 21,887 | 5.27 | 0.618 |
| Fire, climate change | FC | N/A | N/A | 80 | 317,350 | 72,076 | 12,742 | 13.79 | 0.619 |
| Harvesting, fire, climate change | HFC | 418,997 | 73 | 67 | 288,172 | 25,476 | 13,005 | 13.63 | 0.603 |
| Harvesting, fire, oil & gas, climate change | HFOC | 356,851 | 62 | 68 | 275,500 | 23,343 | 15,354 | 11.91 | 0.595 |
| Harvesting, fire, oil & gas, climate change, demographics | HFOCD | 336,151 | 58 | 62 | 269,633 | 20,917 | 15,968 | 12.45 | 0.602 |

[1] Due to the variability of this variable, the mean over 5 repetitions is reported here.

[2] These biodiversity indicators were evaluated seperately for W11 and W13, and the area-weighted mean of the two values are reported here.

The results show that forest planning without taking wildfire and oil & gas, with and without climate and demographic change, is an untenable undertaking. Given that forestry operations require considerable investments of capital and human resources, the creation of an industrial and community infrastructure that relies on the absence of wildfire in order to remain viable is a grave mistake that will have serious long term impacts on society and the economy, as well as on the environment. A critical review of the process of forest management planning in Alberta must be undertaken. The continued developments in oil & gas and the looming, if not already evident, impacts of global climate change make this a priority for Alberta.

# Table of Contents

# List of Tables

# List of Figures

# 1. Introduction

The goal of this project was to evaluate the implications of cumulative impacts of key disturbance agents on the Millar Western Forest Products Ltd. (MWFP) Define Forest Area (DFA) area near Whitecourt, Alberta given a set of assumptions made about global climate change (GCC) and our current understanding of ecosystem function. The project has forecasted landscape states under the combined influences of GCC and natural (wildfire) and anthropogenic (harvesting, oil & gas exploration and extraction) disturbances over a long time horizon, and has evaluated the fate of forest values within the ecosystem (such as biodiversity and forest productivity). While the authors of this report do not claim to predict the precise future state of the forest and of the socially important products and services it provides, the project has brought together current peer-reviewed and expert ecological and socio-economic knowledge to deduce a plausible evolution of the landscape.

To project the future state of the forest under current and GCC conditions, a three tier modeling approach was developed. First, forest dynamics were modeled at the stand scale. Second, this information was scaled up and applied to create a dynamic landscape scale model. Finally, Global Circulation Model (GCM) output was downscaled and integrated into this landscape model. The landscape model simulates harvesting, oil & gas activity (the two most important anthropogenic disturbance agents within the study area), wildfire (the most important natural disturbance agent in the boreal forest), forest succession, regeneration, and the impact of human populations on the incidence of human-caused fires. The scenarios that were tested (each corresponding to a combination of disturbance agents) are presented in Table 1. A number of indicators of sustainability have been evaluated based on the landscape model's output: coarse filter indicators of biodiversity and indicators of forest productivity.

# 1.1   A Primer on Potential Climate Change Impacts

There is growing agreement within the international scientific community that global climate change (GCC) is currently underway.  According to the UN's Intergovernmental Panel on Climate Change (IPCC), "changes in disturbance regimes and shifts in the location of suitable climatically defined habitats may lead to abrupt breakdown of terrestrial and marine ecosystems with significant changes in composition and function and increased risk of extinctions" (IPCC 2001).  While there is no consensus on the exact nature of the impending GCC, there is generalized agreement that there will be important impacts on terrestrial ecosystems over much of the globe.  The extent and intensity of projected GCC suggests that forest ecosystems are at risk.  Notably, important changes are projected for the boreal forest ecosystems of Alberta, where increased losses due to wildfire (Li et al. 2000) and a displacement of continuous forest cover by encroaching aspen parkland (Hogg and Schwartz 1997, Hogg et al. 2002) are anticipated.  Since these boreal forest ecosystems provide a wide range of products and services on which human populations depend (such as clean water, wildlife habitat, recreation, First Nations and other cultural values, carbon sequestration, and timber supply) an understanding of the potential impacts of GCC on forest ecosystems must be developed.  While all impacts of GCC cannot be avoided, there appear to be opportunities to develop adaptation strategies that will minimize detrimental and augment beneficial impacts (IPCC 2001).  In order to develop these adaptation strategies, however, an understanding of the potential impacts must first be developed.

Attempts at modeling the impacts of climate change on vegetation to date have either (i) studied phenomena at the stand or biome scales or (ii) integrated several scales into one modeling exercise.  Studies developed at the stand scale (see Schwalm and Ek (2001) for a review) have modeled climate effects on biomass accumulation, seed production, soil processes and their feed-backs on productivity.  They have employed either gap models (such as JABOWA (Botkin 1972), FORET (Shugart and West 1977), and FORSKA (Prentice et al. 1993)), aspatial hybrid forest growth models (such as FORECAST (Kimmins et al. 1999), or processed-based models such GOTWILA (Gracia et al. 1999) and Tree-BGC (Korol et al. 1996)) to simulate ecosystem dynamics.  Earlier studies addressed the question at the biome scale (VEMAP Members 1995, Cramer 1996, Watson et al. 1996, Neilson et al. 1998).  Generally, these studies calibrated the dependence of plants on climate under current climatic conditions, and then extrapolated future ranges of plants based on climate predictions from GCM output.  In cases where several scales were integrated, either of two approaches were employed: (i) stand scale phenomena was modeled (with the help of gap models) and then scaled up to the landscape scale (Lasch et al. 1999, He et al. 2002, Lasch et al. 2002) or (ii) biome scale potential vegetation was modeled, followed by stand modeling to determine establishment potential (Bradshaw et al. 2000).  The disadvantage with the former approach is that species are generally assumed not to migrate, while the disadvantage with the latter is that it is assumed that there are no barriers to tree migration.  Schwartz et al. (2001) argue that the latter assumption may not be well founded, given the current fragmented state of the forest in many regions of the world and slow tree migration rates.  Therefore, a hybrid approach incorporating elements of both – a stand level response as well as a more regional level shifting of ecological regions coupled to a regeneration model – is required.

# 2. Methods

The following section describes the methods used to create the Athabascan Plains Landscape Model (APLM) and generate the results described later on in the report. The first section describes the analysis and modeling work that preceded the actual building of the model, the second section describes the linkages across scales, and the third section describes the structure and functioning of the model itself.

## 2.1 Study area

The area modeled within the landscape model is the area within the W11 and W13 FMU's located in the Whitecourt area of central Alberta, and is entirely contained within the following coordinates: $53^o$ 53' 46" N and $54^o$ 45' 47" N and $114^o$ 17' 20" W and $116^o$ 32' 55" W. A map of the study area (with the forested area in yellow) is provided in Figure 1.
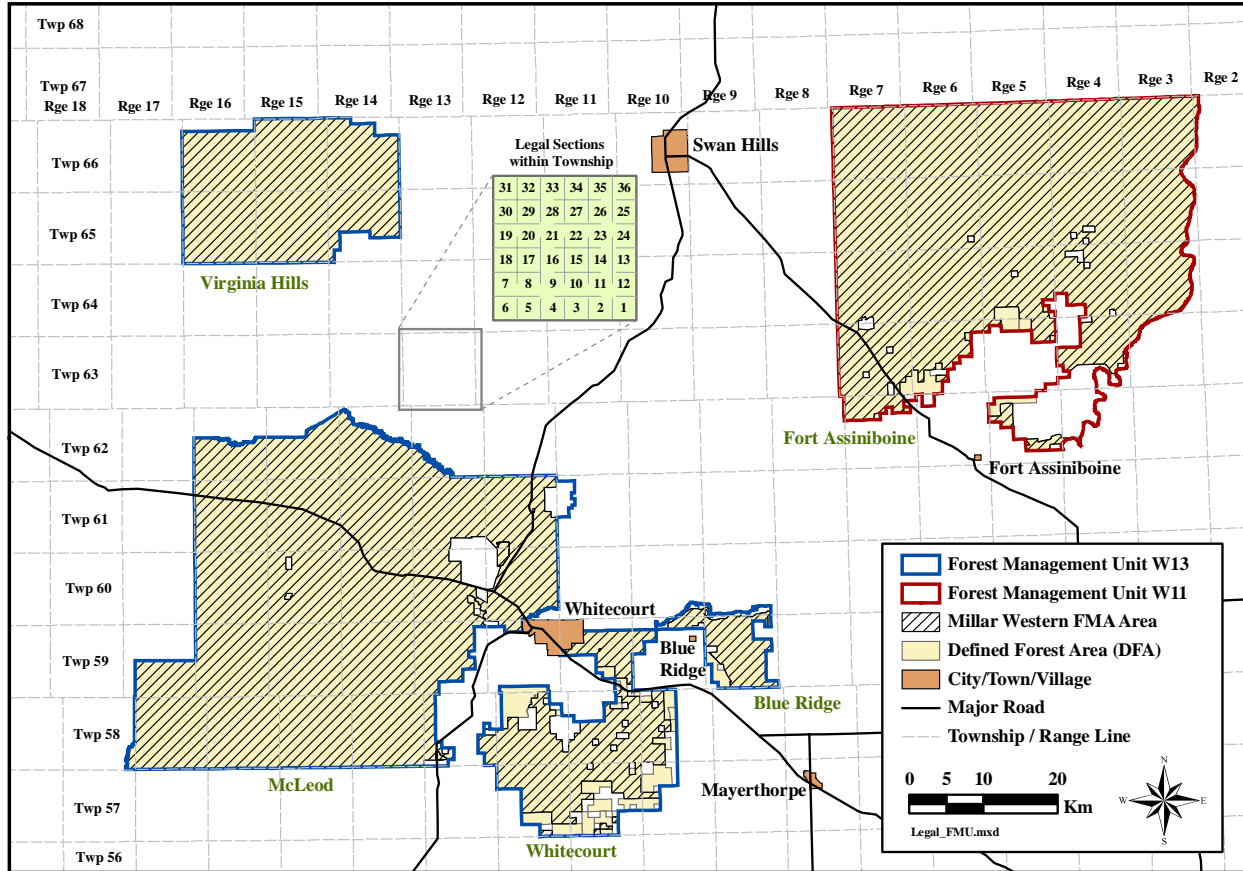
**Figure 1. The study area: The Millar Western 2007 DFMP defined forest area (DFA)[1].**

# 2.2 Data analysis and preliminary modeling

In order to build, parameterize, and drive the landscape model that served to answer many of the questions asked of our research group by MWFP, many types of data analysis, and preparatory and cross-scale modeling were required. For the sake of clarity, the results of the analyses are presented immediately following the description of the methods, rather than in a separate results section.

### 2.2.1 Selection of climate change data

There are a large number of global circulation models, each showing slightly diverging results for the same period in the future and the same assumptions about human populations and energy use. Also, within the Inter-governmental Panel on Climate Change (IPCC) climate change projection scheme, there are a range of possible futures used to generate climate change scenarios. The impacts of these scenarios on the resulting climate modeling are important. It is important to state here that **all** scenarios were deemed reasonable and possible by IPCC experts. In choosing a climate change scenario, we had one main objective: we wanted to choose a scenario that was likely to show some impact of climate change. This objective led us to choose the A1 scenario from IPCC's SRES (IPCC 2001). An illustration of historical global mean

surface temperature and the various IPCC scenarios with their temperature trends over time is shown in Figure 2.  As for the choice of climate model, we required output that contained data on mean, maximum and minimum temperatures, as well as data on solar radiation (for FORECAST modeling and the prediction of climate moisture index), relative humidity, and wind speed (for the generation of fire weather under climate change).  Therefore the CCSR-NIES model was selected, since its available output contained all the required data.
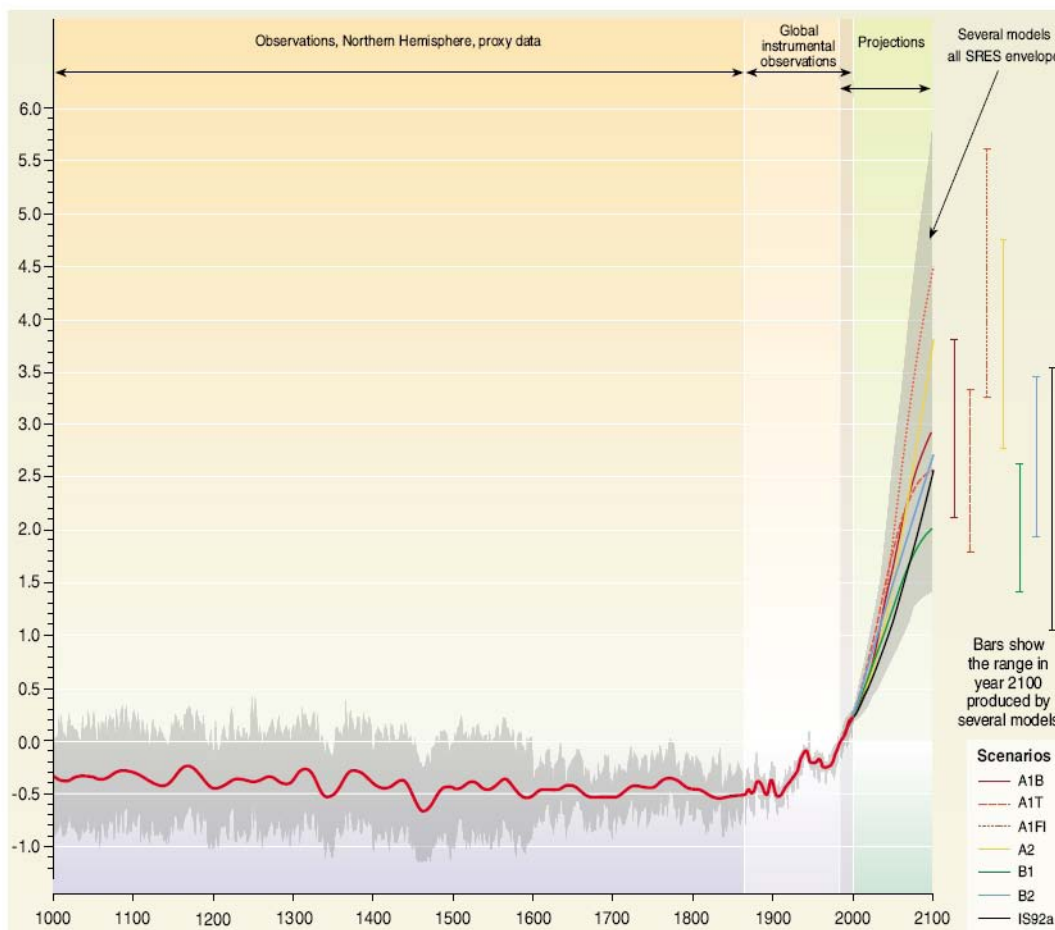


**Figure 2.  Global mean surface temperature trends over time, estimated from proxy sources (1000 – 1870), measured with instruments (1870 – 1999), and projected for the different IPCC scenarios (1999 – 2100).  Drawn from IPCC (2001).**

Since we were interested in showing the impacts of a strong increase in temperature, we chose one of the stronger CC scenarios, the A1 scenario (roughly, the mean of A1B and A1T).

## 2.2.2    Down-scaling Global Circulation Model (GCM) data to the DFA

Data on climate change is generally available at the global scale, and for the simulation of local events, such as fire, such data is inappropriate.  There are now regional climate models producing output at the regional scale (Plummer *et al*., 2006), but at the time of the establishment of this modeling framework, none of these models was available.  For the downscaling of climate data, there existed two classes of methods: statistical downscaling and the adjustment of local weather with GCM data.  The former involves establishing statistical linkages between upper and lower atmosphere variables and weather observed on the ground; from a review of available literature at the time, we felt that there was insufficient basis to maintain such assumptions.  Therefore the latter method was adopted.

Historical daily weather data was obtained from Alberta's Agriculture, Food, and Rural Development, spanning a period from 1961 to 1990, for each township and range covering the span of the forest management area (for townships 57 to 66, and ranges 3 to 17, for a total of 150 townships).  This period corresponds to the reference period generally used in climate change research as the baseline, or no climate change, period.  We received data for mean, minimum and maximum temperatures, precipitation, relative humidity, wind speed and direction, and solar radiation.  For a description of the methods used to generate this data, please refer to Alberta Agriculture (2006).  In order to generate weather streams under climate change, this historical data was adjusted using the monthly change parameters presented in Table 2.  As an example, to calculate the mean temperature for May 26th of the eighth year of simulation under climate change, the adjustment parameter for mean temperature for May (+4.61 deg. C) was added to the mean temperature from May 26th 1968 (the eighth year of the historical weather record).  In order to avoid negative precipitation, wind speed, relative humidity, and radiation values, the climate change values for these variables were obtained by adding the percentages indicated in the table to the historical value (which is equivalent to multiplying the original value by 1+percentage/100).

**Table 2.    Output from the CCSR-NIES global circulation model that was used to adjust the historical weather stream for the DFA[1].**

| Month | Absolute Temperature Change | | | Absolute Change | Percent Change | | |
|---|---|---|---|---|---|---|---|
|  | Maximum | Minimum | Mean | Radiation | Precipitation | Relative Humidity | Wind |
| 1 | 8.11 | 8.41 | 8.32 | 5.6313 | 28.11% | -0.01% | -4.37% |
| 2 | 8.32 | 8.86 | 8.75 | 14.9653 | 26.51% | -0.07% | -13.47% |
| 3 | 8.30 | 8.53 | 8.53 | 26.1007 | 21.58% | -2.09% | -16.29% |
| 4 | 6.48 | 6.86 | 6.83 | 6.2820 | 34.27% | -0.27% | -13.23% |
| 5 | 4.59 | 4.64 | 4.61 | 3.1210 | -6.13% | 2.55% | -0.08% |
| 6 | 5.27 | 5.19 | 5.24 | 16.9380 | 21.31% | 4.64% | -10.88% |
| 7 | 6.81 | 6.48 | 6.69 | 31.5780 | 17.66% | -1.24% | -16.89% |
| 8 | 7.09 | 6.73 | 7.00 | 24.3810 | -2.24% | -7.01% | -13.32% |
| 9 | 5.57 | 5.45 | 5.53 | 8.0990 | -0.18% | -4.29% | -4.29% |
| 10 | 6.20 | 5.84 | 5.94 | 4.2004 | 3.16% | -0.27% | -2.25% |
| 11 | 8.61 | 8.39 | 8.48 | 2.2838 | 18.38% | -0.06% | 3.33% |
| 12 | 9.66 | 9.93 | 9.79 | 3.4732 | 26.88% | -0.02% | 9.62% |

## 2.2.3    Associating weather streams and fire events

Once the weather streams under both historical conditions and climate change were obtained (as described in the previous section), each day's fire weather indices could be calculated, for each of the 150 townships.  The Fire Behaviour Prediction System was used to derive daily values for Fine Fuel Moisture Code (FFMC), Build Up Index (BUI), and Fire Weather Index (FWI), for the period from January 1st 1961 to December 31st 1990, and the corresponding 30-year period under climate change.  An example is provided for the month of July, 1961 (Table 3).  This 30-year fire record, which corresponds to the 30-year baseline most commonly used in climate research, serves as the basis for fire modelling with the APLM. To simulate 200 years of fires, the model will cycle through this 30-year record (almost 7 full cycles to produce 200-year simulations).

In the 1961 to 1990 fire history for the DFA bounding box (the area within a rectangular box, aligned on latitudes and longitudes, delimited by the DFA's northern-, southern-, eastern-, and western-most points), there are a total of 222 fires. Fires were retained if greater or equal to 1 ha, if they occurred on forested land, and if not carried over from one fire season to the next; carry-over fires were excluded since these fires are not actively spreading during the carry-over period, and with the FBPS, fires are either actively spreading or extinguished.  Among these 222 fires, the longest fire's duration is slightly less than 8 days; therefore, fires in the APLM were limited to an 8-day duration, each day possessing its own fire weather drawn from either the historical or CC fire weather record, depending on the assumptions for the scenario being simulated.  As will be explained in the section on the fire model, fires may be extinguished prior to this 8-day limit, depending on the conditions encountered by the fires. Through the use of a relational database, 8 days of historical fire weather data and 8 days of climate change fire weather data (FFMC, BUI, wind speed, and wind direction) were associated to each of the DFA's 222 fire events. The

---

[1] Change values expressed as absolute change were added to historical values, and others were applied as a percent change (this is done in order to avoid negative precipitation, humidity, and wind values).

established link was based on the fire event's start day and township of origin (since each township has its own weather). From this association, two tables of fire weather were generated (one table for historical and one table for CC conditions) with 222 rows and 33 columns (1 index column and 4 weather variable columns repeated 8 times, once for each day of the fire events maximum duration).

**Table 3.    Example of Generated Weather Streams for Fire Events Under Climate Change[2].**

| | | | | | No Climate Change | | | | Climate Change | | | |
| | | | | | | | Wind | | | | Wind | |
| Township | Range | Year | Month | Day | FFMC | BUI | Speed | Azimuth | FFMC | BUI | Speed | Azimuth |
|---|---|---|---|---|---|---|---|---|---|---|---|---|
| 57 | 3 | 1961 | 7 | 1 | 47.3 | 2.6 | 25.0 | 303 | 53.2 | 3.6 | 20.8 | 303 |
| 57 | 3 | 1961 | 7 | 2 | 68.2 | 4.6 | 15.0 | 132 | 74.2 | 6.4 | 12.5 | 132 |
| 57 | 3 | 1961 | 7 | 3 | 79.2 | 7.3 | 10.0 | 231 | 83.2 | 9.8 | 8.3 | 231 |
| 57 | 3 | 1961 | 7 | 4 | 84.2 | 10.3 | 11.0 | 173 | 86.6 | 13.5 | 9.1 | 173 |
| 57 | 3 | 1961 | 7 | 5 | 86.0 | 13.4 | 19.0 | 123 | 87.5 | 17.2 | 15.8 | 123 |
| 57 | 3 | 1961 | 7 | 6 | 73.9 | 12.2 | 24.0 | 117 | 76.7 | 15.7 | 19.9 | 117 |
| 57 | 3 | 1961 | 7 | 7 | 69.1 | 10.8 | 19.0 | 145 | 73.1 | 14.0 | 15.8 | 145 |
| 57 | 3 | 1961 | 7 | 8 | 81.2 | 13.3 | 28.0 | 284 | 84.1 | 17.2 | 23.3 | 284 |
| 57 | 3 | 1961 | 7 | 9 | 85.5 | 16.1 | 29.0 | 286 | 87.2 | 20.8 | 24.1 | 286 |
| 57 | 3 | 1961 | 7 | 10 | 85.7 | 18.6 | 29.0 | 293 | 87.3 | 24.0 | 24.1 | 293 |
| 57 | 3 | 1961 | 7 | 11 | 85.7 | 20.7 | 21.0 | 321 | 87.1 | 26.6 | 17.5 | 321 |
| 57 | 3 | 1961 | 7 | 12 | 85.8 | 22.7 | 16.0 | 335 | 87.0 | 29.2 | 13.3 | 335 |
| 57 | 3 | 1961 | 7 | 13 | 86.9 | 25.8 | 17.0 | 160 | 88.2 | 33.0 | 14.1 | 160 |
| 57 | 3 | 1961 | 7 | 14 | 74.3 | 21.6 | 17.0 | 256 | 78.6 | 27.1 | 14.1 | 256 |
| 57 | 3 | 1961 | 7 | 15 | 50.0 | 14.3 | 19.0 | 2 | 54.5 | 18.1 | 15.8 | 2 |
| 57 | 3 | 1961 | 7 | 16 | 57.6 | 15.1 | 23.0 | 98 | 62.0 | 19.2 | 19.1 | 98 |
| 57 | 3 | 1961 | 7 | 17 | 71.9 | 16.6 | 16.0 | 335 | 76.3 | 21.4 | 13.3 | 335 |
| 57 | 3 | 1961 | 7 | 18 | 75.4 | 18.9 | 12.0 | 255 | 78.2 | 24.4 | 10.0 | 255 |
| 57 | 3 | 1961 | 7 | 19 | 82.4 | 21.3 | 25.0 | 281 | 84.5 | 27.5 | 20.8 | 281 |
| 57 | 3 | 1961 | 7 | 20 | 84.6 | 24.1 | 14.0 | 275 | 86.2 | 30.9 | 11.6 | 275 |
| 57 | 3 | 1961 | 7 | 21 | 84.7 | 26.4 | 15.0 | 218 | 86.3 | 33.8 | 12.5 | 218 |
| 57 | 3 | 1961 | 7 | 22 | 84.7 | 28.4 | 14.0 | 3 | 86.3 | 36.4 | 11.6 | 3 |
| 57 | 3 | 1961 | 7 | 23 | 49.8 | 12.8 | 26.0 | 107 | 56.9 | 15.1 | 21.6 | 107 |
| 57 | 3 | 1961 | 7 | 24 | 40.4 | 10.2 | 27.0 | 2 | 45.0 | 11.9 | 22.4 | 2 |
| 57 | 3 | 1961 | 7 | 25 | 60.4 | 11.2 | 25.0 | 308 | 66.7 | 13.4 | 20.8 | 308 |
| 57 | 3 | 1961 | 7 | 26 | 45.2 | 7.2 | 12.0 | 298 | 51.1 | 9.1 | 10.0 | 298 |
| 57 | 3 | 1961 | 7 | 27 | 63.4 | 8.6 | 14.0 | 348 | 69.9 | 11.1 | 11.6 | 348 |
| 57 | 3 | 1961 | 7 | 28 | 66.2 | 9.7 | 14.0 | 25 | 70.1 | 12.7 | 11.6 | 25 |
| 57 | 3 | 1961 | 7 | 29 | 73.6 | 10.7 | 19.0 | 82 | 77.1 | 14.2 | 15.8 | 82 |
| 57 | 3 | 1961 | 7 | 30 | 77.1 | 11.8 | 13.0 | 87 | 79.8 | 15.8 | 10.8 | 87 |
| 57 | 3 | 1961 | 7 | 31 | 80.9 | 13.6 | 16.0 | 180 | 83.0 | 18.2 | 13.3 | 180 |

## 2.2.4    Analysis of fire data: seasonality of fire events

In order to generate new fire events under the assumption of demographic change, patterns needed to be derived regarding the seasonality of fire events. Historical fire events, from the

---

[2] The box on the left (in blue) shows the fire weather stream for one event, starting on the 5th of July 1961, under the no climate change assumption, and the box on the right (in red) highlights the weather stream for the same event under the CC assumption.

reference period of 1961 to 1990 were plotted by cause and by month of occurrence; Figure 3. This analysis clearly shows patterns for both human and lightning caused events. Lightning caused events show a uni-modal distribution with a peak in July, while human-caused fire events clearly show a bi-modal distribution, with a large peak in May and a second smaller peak in October (the peaks coincide with seasonal recreational use of the forest, with fishing principally in the spring and hunting in the fall). Therefore, it was deemed important to respect this frequency distribution of events when generating new fire events.
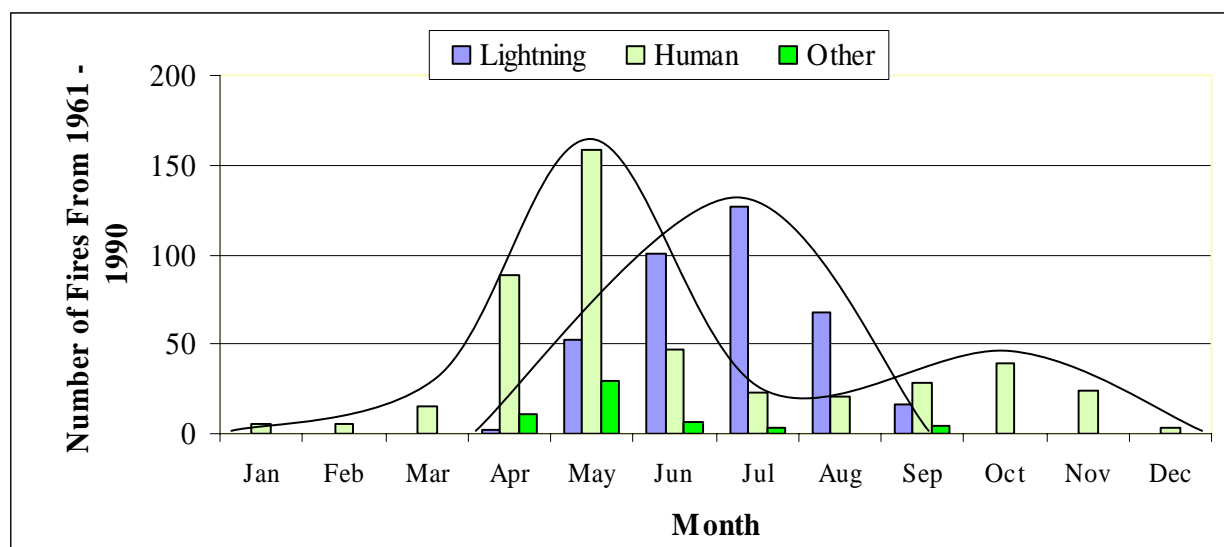


**Figure 3. Seasonal trends in the DFA's fire history from 1961 to 1990. The distribution of human caused fires by month over the 30-year fire record was used to derive the distribution of new fire events that result from an increase in the human population of Alberta.**

## 2.2.5 Assigning initial Forecast run to inventory data

The APLM uses the FORECAST run as the fundamental unit of classification for composition and dynamics. That is to say that, once a FORECAST run is assigned to a cell within the model, the trajectory of that cell and all its characteristics are determined by data that was generated by the FORECAST model (Duchesneau *et al.*, 2007). Thus, the dynamics of stands (or, more specifically, cells) within the APLM exactly follow the dynamics of stands, under both current and climate change conditions, as those modelled by Duchesneau *et al.* (2007). In order to initiate the model, it was therefore necessary to generate a grid of FORECAST run assignments for the model's year 0. Millar Western's landbase for the DFA (Landbase version 8) was used as the basis for this assignment. First, the non forested codes assigned within the landbase were conserved, with the exception of code "1111", regenerating white aspen; these cells were assigned to high density aspen stands of age 0. All area that did not sustain a deletion as part of the landbase net-down process was considered to be productive and eligible for harvest.

The percentage by leading species and secondary species and the density class data were used to generate basal area by species and density class for each of the polygons, the first step in

assigning FORECAST runs to inventory polygons. Data from the permanent sample plots (PSP) were used to generate regression models that predict total basal area from stand age; statistics from the analyses are presented in Table 4. This total basal area was then multiplied by the percentages by species data in order to obtain the polygon's basal area by species. FORECAST runs were split into age classes (40 year per class), and each 40-year segment was assigned a leading and secondary species, based on basal area by species. Then, each segment's basal area data was placed in the corresponding composition class table. Thus, there was one table per composition class, and a given age class segment within a FORECAST run could be assigned to a composition table independently of the other age classes. Then each polygon was compared to each of the FORECAST run segments of the corresponding composition class, and the Euclidean distance (in the 2 dimensional space described by basal area by lead and secondary species) from each of the candidate FORECAST run segments and the polygon was calculated. The FORECAST run closest to the polygon was selected as the initial FORECAST run for the model (Figure 4).

**Table 4.    Statistics for the regression models predicting basal area from stand density class, stand age, and the interaction between the two.**

| Density | Model Results | |
|---|---|---|
| Class | R-Square | P-Value |
| A | 0.0004 | 0.8889 |
| B | 0.1271 | <0.0001 |
| C | 0.1161 | <0.0001 |
| D | 0.0769 | <0.0001 |
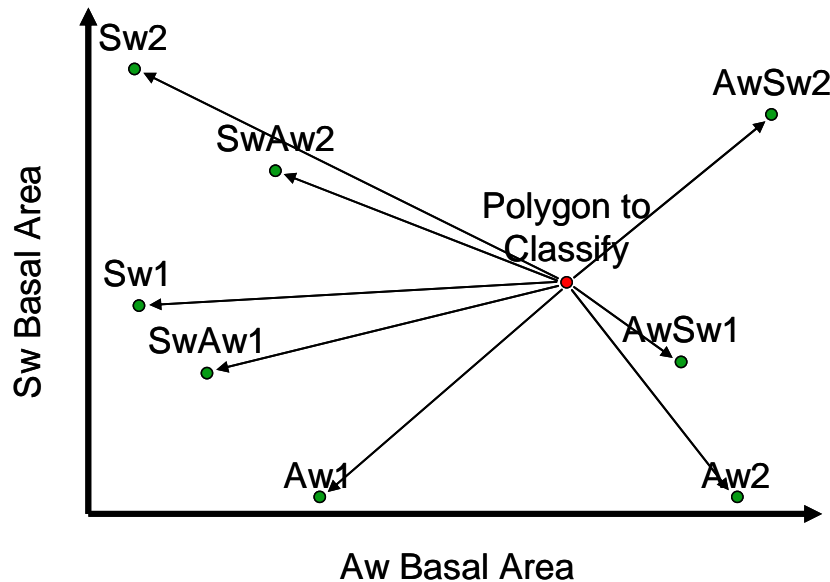


**Figure 4.   Illustration of the method applied to assign a polygon from the forest inventory (red dot) to a FORECAST run (green dots) during pre-processing.**

At the end of the process, BAP strata was assigned to all polygons using the tables described below (in Section 2.2.12 - *Assigning BAP strata and age to FORECAST output*), and this BAP strata assignment was compared to the BAP assignment of the TSA. The result of this comparison is presented here: Table 5; we can see that generally runs are assigned to the same BAP strata, but that there are differences. Some of the differences in assignment can be attributed to the difference in method to assign BAP strata to polygons. FORECAST runs were manually assigned to BAP strata through visual inspection of the basal area over time graphs, and this data (basal area by species over time) can be very dynamic. Thus, we judge that most of the differences between TSA and APLM initial BAP strata assignment result from the difficulty inherent in assigning a BAP strata to FORECAST output.

**Table 5.    Comparison of initial BAP strata for TSA (columns) and APLM (rows).**

| APLM initial state | AW_PL | AW | AW_SWSB | PL_DEC | PL | SB | SWSB_DEC | SW | BW | LT | PB | PB_CON | 1111 | Total |
|---|---|---|---|---|---|---|---|---|---|---|---|---|---|---|
| AwPl | 2,775 | 2,029 | - | 1,258 | 3,227 | - | - | - | 26 | - | 4 | 3 | - | 9,322 |
| Aw | 37 | 19,828 | 1,640 | - | - | - | 127 | - | 308 | - | 1,887 | 329 | 152 | 20,813 |
| AwSw | - | 2,547 | 4,395 | - | - | 55 | 3,313 | 2,731 | 100 | 7 | 46 | 139 | - | 13,333 |
| PlAw | 13 | - | - | 2,839 | 1,963 | - | - | - | - | - | - | - | - | 4,815 |
| Pl | - | - | - | 660 | 22,790 | 38 | 30 | 1,380 | - | - | - | - | - | 24,898 |
| SbLow | - | - | - | - | - | 12,686 | 89 | 4 | - | 1,363 | - | - | - | 14,142 |
| SbUp | - | - | - | 1 | - | 6,531 | 183 | 108 | - | 3,342 | - | - | - | 10,165 |
| SwAw | - | - | 129 | - | - | - | 3,684 | 1,690 | - | - | - | 7 | - | 5,510 |
| Sw | - | - | - | 28 | 230 | 6 | 705 | 7,453 | - | - | - | - | - | 8,422 |
| Total | 2,825 | 24,404 | 6,164 | 4,786 | 28,210 | 19,316 | 8,131 | 13,366 | 434 | 4,712 | 1,937 | 478 | 152 | |

Shaded cells indicate the closest correspondence between the BAP strata and the APLM cover types.

## 2.2.6    Modeling the migration of ecological regions within the bounds of the DFA

Since the DFA sits at the northern limit of the Aspen Parkland ecoregion, and since the work of Hogg (Hogg 1994, Hogg 1997, Hogg and Schwartz 1997, Hogg et al. 2002) has suggested that climate change may result in the conversion of forested land to aspen parkland, we sought to predict how much forested land would shift to aspen parkland under the assumption of climate change. In order to do so, the weather streams adjusted for climate change (described above) and elevation maps for the DFA were used to calculate the climate moisture index (CMI) for the area of the DFA. Area with CMI values below zero were considered to shift to Aspen Parkland. An estimated 11,577 ha of forested land, mostly in W11, will shift to aspen parkland under the climate change assumptions described above, given the results presented by Hogg (1994 and 1997). This area represents 2.7% of the total forested area for the DFA. The figure presented here (Figure 5) illustrates, in blue, the area that is predicted to shift to parkland. While this encroachment may become important in the future, its impact was judged insufficiently interesting in terms of landscape dynamics to be included in the simulations under climate change with APLM. Therefore, the conversion to aspen parkland was not carried out during the simulation of scenarios.
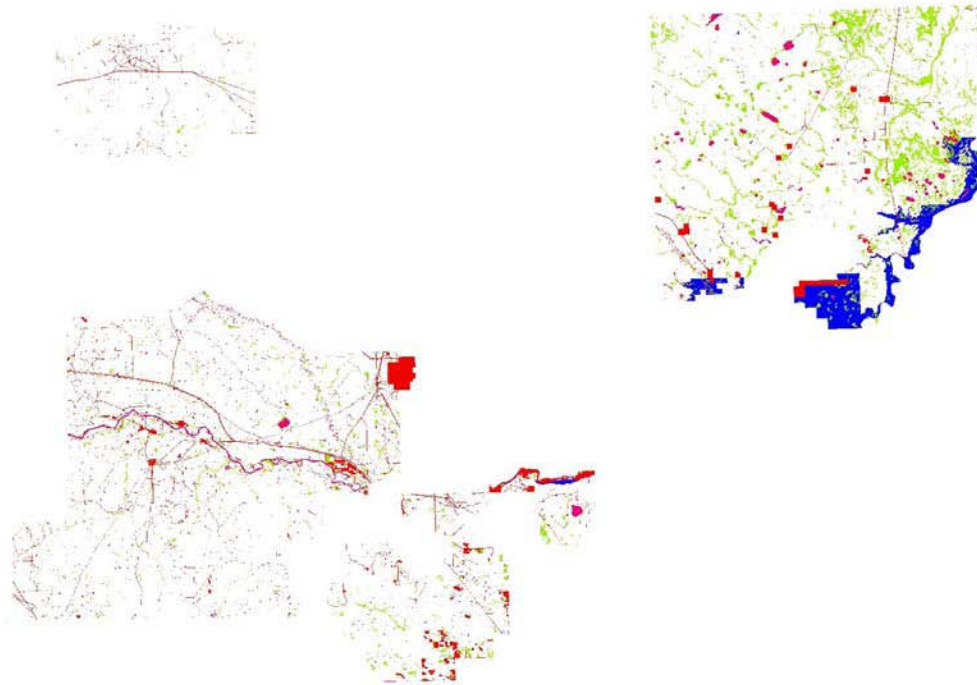
**Figure 5.  Map of non-forested area within the DFA, with expected encroachment by aspen parkland into the DFA due to climate change (in blue)[3].**

### 2.2.7    Analysis of oil & gas patterns on the DFA

The patterns of oil & gas were analyzed for the DFA in order to be able to simulate oil & gas developments in the future.  From the forest inventory, the number of wells per township was determined.  Also, since dates are provided with each of the well sites, it was possible to generate a time series of number of new well sites annually, and the area each represents.  This time series is presented in Figure 6; no clear temporal trend is obvious.  An attempt was made to relate the number of wells introduced annually to various indicators of the oil & gas industry (such as the price of crude, the US and world demand and supply, and the pump price), but no significant results could be obtained.  Therefore, the mean value of new well sites annually, 17, was used in the model.  There is currently research being carried out that is attempting to relate economic indicators

---

[3] The Climate Moisture Index method of Hogg (1999) was applied to predict the extent of aspen parkland within DFA boundaries, using an elevation map for the DFA, weather records by township and range, and projected climate change values (CCSR-NIES A1 scenario).

of oil and gas activity to the impacts of the oil and gas industry on the landscapes of Alberta (e.g., Adamowicz and Habteyonas at the University of Alberta). Future modeling work on this subject should benefit from this work in order to provide estimates of oil and gas activity that better reflect the expected behaviour the industry in the future.
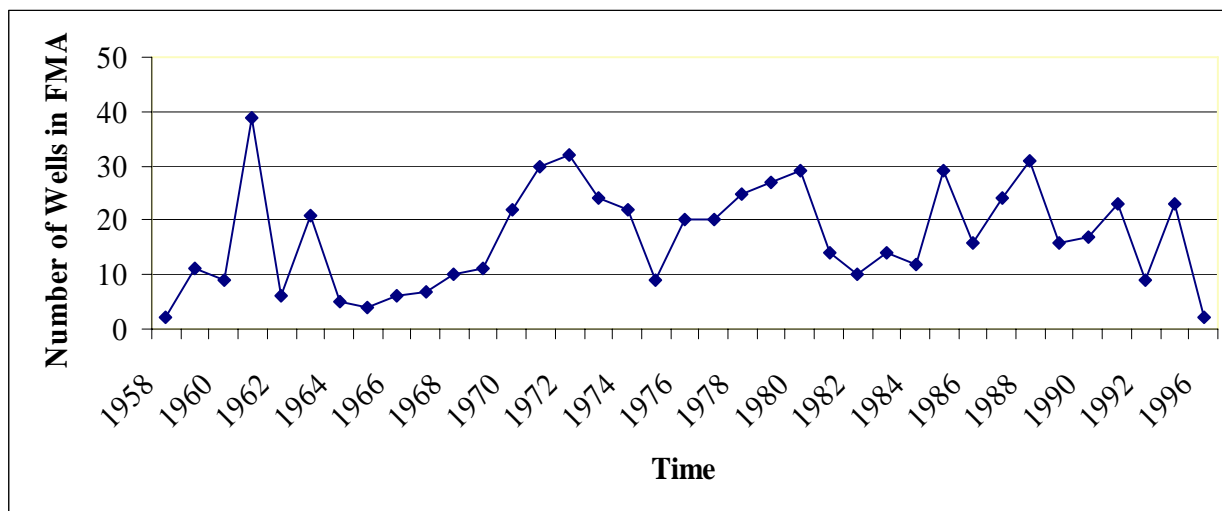


**Figure 6.  Number of Wells on DFA from 1958 to 1996.**

It was also necessary to identify the length of seismic to set down annually within the model. Since it was assumed that seismic developments generally accompany the installation of wells, an analysis relating the number of wells per township to the length of seismic in the township was conducted.  A significant relationship was obtained after log-transforming the number of wells data.  The regression is presented in Figure 7.
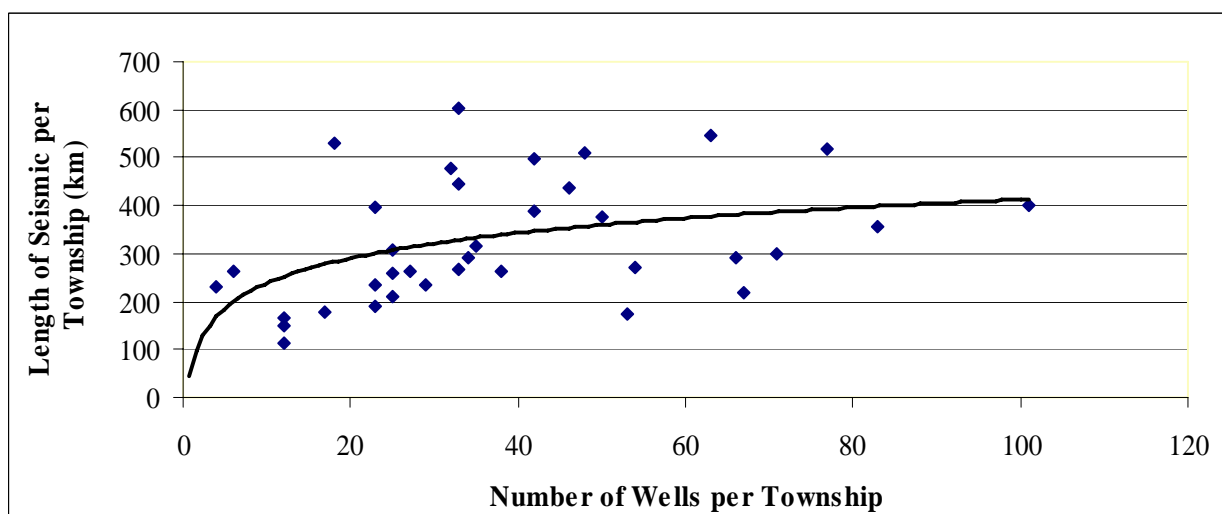


**Figure 7.  Length of Seismic Lines per Township in relation to the Number of Wells per Township.**

## 2.2.8    Modeling the cumulative impact of seismic lines at the 1 ha scale

The cumulative impacts of multiple seismic lines within the same hectare were of particular interest.  Since the model works at a scale of 1 ha, it was impossible to estimate the exactly how much area was occupied by seismic within the model itself.  Therefore, a separate modeling exercise was devised to derive the impact of several seismic lines over the same ha.  This seismic model, of a 1 ha extent, runs lines of a set width (defined by the user) and measures, at each pass, how much area is occupied by lines, and how much area is free of lines.  By running the model for 5 replicates of 400 lines, it was possible to generate a dataset from which a regression could be run.  An example of such a modeling exercise (with 4 m seismic lines) is presented in Figure 8.  The exercise was run for seismic widths from 1m to 8m and results of the runs are presented in Figure 9 for seismic lines of 4m, and in Figure 10 for seismic lines of 8m.  Non-linear regressions were run on the data, using the following equation:

$$TAD = maxTAD * (1 - \beta^{p})$$ (Eq. 1)

Where :

TAD: Total area disturbed;

MaxTAD: Horizontal asymptote;

$\beta$: Coefficient to estimate; and

p: Number of passes.

The estimated parameters from this equation were used in the landscape model to estimate the amount of area occupied by seismic with each pass crossing a cell, and in order to derive the initial amount of seismic passes in each of the model cells at the beginning of simulation.
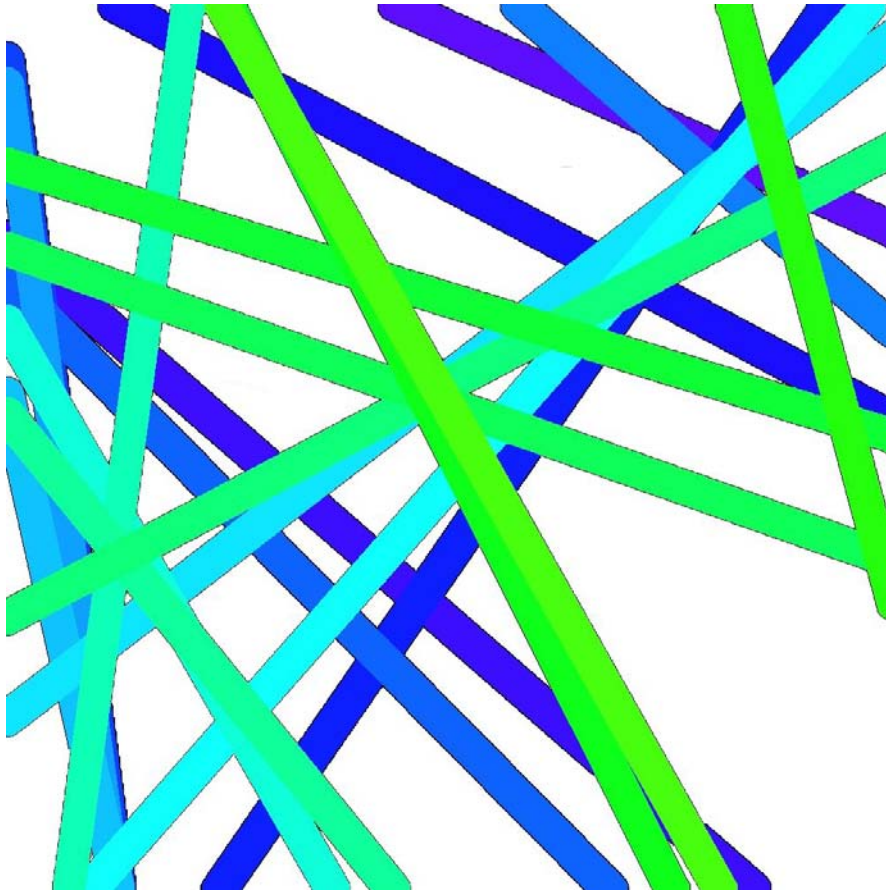
**Figure 8.  Simulation of the Cumulative effects of 4m Seismic lines, on a 1 ha plot[4].**

---

[4] Seismic lines were dropped, one by one, onto this 1 ha area, and at every time step, the area occupied by seismic was tallied; this data was used to establish the relationship between the number of seismic lines (of a given width) per ha and the area occupied by seismic.
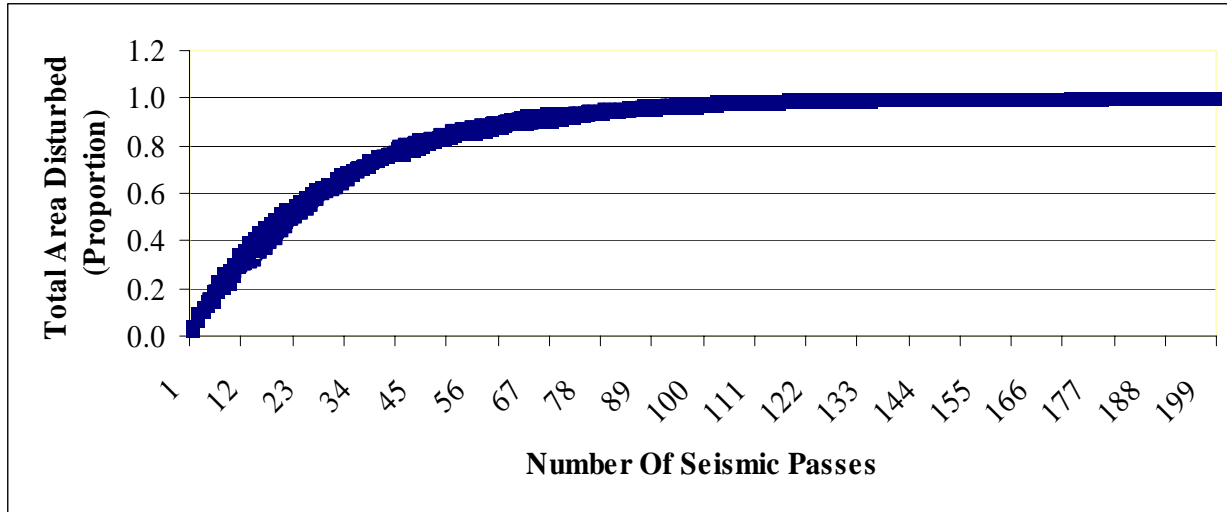
**Figure 9.** **Cumulative proportion of a 1ha plot that is disturbed as a function of the Number of Seismic Passes (4 m Wide Lines).**
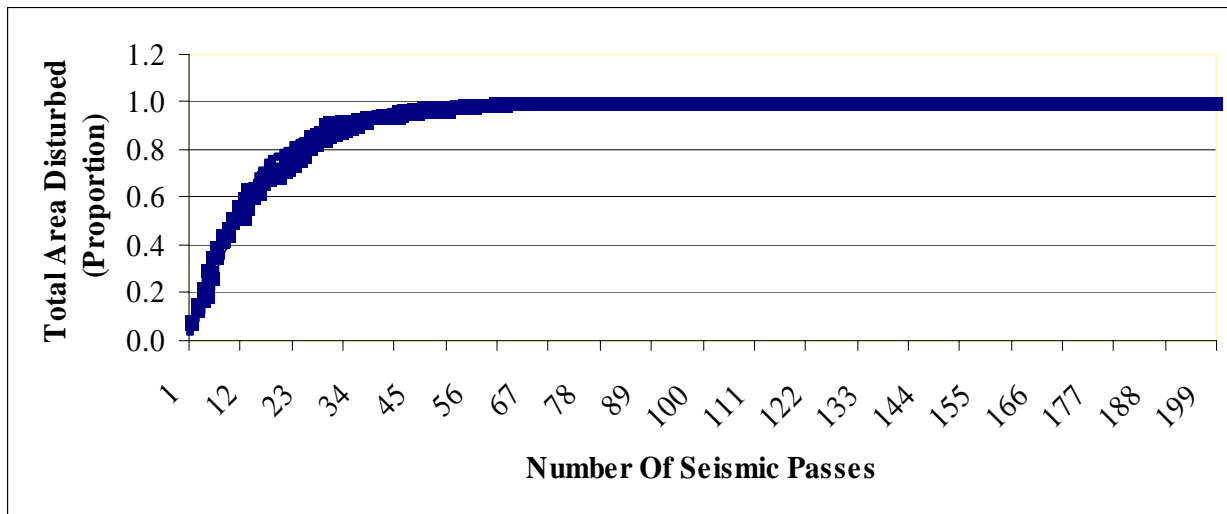


**Figure 10.** **Cumulative proportion of a 1ha plot that is disturbed as a function of the Number of Seismic Passes (8 m Wide Lines).**

### 2.2.9    Harvestable volumes and harvest target parameters

In order to calculate the annual allowable cut within the landscape model, it was necessary to estimate the merchantable volume present in any given cell at the targeted harvest age. To do this, merchantable volume data from the FORECAST runs of Duchesneau *et al*. (2007) were analyzed by composition class (there are 40 composition classes drawn from the FORECAST work, all having identical initial stem densities and compositions) in order to obtain a mean volume per hectare at the target harvest age (THA). The first THA was obtained as the minimum harvest age plus 5 years, and the second as minimum harvest age (MHA) plus 10 years. For the simulations on which this report is based, only the second (MHA + 10 years) of

these was used.  The minimum harvest ages were obtained from The Forestry Corp. and are the same ages as those applied within the timber supply analysis.

It should be noted that the APLM uses yield data that were derived from FORECAST model output (FORECAST outputs data on merchantable volume). Care was taken to ensure that yields from FORECAST coincide with standard yield data for Alberta, in particular through a step of calibration of the FORECAST model's yields with the Mixedwood Growth Model (MGM) (Government of British Columbia, 2007), as described by Duschesneau *et al.* (2007). A graph showing the relationship between the Millar Western yield curves and the FORECAST yield curves is shown in Figure 18.  Issues related to harvest target calculations and their realism are discussed in the section on the landscape model, in the sub-section on the growing stock sub-model.  A table of minimum harvest ages and volumes at target harvest ages are presented in Table 6.

**Table 6.    Parameters for the calculations of AAC based on Species composition, Harvest Age and Stand Volume.**

| Species Composition | | | | Harvest Ages (yr) | | | Volume (cu.m) | | | Regression Coefficients | | | |
|---|---|---|---|---|---|---|---|---|---|---|---|---|---|
| 1st | Initial density | 2nd | Initial density | Min | Target 1 | Target 2 | Min | Target 1 | Target 2 | Int | Coeff | R-sq | P-value |
| SW | 1,875 | - | - | 86 | 91 | 96 | 202.8 | 217.3 | 231.8 | -46.812 | 2.902 | 0.720 | 9.60E-140 |
| SW | 375 | - | - | 86 | 91 | 96 | 53.2 | 57.1 | 61.0 | -13.319 | 0.774 | 0.711 | 2.18E-136 |
| AW | 1,125 | - | - | 81 | 86 | 91 | 193.2 | 206.4 | 219.6 | -20.564 | 2.639 | 0.793 | 1.22E-172 |
| AW | 3,125 | - | - | 81 | 86 | 91 | 209.6 | 223.0 | 236.4 | -7.305 | 2.678 | 0.687 | 8.43E-128 |
| PL | 2,125 | - | - | 76 | 81 | 86 | 158.0 | 171.3 | 184.6 | -44.601 | 2.665 | 0.790 | 1.08E-170 |
| PL | 3,875 | - | - | 76 | 81 | 86 | 129.8 | 141.4 | 152.9 | -45.635 | 2.308 | 0.727 | 2.51E-142 |
| SB | 1,875 | - | - | 91 | 96 | 101 | 60.5 | 64.5 | 68.5 | -12.248 | 0.800 | 0.811 | 1.46E-182 |
| SB | 2,375 | - | - | 91 | 96 | 101 | 69.8 | 74.3 | 78.8 | -12.680 | 0.906 | 0.818 | 3.76E-186 |
| SW | 1,875 | AW | 875 | 86 | 91 | 96 | 266.6 | 284.9 | 303.2 | -47.829 | 3.656 | 0.823 | 1.75E-189 |
| PL | 2,125 | AW | 875 | 66 | 71 | 76 | 174.0 | 190.6 | 207.2 | -44.671 | 3.314 | 0.861 | 1.31E-215 |
| AW | 875 | SB | 1,875 | 86 | 91 | 96 | 221.9 | 236.5 | 251.2 | -29.776 | 2.927 | 0.816 | 1.98E-185 |
| SW | 375 | SB | 375 | 86 | 91 | 96 | 65.0 | 69.7 | 74.4 | -15.990 | 0.942 | 0.733 | 5.63E-145 |
| AW | 375 | SB | 375 | 86 | 91 | 96 | 153.7 | 164.2 | 174.8 | -27.542 | 2.108 | 0.847 | 3.81E-205 |
| AW | 1,625 | SW | 625 | 86 | 91 | 96 | 259.0 | 275.6 | 292.3 | -27.646 | 3.333 | 0.771 | 9.57E-162 |
| AW | 375 | SW | 375 | 86 | 91 | 96 | 180.0 | 192.4 | 204.8 | -33.440 | 2.482 | 0.845 | 5.66E-204 |
| AW | 1,625 | SB | 625 | 86 | 91 | 96 | 229.9 | 244.4 | 259.0 | -20.220 | 2.908 | 0.786 | 9.93E-169 |
| SB | 1,625 | PL | 1,125 | 91 | 96 | 101 | 157.6 | 168.1 | 178.6 | -33.272 | 2.098 | 0.841 | 4.53E-201 |
| AW | 625 | PL | 625 | 66 | 71 | 76 | 156.2 | 170.5 | 184.8 | -32.087 | 2.853 | 0.858 | 3.28E-213 |
| PL | 625 | SB | 625 | 76 | 81 | 86 | 78.8 | 85.3 | 91.8 | -19.716 | 1.297 | 0.661 | 4.72E-119 |
| PL | 625 | SW | 625 | 86 | 91 | 96 | 153.5 | 164.4 | 175.4 | -35.069 | 2.192 | 0.713 | 5.88E-137 |
| SW | 1,375 | SB | 1,125 | 86 | 91 | 96 | 184.1 | 197.3 | 210.4 | -42.148 | 2.631 | 0.738 | 5.61E-147 |
| PL | 3,875 | SB | 625 | 76 | 81 | 86 | 115.0 | 125.2 | 135.4 | -39.928 | 2.038 | 0.745 | 6.49E-150 |
| AW | 3,125 | SW | 1,375 | 86 | 91 | 96 | 279.9 | 298.4 | 316.8 | -36.907 | 3.684 | 0.743 | 3.64E-149 |
| PL | 3,375 | SW | 1,375 | 76 | 81 | 86 | 143.0 | 155.6 | 168.2 | -48.507 | 2.520 | 0.691 | 3.52E-129 |
| AW | 2,375 | SW | 2,375 | 86 | 91 | 96 | 277.9 | 296.9 | 315.9 | -48.873 | 3.800 | 0.770 | 3.01E-161 |
| PL | 3,125 | AW | 1,375 | 66 | 71 | 76 | 156.0 | 171.5 | 187.0 | -48.697 | 3.102 | 0.799 | 1.80E-175 |
| SB | 2,375 | PL | 1,875 | 91 | 96 | 101 | 161.1 | 171.9 | 182.7 | -35.711 | 2.163 | 0.822 | 1.29E-188 |
| SW | 2,375 | PL | 1,375 | 86 | 91 | 96 | 220.2 | 236.2 | 252.2 | -55.193 | 3.202 | 0.725 | 1.30E-141 |
| SW | 2,375 | SB | 2,375 | 86 | 91 | 96 | 169.5 | 181.7 | 193.9 | -40.797 | 2.445 | 0.750 | 4.93E-152 |
| AW | 3,125 | PL | 2,125 | 66 | 71 | 76 | 182.7 | 200.1 | 217.5 | -46.980 | 3.480 | 0.766 | 2.81E-159 |
| AW | 3,125 | SW | 125 | 86 | 91 | 96 | 232.3 | 246.4 | 260.5 | -10.468 | 2.823 | 0.703 | 2.45E-133 |
| PL | 3,875 | SW | 125 | 76 | 81 | 86 | 130.2 | 141.8 | 153.3 | -45.666 | 2.314 | 0.724 | 2.54E-141 |
| SB | 2,375 | SW | 125 | 91 | 96 | 101 | 86.4 | 92.0 | 97.7 | -16.313 | 1.129 | 0.800 | 3.58E-176 |
| AW | 3,125 | SB | 125 | 86 | 91 | 96 | 227.2 | 240.9 | 254.7 | -9.245 | 2.749 | 0.700 | 1.95E-132 |
| AW | 3,125 | SW | 2,375 | 86 | 91 | 96 | 272.5 | 291.1 | 309.8 | -48.206 | 3.729 | 0.739 | 3.59E-147 |
| PL | 3,875 | AW | 3,125 | 66 | 71 | 76 | 134.9 | 149.1 | 163.2 | -52.144 | 2.834 | 0.729 | 3.22E-143 |
| PL | 3,875 | SB | 2,375 | 76 | 81 | 86 | 87.9 | 95.3 | 102.8 | -25.102 | 1.487 | 0.826 | 2.07E-191 |
| PL | 3,875 | SW | 2,375 | 76 | 81 | 86 | 129.4 | 140.9 | 152.4 | -44.956 | 2.295 | 0.595 | 1.12E-99 |
| AW | 3,125 | SB | 2,375 | 86 | 91 | 96 | 268.1 | 286.0 | 303.8 | -38.367 | 3.564 | 0.750 | 4.25E-152 |
| AW | 3,125 | PL | 625 | 66 | 71 | 76 | 186.8 | 202.6 | 218.3 | -21.703 | 3.159 | 0.766 | 2.29E-159 |

## 2.2.10    Analysis of human population and fire data, and generation of new fire events

Fire, fire weather, and population data were analyzed in order to determine if there was a link among population, weather, and the occurrence of fire within the DFA.  A significant relationship was detected among these, a relationship expressed by the following regression model:

numFires = pop35to44 + highFwi                                                                          (Eq. 2)

Where:

NumFires: Number of fires within the DFA for a given year;

Pop35to44: Population of Alberta between the ages of 35 and 44; and

HighFwi: Number of high fire weather index days for a given year.

The regression resulted in a significant model, and the results are presented in Table 7.  These results, combined with the population projections of the DFMP process's demographics group (Loreto and McCormack, 2007), were used to project the number of fire events in the future, given climate and demographic change.  The results of this exercise are presented in Table 8.

**Table 7.    Regression results predicting the number of human caused fires from Population (Alberta 35-44) and the number of High Fire Weather Index days.**

| Element | Parameter Estimate | T-Value | R-Square | P-value |
|---|---|---|---|---|
| Model | | | 0.9171 | 0.0020 |
| Intercept | 0.79093 | 0.46 | | 0.6648 |
| Alberta population 35-44 | 0.00001122 | 2.86 | | 0.0353 |
| high Fwi days | 1.16019 | 6.4 | | 0.0014 |

**Table 8.    Projected Number of anthropogenic Fires based on Climate and Demographic Change (from Loreto and McCormack, 2007).**

| Year Of Cycle | Historical | | | Projected | | | |
|---|---|---|---|---|---|---|---|
| | Population Alberta 35-44 | HighFwiS NoCC | Number Of Fire Events | Population Alberta 35-44 | HighFwiS NoCC | Number Of Fire Events Demo Only | Number Of Fire Events Demo and CC |
| 1 | 172,623 | 12.1 | 17 | 814,288 | 26.7 | 24.0 | 40.9 |
| 2 | 172,623 | 2.3 | 5 | 818,651 | 4.6 | 12.6 | 15.3 |
| 3 | 172,623 | 8.6 | 4 | 823,038 | 22.4 | 20.0 | 36.0 |
| 4 | 172,623 | 6.6 | 28 | 827,444 | 19.7 | 17.7 | 32.9 |
| 5 | 172,623 | 6.8 | 7 | 831,872 | 16.6 | 18.0 | 29.3 |
| 6 | 184,532 | 6.5 | 12 | 836,301 | 18.0 | 17.8 | 31.1 |
| 7 | 184,532 | 33.9 | 19 | 840,722 | 61.8 | 49.5 | 81.9 |
| 8 | 184,532 | 7.1 | 19 | 845,113 | 14.4 | 18.5 | 27.0 |
| 9 | 184,532 | 6.6 | 5 | 849,460 | 18.7 | 18.0 | 32.0 |
| 10 | 184,532 | 7.1 | 27 | 853,763 | 22.1 | 18.6 | 36.0 |
| 11 | 193,155 | 5.0 | 15 | 858,019 | 17.8 | 16.2 | 31.0 |
| 12 | 193,155 | 7.2 | 2 | 862,221 | 18.0 | 18.8 | 31.4 |
| 13 | 193,155 | 5.2 | 5 | 866,363 | 11.2 | 16.6 | 23.5 |
| 14 | 193,155 | 5.0 | 6 | 870,451 | 9.7 | 16.3 | 21.8 |
| 15 | 193,155 | 1.2 | 8 | 874,487 | 9.2 | 12.0 | 21.3 |
| 16 | 205,820 | 9.6 | 12 | 878,489 | 23.4 | 21.8 | 37.8 |
| 17 | 205,820 | 2.4 | 10 | 882,464 | 19.6 | 13.4 | 33.4 |
| 18 | 205,820 | 2.3 | 8 | 886,415 | 12.4 | 13.4 | 25.2 |
| 19 | 205,820 | 1.5 | 9 | 890,341 | 7.6 | 12.5 | 19.6 |
| 20 | 205,820 | 16.2 | 19 | 894,244 | 34.1 | 29.6 | 50.4 |
| 21 | 259,320 | 7.4 | 7 | 898,118 | 29.5 | 19.5 | 45.1 |
| 22 | 259,320 | 6.5 | 14 | 901,953 | 18.5 | 18.5 | 32.4 |
| 23 | 259,320 | 3.1 | 10 | 905,740 | 12.4 | 14.6 | 25.3 |
| 24 | 259,320 | 3.8 | 12 | 909,471 | 18.0 | 15.4 | 31.8 |
| 25 | 259,320 | 7.4 | 9 | 913,134 | 25.2 | 19.6 | 40.2 |
| 26 | 330,130 | 12.9 | 9 | 916,717 | 25.4 | 26.1 | 40.6 |
| 27 | 330,130 | 11.6 | 20 | 920,211 | 43.8 | 24.6 | 61.9 |
| 28 | 330,130 | 15.7 | 24 | 923,597 | 44.2 | 29.4 | 62.4 |
| 29 | 330,130 | 4.8 | 12 | 926,866 | 19.4 | 16.8 | 33.7 |
| 30 | 330,130 | 6.7 | 17 | 930,007 | 22.6 | 18.9 | 37.5 |

## 2.2.11    Analysis of linkages between fire behaviour and climate

Considerable effort was spent to relate the behaviour of fires and various climatic indicators that are thought to influence the behaviour of fire.  Fire duration, extent, fire frequency and seasonality were all statistically modeled as dependents of various FBP system indices (FFMC, BUI, DC, FWI), and annual, seasonal, and daily measures of temperature, precipitation, and wind.  Under certain conditions, significant correlation was found, but given the volume of statistical tests run, these were considered to be spurious.  Further work should seek to relate the behaviour and incidence of fire to climatic variables expected to be influenced by climate change. Notably, attention should be given to the length of the fire season and climatic indicators.

## 2.2.12    Assigning BAP strata and age to FORECAST output

In order to output data from the model that could be analyzed with the BAP toolbox, it was necessary to assign BAP strata and BAP age to the different phases of each of the FORECAST runs.  Each of the 200 FORECAST runs was inspected visually and BAP strata and BAP ages were assigned, as illustrated in Figure 11.  BAP age was set to zero whenever the stand re-initiates in FORECAST (as indicated by the "0" in the same figure).  Thus, the landscape model by tracking FORECAST run and time since stand establishment could look up values for BAP strata and age.
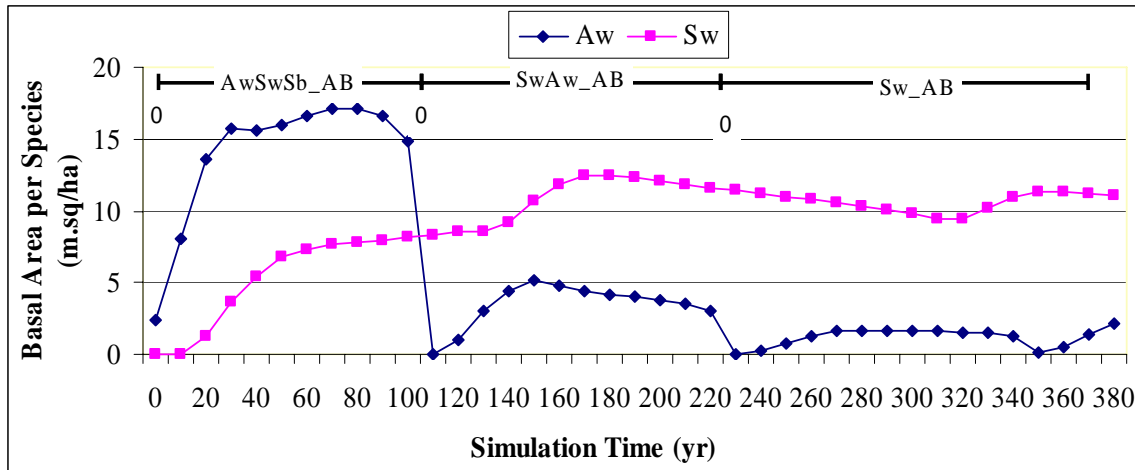


**Figure 11. Assignment of BAP Strata to a FORECAST run, based on Basal Area per Species (aspen and spruce) over Simulation Time[5].**

## 2.2.13    Assigning FBP fuel type to FORECAST output

A simple set of rules was scripted in order to assign FBP fuel type to every year of every forecast run.  The figure presented here, Figure 12, illustrates the decision tree for the assignment.  These decision rules are based on the FBP system, developed by the CFS.

---

[5] AwSwSb_AB is a low density aspen dominated stand with white and black spruce; SwAw_AB is a low-density white spruce dominated stand with sub-dominant aspen; and Sw_AB is a low density white spruce stand.

StandAge < 20

yes                                                no

O1A                    Deciduous > 70%

yes                                    no

D1                    Deciduous > 30%

yes                                    no

M1M2                          Pine > 50%

yes                                    no

StandAge < 40                              Sb > 30%

yes            no              yes              no

C3            C4              C7              C2
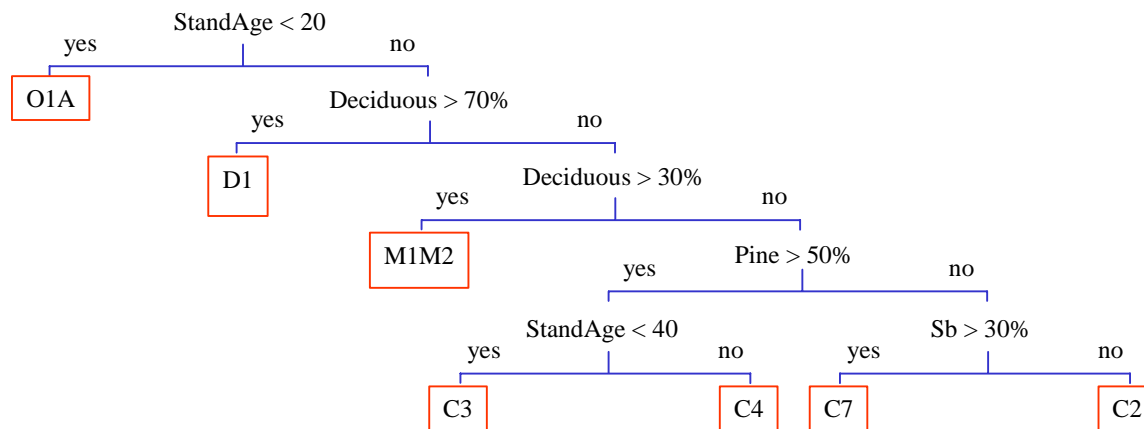
**Figure 12.  Decision tree for Assignment of Fuel Type to FORECAST Output.**

## 2.2.14   Completion of the pipeline network on the DFA

The rasterization of the pipeline and well site geographic data at a one hectare scale yielded maps with discontinuous pipeline over the extent of the DFA.  Meanwhile, the pipelining sub-model (described below) needed to be able to add pipeline between new well sites and the existing network in an efficient manner.  It was thus deemed important to establish one continuous network of pipeline over the entire area of the DFA, so that new segments could be attached to this continuous network without undue computational cost and for the pipelining model to be as streamlined as possible.  The map of the completed pipeline network is shown in Figure 13.  The algorithm used to generate this complete pipeline network is the same as the one applied to the pipelining sub-model, and is described in section 2.4.12.
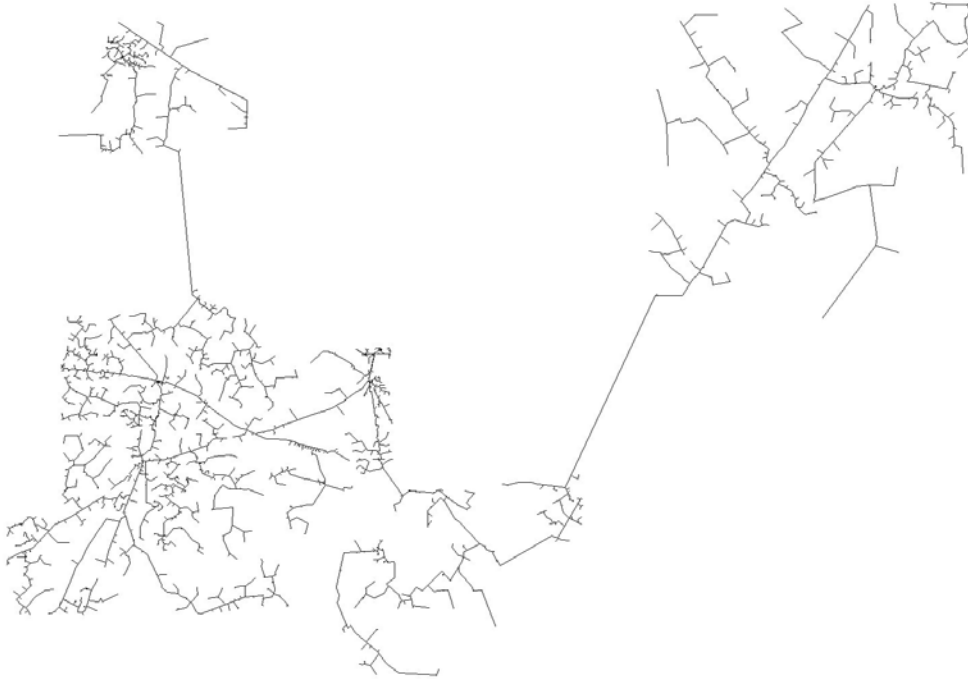
**Figure 13. Map of Linked Pipeline Network for the DFA. In order to facilitate the modeling of pipeline development within the APLM, all components of the existing oil and gas network (wells and pipelines) were linked before scenarios were run.**

## 2.3 Cross-scaling for the modeling of cumulative impacts at the landscape scale

Since the processes that are relevant to answering the questions asked of this work group operate at several distinct scales, some consideration was needed in transferring knowledge and information from one scale to another. The most important cross-scaling elements are the following:

- scaling of climate change data from the global scale to the landscape and township scale,

- scaling of stand information (e.g., volume) to the landscape scale,

- influencing landscape species composition with stand scale processes, and

- influencing the landscape scale fire regime with stand fuel composition.

The most important of these was the scaling from stand scale dynamics to the landscape.

FORECAST is the driving engine for the forest growth and succession to be implemented at the landscape scale using the SELES modeling tool. All stand scale information on composition, merchantable volume, and basal area was generated by the stand scale model FORECAST. Duchesneau (2006) used inventory data, Mixedwood Growth Model (MGM, Titus) output, and output from custom built ecological process models to parameterize the stand scale modeling tool FORECAST. While FORECAST does not take climate or weather directly into account, it was possible to estimate the impacts of climate change on the ecological processes through the use of these custom built process models. Both photosynthesis and organic matter decomposition were modeled under climate change assumptions (adjusted temperature, $CO^2$, and solar radiation), and used to generate parameters that were then used to calibrate FORECAST. See "Impacts of Climate Change at the Stand Scale", a Millar Western 2007 DFMP Report, for an extensive account of the work carried out at the stand scale. These results show that productivity should increase on certain, more productive, sites and decrease on other sites.

The two modeling platforms, FORECAST and the APLM, were not computationally coupled (i.e., they were operating independently). Therefore, it was necessary to anticipate the data requirements of the landscape model and define the nature of data communication between the stand scale models and landscape model. A database consisting of annual stand-level data was compiled from FORECAST and made available to the landscape model. Data on merchantable volume for deciduous and conifer and basal area by species, as well as data generated from FORECAST output (data on fuel type and BAP age and strata, as described above), were stored as ASCII files, and the APLM retrieved the information as needed.

## 2.4 Landscape scale processes

To determine the long-term combined impacts of GCC and other ecosystem drivers (fire, harvesting, and the oil & gas industry) on timber supply, biodiversity, and other forest values at the landscape scale, we have developed a spatio-temporal landscape dynamics model with the SELES modeling tool (Fall and Fall 2001), which we have called the Athabascan Plains Landscape Model (the APLM). The model's start point is defined by a set of initial conditions:

- initial FORECAST runs, derived from the inventory (as described above),

- digital elevation model,

- initial stand age, taken from the net landbase (F_AGE),

- initial oil & gas pipelines and wells (from the AVI),

- ecosite assignments (from GDC for W13 and Forestry Corp. for W11),

- initial non-forested land, from the net landbase (all area with numerical F_BAP),

- initial productive forest, from the net landbase (all area with F_DEL equal to NONE),

- initial recent disturbance, from the net landbase,

- initial number of seismic passes per cell (as described above), and

- township and range

A set of sub-models (also known as landscape events in the SELES vocabulary) define the behaviour of the model. There are sub-models for the processes of fire, harvesting, natural regeneration, oil and gas components (seismic lines and well site and pipeline establishment), growing stock calculations, tree planting, and succession. There are also sub-models for non-biological process related to the model itself (data reporting, for example). In a given time step, the SELES model applies the programming (essentially a set of instructions in the form of equations and rules) contained in the sub-models to modify the initial condition of the forest, in order to produce an outcome state of the forest. In the next time step, the model uses this outcome state as the initial state, and repeats this loop for as many time step as required (Figure 14).
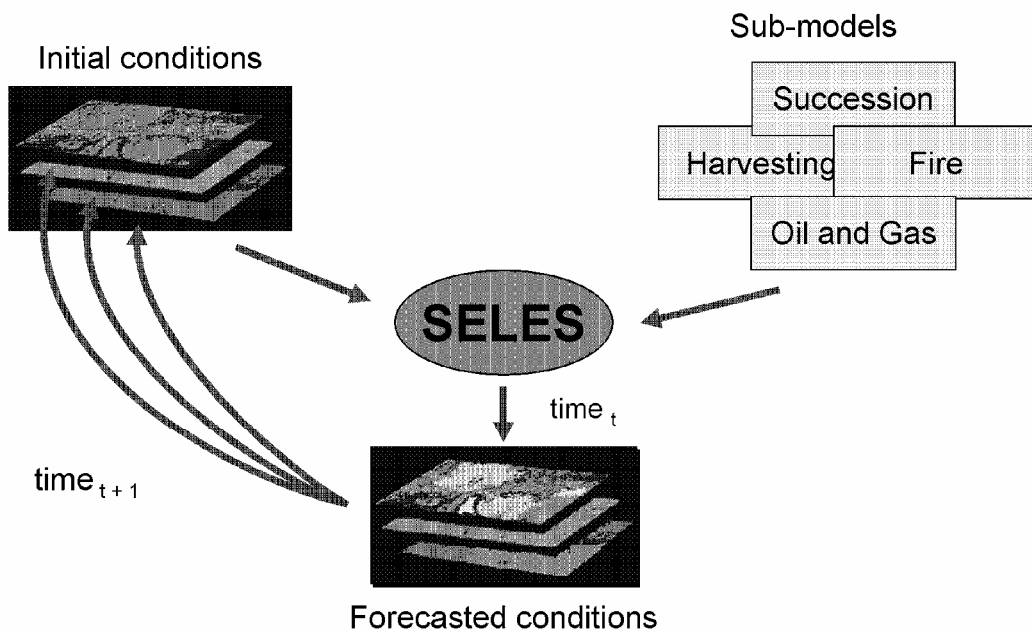


**Figure 14. Illustration of the role of SELES in using sub-models to modify the initial state of the landscape in order to generate predicted states, at time t.**

**The diagram also illustrates how the predicted state is used as the initial state in the next time step.**

Input data stored in tables is also used by the model in order to influence behaviour (e.g., data on fire weather, merchantable volume). Thus, the various sub-models interact with the landscape in order to simulate the behaviour of the forested ecosystem of the Whitecourt DFA. A diagram of

the major model components and the linkages is provided in Figure 15. Each of the sub-models that make up the model is described in the sections that follow.
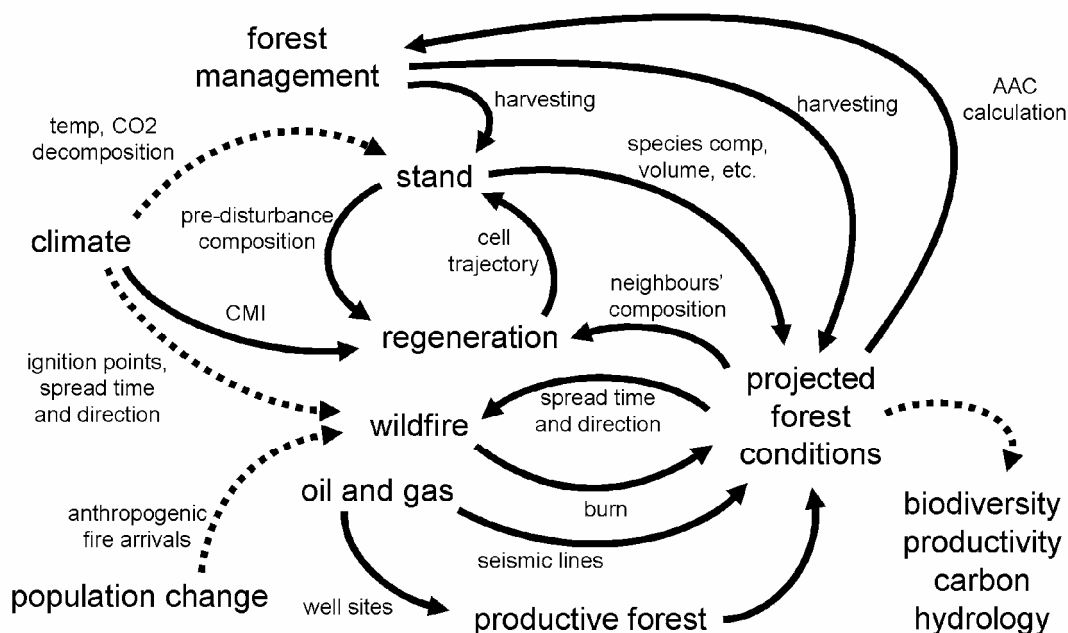


**Figure 15. Illustration of the conceptual model that served as the basis for the implementation of the APLM[6].**

## 2.4.1 The mechanistic fire sub-model

The Canadian Forest Fire Danger Rating System (CFFDRS, Stocks et al. 1989) and related sub-systems (Fire Weather Index and Fire Behaviour Prediction) were used as the basis for the development of the mechanistic wildfire sub-model. The CFFDRS, widely used by researchers and field foresters alike, requires daily fire weather (FFMC, BUI, wind speed, and direction), fuel type (derived here from FORECAST output and tracked by the landscape model), and elevation in order to calculate fire spread direction and speed. See Figure 16 for an illustration of the components of the mechanistic fire model.

---

[6] Dotted lines indicated that linkages are made implicitly, that is in a pre-processing step before the actual simulations were run. The dotted line at the rights leads to analyses that were to take place after simulations were completed. Well sites can be established on non-forested land, though this has impact on neither the model nor its output.
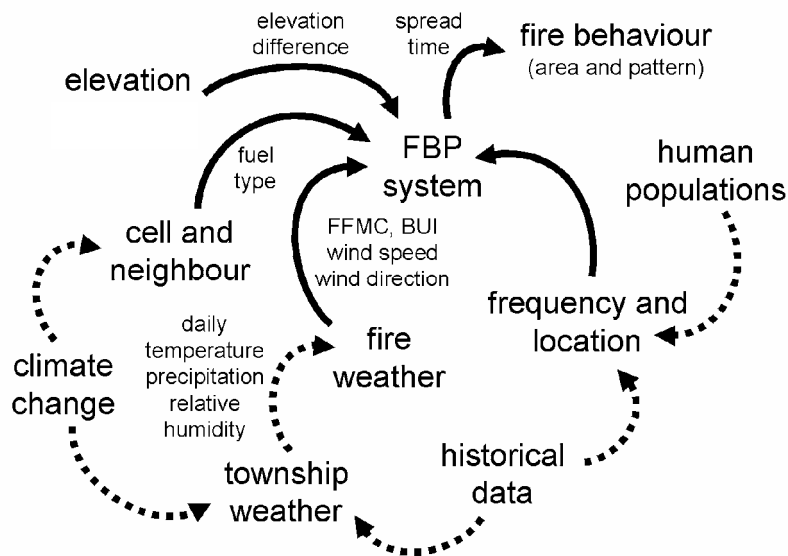
**Figure 16. An illustration of the structure of the mechanistic fire model, which was based on the Canadian Forest Service Fire Behaviour Prediction System.**

**Dotted lines indicate linkages that were made outside the model, in pre-processing steps.**

All equations applied in the model are based on the original documents of the CFS (FCFDG 1992, Stocks at al. 1989) and on more recent updates to the equation system by Wotton et al. (2000). For the version of the fire sub-model described herein, only spread rate (having taken into account foliage moisture, wind, and slope effects, as per CFFDRS) is calculated. Severity and crown-fraction burned have not been considered, since the successional pathways that were implemented (based on stand-scale simulations of forest growth under current and future climates) only simulate post-harvest and post-fire conditions; there is no detail on the amount of crown fraction burned or severity of the fire.

Within the fire sub-model, the time required to spread is calculated and the fire event moves on to the recipient cell, at which point the calculation of spread rate begins again. Each fire event is assigned, at initiation, a stream of daily values for fine-fuel moisture code (FFMC), build-up index (BUI), wind speed and wind direction, which are drawn from a table (with one record for each fire to be simulated). The creation of this table takes place before simulation begins, and is described above in Section 2.2.3. For a given fire, the FWI index values are carried by all cells to which the fire spreads. A fire will only spread if (i) the recipient cell is combustible (has been assigned a FBP fuel code) and (ii) if the spread rate is above the minimum of value 0.1 meters per minute (K. Frederik, pers. comm.).

The difficulties involved with implementing the CFFDRS in a raster environment stem from the fact that the FBP system was developed for continuous (vector-based) space. Attempting to reproduce CFFDRS spread in a discontinuous (raster-based) space leads to inaccurate fire shapes (as compared to a vector-based implementation), and ultimately, to discrepancies in the area burned by the raster-based model relative to the area burned under the same conditions in the

vector based model. These inaccuracies are caused by artefacts resulting from the discontinuity of space (Feunekes, 1991).

The calculation of spread rate implemented in this fire sub-model follows the FBPS very closely. The key difference lies in how the wind-speed-equivalent slope vector  (SV) is added to the wind-speed vector (WV) to arrive at the resultant combined wind and wind-equivalent slope vector (WSV) in the direction of spread (i.e., in the direction of one of the 8 neighbours). The model uses an 8-point spread template (a burning cell can spread to all 8 of its immediate neighbours), and for each of these 8 spread directions, the same calculation is carried out. In order to obtain the magnitude of WSV, a vectorial summation of WV and SV is carried out. Unlike the operation carried out in the FBPS, however, the magnitude is calculated using the spread direction as the reference axis. Since the direction of each neighbour is known, and the slope between the two can be obtained as the difference between the cells' elevations divided by the distance between the cells' centers (equal to 1 for cardinal neighbours and 1.4142 for others), the required information is simply obtained. In this way, for each of the 8 spread directions, the cumulative influence of wind and slope can be taken into account.

Once the sub-model was completed it was calibrated to overcome the artefacts introduced by the passage from a vector based model system to a raster based system, by the introduction of a multiplier on the calculated spread rate.  To this end, 40800 8-hour simulations were run over a range of fire weather and fuel conditions (all combinations of 17 fuels, 20 FFMC, 10 wind speeds, and 12 BUI), each in an iterative mode so as to obtain a correction factor on the spread rate that would bring the area burned at the end of an 8-hour period to within 1% (or 3% or 5 ha at the end of 30 iterations).  Correction factors ranged from 0.125 to 1.95 with a mean value of 0.83.

A record of the number of fire events for each year between 1961 and 1990 (inclusively) was set up in a table, and the corresponding fire weather over a period of 8 days for each of these fire events was set up in another table.  When a given year is reached by the APLM, the mechanistic fire sub-model launches as many instances of the fire sub-model as there are active townships (active townships are identified as townships having at least 75% of their area within the DFA), and each of these instances initiates as many fires as are there are fires in the fire record for that year and township.  Once these fire events are initiated, each event then reads in the appropriate fire weather for each fire it is simulating.  Originally the intent was to assign one fire event instance per township and range, for a total of 150 fire event instances.  However, because fires can only spread within the bounds of the DFA, this concentrated fires to an unacceptable level in certain townships (those actually in the DFA), and left other townships untouched by fire.  And so fires were allowed to initiate in any cell within the DFA.  Fires burn for a period of 8 hours, a period defined as the maximum period for active fire spread by the CFS (CFS, 1992).  At the end of this 8 hour period, the events read in the following day's fire weather, and so on up to a maximum of 8 days.

Once the mechanistic fire sub-model was introduced into the APLM and allowed to burn area, we found that the application of fire indices (FFMC and BUI) calculated from daily mean values combined with the permeability of the landscape caused a very large proportion of the landscape to burn within a few years.  Thus, while the burn rate of the fuels was correct and well calibrated for fixed conditions of fuel type, wind, FFMC, and BUI, it would seem that the implementation

of the fire model using daily mean weather at the landscape scale over large periods leads to unreasonably short fire return intervals. Therefore, we repeated the 30-year fire events loop over a 200 year period and applied a global correction factor to spread rates (a simple multiplier on the rate of spread) within a binary search algorithm, until over the course of simulation a fire return interval was obtained that was comparable to that observed from historical records (see Doyon and Duinker 1999). The correction factor obtained in this way was 0.17, and it yielded a fire return interval over 5 repetitions of a 200 year simulation of 87.7 years. In this way, the mechanistic fire model could be run with and without climate change adjusted fire weather (see section above "Generation of weather streams for fire events under climate change"), to obtain the behaviour of the fire regime under climate change and historical climate, respectively.

Mechanistic wildfire events set stand age to zero, track the area burned, and invoke the natural regeneration sub-model (see "natural regeneration", below).

### 2.4.2    The mechanistic fire reporting sub-model

This sub-model accompanies the previous and outputs indicator data. It was necessary to set this as a separate sub-model since there were multiple mechanistic fire sub-model events running simultaneously and it was impossible to know beforehand, which would be the last extinguished (and therefore the most appropriate to report on all fire events).

### 2.4.3    The empirical fire sub-model

An empirical fire model (where the area to burn is dictated to the model based on historical fire data, in this case as a mean area to burn annually and a standard deviation) was also developed for the project and applied when no influence of climate change was required. The model was applied since it is computationally lighter and required fewer assumptions than the mechanistic fire sub-model. Thus, it was used for the simulation of the natural disturbance regime, the harvesting and fire simulations, and the simulation of fire with harvesting and oil & gas activity. The sub-model draws fire sizes randomly from a negative exponential distribution (the sub-model can also be set to a lognormal exponential distribution, but this distribution proved to be too variable to produce an equilibrium state; see Armstrong (1999) for details), and draws fire event sizes from a negative exponential distribution, with a mean of 1,100 ha. The sub-model was set to continue generating fire events until the annual target area to burn was achieved; this was necessary since the non-forested patches within the DFA could cause fires to extinguish before their target area was reached. A systems diagram for the empirical fire model is provided in Figure 17.
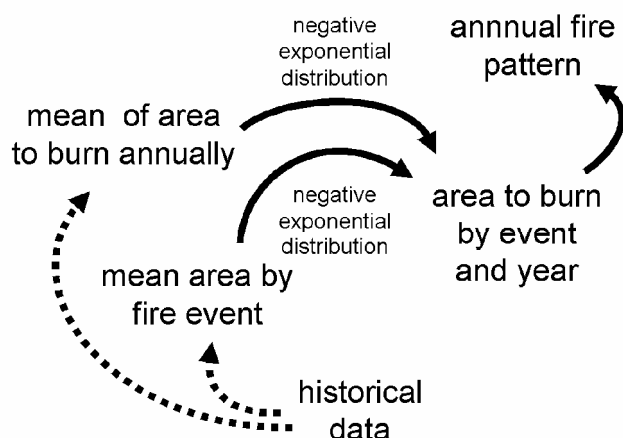
**Figure 17. Illustration of the structure of the empirical fire model. Dotted lines indicate linkages that were made outside the model, in pre-processing steps.**

As with the mechanistic fire sub-model, the empirical model sets stand ages to zero, tracks the area burned annually, shifts cells to a salvageable status if the age is greater than or equal to the minimum harvest age (after reducing the merchantable volume by 50%), and invokes the natural regeneration sub-model (see "natural regeneration", below).

### 2.4.4 The salvage harvesting sub-model

Since modeling within the APLM can involve wildfire, it was deemed important to include a salvage harvesting component in the model's dynamics. After fires have passed through the DFA, the salvage harvesting sub-models finds salvageable volume in the DFA, and harvests this volume, deducting the volume against the target volume to harvest that year. With each new cell to harvest, the sub-model ensures that the amount harvested does not surpass the limit imposed by the scenario. This limit has been set to 100% of the annual harvest target.

### 2.4.5 The harvesting sub-model

The harvesting sub-model applies an "oldest first" rule to harvesting. Minimum stand ages are applied based on information provided by the Timber Supply Analysis (TSA) group (see Table 6). The sub-model applies clear cut harvesting as the only form of harvesting within the DFA.

The harvesting sub-model sets stand age and merchantable volume to zero and tracks the volume harvested, for conifer and deciduous separately. It also invokes the tree-planting sub-model (presented below) in cells that have been harvested.

### 2.4.6 The harvest reporting sub-model

As with the mechanistic fire sub-model, a separate sub-model for the reporting of the harvest activities was created.

## 2.4.7    The tree planting sub-model

This is a simple sub-model that treats cells that have been harvested.  It essentially assigns a new FORECAST based on either of two sets of decision rules.  The first and simplest simply assigns the same FORECAST run as before harvesting.  The second applies a set of rules that assigns FORECAST run based on the composition of the stand at the time of harvesting.  To do this, the model looks up the amount of basal area per species, determines what is dominant and sub-dominant, and assigns the FORECAST run accordingly.  Table 9 presents the different possible compositions at harvest and the initial densities of the FORECAST runs that are applied to the harvested cells by the tree planting sub-model.  While aspen is generally not planted, it is included in the table since it is part of post-harvest successional pathways.

**Table 9.    Initial stem densities of the FORECAST runs assigned to recently harvested cells, based on the composition of the stand at harvest.**

| Composition at Harvest | | FORECAST to Regenerate Density | |
|---|---|---|---|
| Dominant | Sub-Dominant | Dominant | Sub-Dominant |
| Aw | - | 1,125 | - |
| Pl | Aw | 2,125 | 875 |
| Pl | - | 2,125 | - |
| Sb | Aw | 1,875 | 875 |
| Sb | - | 1,875 | - |
| Sw | Aw | 1,875 | 875 |
| Sw | - | 1,875 | - |

## 2.4.8    The growing stock sub-model

This sub-model inventories all merchantable volume, classifies the landbase into available for harvest, unavailable, and available for salvage harvesting at every time step, and calculates the annual harvest target for the harvesting and salvage harvesting sub-models.

The harvest target is calculated by summing the harvest targets by species composition group and then subtracting from this amount the volume harvested by the seismic line sub-model (Eq. 3).

$$harvestTarget = corrFactor \cdot \left[ \sum_{i=1}^{g} ( area_i \cdot volAtTha_i / tha_i ) \right] - volFromSeismic \qquad \text{(Eq. 3)}$$

Where harvestTarget is the annual harvest target, in cubic meters per year,

corrFactor is a correction factor applied to generate sustainable yield,

g is the number of composition groups,

$area_i$ is the area occupied by the ith species composition group in ha,

volAtTha$_i$ is the volume of the ith group at target harvest age, in cubic meters per ha,

tha$_i$ is the target harvest age, in years, and

volFromSeismic is the volume harvested by seismic in that year.

Composition groups are the 40 groups of identical initial composition and stem density, on which the FORECAST simulations were based (Duchesneau *et al*., 2007); a complete list of the 40 groups and their corresponding parameters is provided in Table 6. It was these 40 groups, simulated over 5 site types and 2 climates that yielded the 400 final FORECAST runs (Duchesneau *et al*., 2007). The estimation of volume harvested from seismic is described in the section on the seismic line sub-model. The correction factor is applied in order to obtain a sustained yield over the course of the simulation time horizon for the harvesting only scenario. This value is obtained by applying a search algorithm to the simulation of the harvesting only scenario. The algorithm essentially runs several simulations until the highest possible correction factor that does not result in an annual shortfall in harvest volume (less volume harvested than is established by the harvest target) is found (to 2 decimal places). This correction factor is then applied to all other scenarios; in this way, the sustainable harvest rate under the harvesting only scenario is used as the baseline harvest rate. Under the other scenarios, which include fire and other factors that will limit the volumes that can be harvested, the number of shortfalls and the mean volume actually harvested can be tracked for each of the simulations and output as indicator data.

As mentioned previously, care was taken to emulate the TSA's harvested volumes with the APLM. Merchantable volumes, which were drawn from the simulation work also prepared for the 2007-2016 DFMP (described in greater detail in the section 2.3 and in the report of Duchesneau *et al*., 2007), had been calibrated against Millar Western's growth and yield data (Figure 18). However, several factors will lead to differences in the estimation of harvestable volume by the APLM and the TSA. Most notably, the TSA results from an optimization of harvesting over time, while the APLM does not. Also, the trajectories that a stand may follow are more limited in number in the APLM than in the TSA. Within the APLM, there are no constraints on the spatial distribution of harvest blocks; this will also have an influence on the achievable harvest rates for the DFA. Therefore, the harvest rates obtained by the different scenarios run by in APLM should not be compared to those obtained by the TSA (although this exercise would be of interest), but rather, they should be compared to the harvesting-only harvest rate, the baseline for comparison.
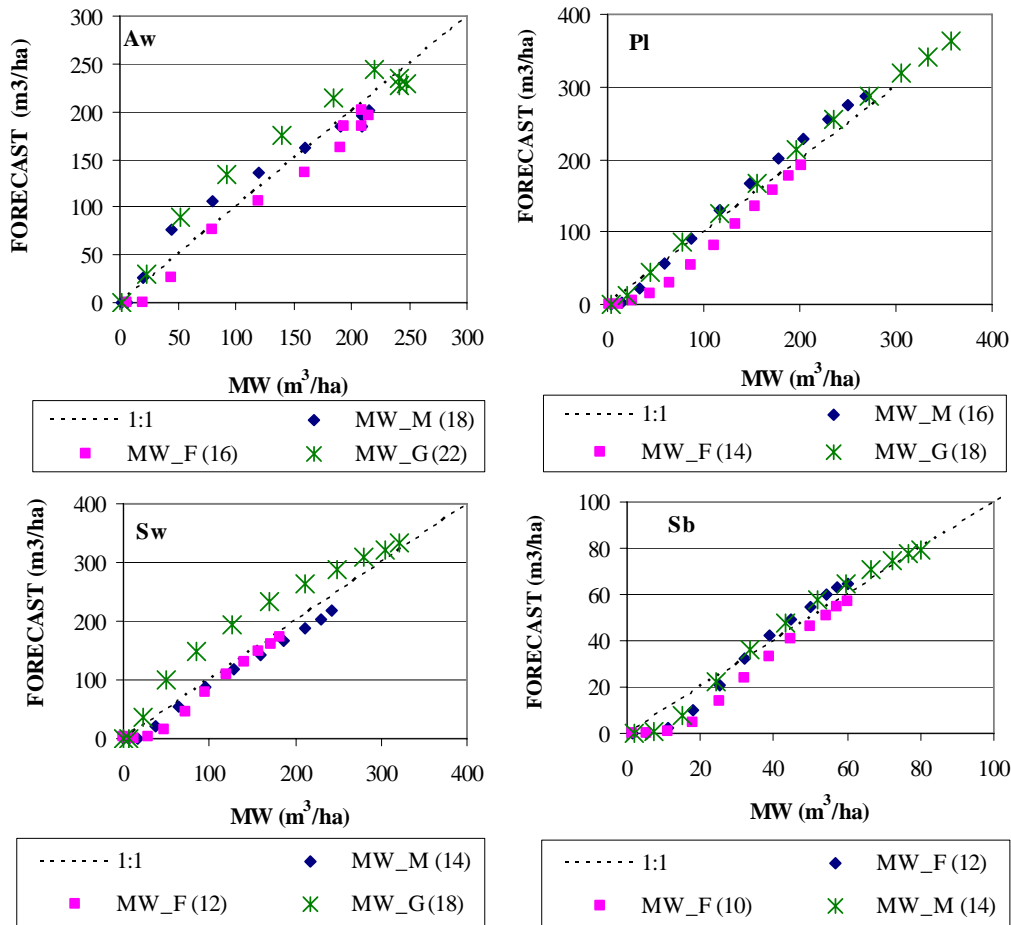
**Figure 18. Relationship between merchantable volume (m3/ha) from Millar Western's DFA growth and yield data for managed stands (MW) and from FORECAST model output for four species.**

**Tags in the legend correspond to the following: MW = Millar Western data; _F = fair sites, _M= medium sites; _G= good sites. Numbers in parentheses is the site index used for the FORECAST simulations. This figure is drawn from the report "The influence of global climate change on the productivity of forest ecosystems" (Duchesneau *et al*., 2007), also prepared for the Millar Western 2007-2016 DFMP.**

## 2.4.9    The stand succession sub-model

Conceptually, having determined initial composition of a cell (and its FORECAST run) succession within the APLM is extremely simple. The evolution of a cell amounts to looking up stand characteristics in a table of data, data that was generated by the FORECAST stand model (Duchesneau *et al*., 2007). Therefore, the succession sub-model does little in the way of what is generally conceived as succession, but rather serves to update age, and generate output data both

in the form of rasters (for BAP age and strata) and tabular data (such as tracking forested and non-forested area, the amount of area as seismic, etc.).  The sub-model also "ages" certain features, such as seismic lines and salvageable volume.  For salvageable volume, it removes 50% of the standing volume every year (so the volume is 50% of initial the first year, 25% the second year), and if the age of the burn is above the maximum life span for salvageable wood (for this exercise, this is set to 2 years), it sets the salvageable volume of the cell to zero.  For seismic, it re-arranges the seismic pass data within cells, so that seismic lines gradually diminish, at a rate that will maintain existing abundances on the landscape if historical rates of seismic activity are maintained (this decay rate was found to be 1. 372%, annually).  This implies that over time seismic lines are regenerated.

## 2.4.10   The natural regeneration sub-model

When a cell within the model has been disturbed by one of the wildfire sub-models, the natural regeneration sub-model is invoked for that cell (Figure 19).  The sub-model works on the principles and equations developed by Greene and collaborators and it is applied to determine both *in situ* and *ex situ* regeneration.  Modifications were brought to these equation systems based on the work of Hogg (Hogg and Schwartz 1997), in order to take CC into account.
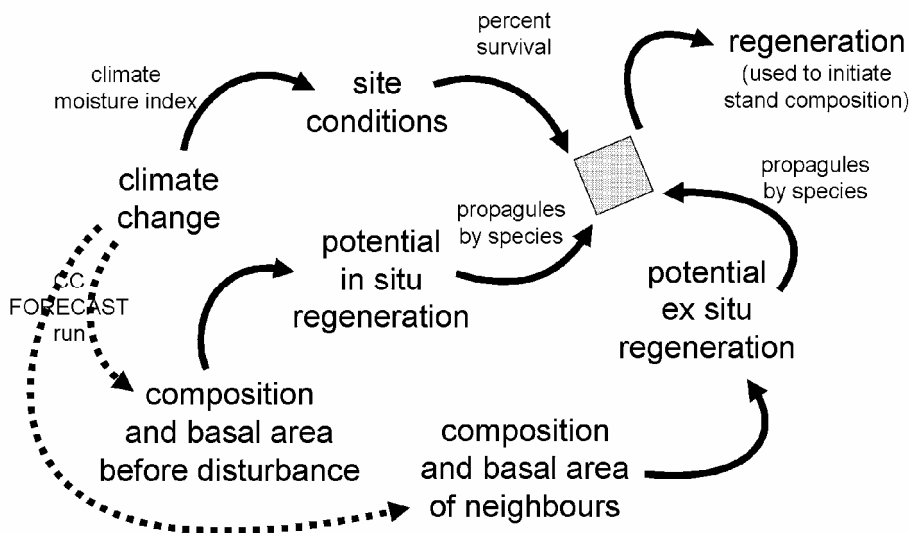


**Figure 19. Structure of the natural regeneration sub-model, indicating the contributions of in situ and ex situ regeneration.**

**Dotted lines indicate linkages that were made outside the model, in pre-processing steps.**

For *in situ* regeneration, the sub-model uses the amount of basal area by species present when the fire occurred (taken from the tables produced by Duchesneau *et al*. (2007) through the use of FORECAST run and stand age) to derive the number of stems that will establish on the site; the equations were drawn from Greene and Johnson (1999).  For aspen regeneration, an ecosite-specific regeneration moisture index is applied; this moisture index was based on the assumption

that there is a moisture optimum for regeneration, and that the function linking moisture regime (taken from Beckingham's ecosite classification) is a convex hyperbola. An illustration of the function and the equation for the function is given in Figure 20. The moisture index, which takes on values between 0 and 1, multiplies the final estimate of regenerating aspen stems to scale down regeneration from the optimum at site moisture index of 5. For white spruce regeneration *in situ*, the *ex situ* equations of Greene (described in the next section) are applied with a dispersal distance of 1 meter.



The graph shows a curve with the equation $y = -0.0625x^2 + 0.625x - 0.5625$, with "Moisture modifier parameter" on the y-axis (ranging 0 to 1.2) and "Moisture index" on the x-axis (ranging 0 to 10).
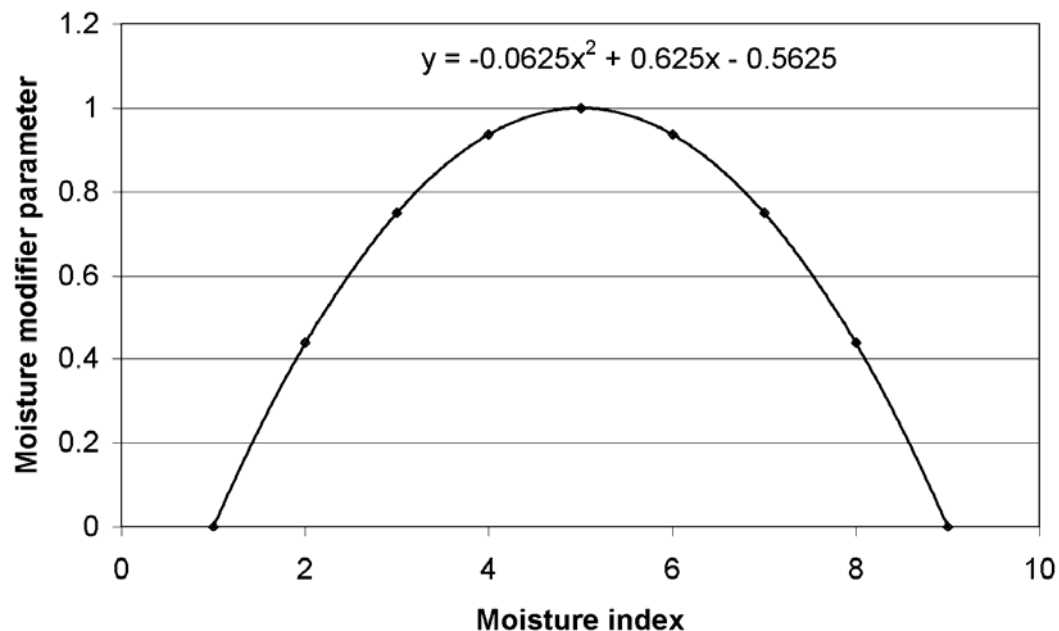
**Figure 20. The modifier for *in situ* aspen regeneration, which scales regeneration down from its optimum at a site moisture index of 5 (based on Beckingham's ecosite classification).**

For *ex situ* regeneration, the sub-model first seeks to determine the amount and type of seeds in the nearest seed-bearing neighbour to the north, south, east, and west (see Figure 22). This distance must be inferior to a set maximum distance (here applied to 500m) for the model to consider the cell a source cell; a cell's trees must have an age of at least 25 years in order to bear seeds. Once these source cells have been identified, the number of seeds in these cells (Greene and Johnson 1994) and the dispersion of seeds from these sources to the target cell (the cell to be regenerated) is calculated (Greene and Johnson 1996, Greene 2000, Calogeropoulos et al. 2003), and the number of potential seedlings is established for each species. A survival index is then calculated based on a competition index derived from the vegetation competition code of Beckingham's ecosite classification system (Figure 21, Eq. 2); a post burn seedbed index (Charron and Greene 2002); and a CMI index (based on the work of Hogg and Schwartz, 1997). The number of established seedlings is obtained by multiplying the number of seeds dispersed into the cell to regenerate by this survival index, the percent open cone index (Muir and Lotan 1985, Gauthier et al. 1996, Radeloff et al. 2003), the dispersal index (Greene and Johnson 1996,

Greene 2000), and invasion time (Greene and Johnson 1998, Calogeropoulos et al. 2003); the generalized equation for this calculation is given (Eq. 3).
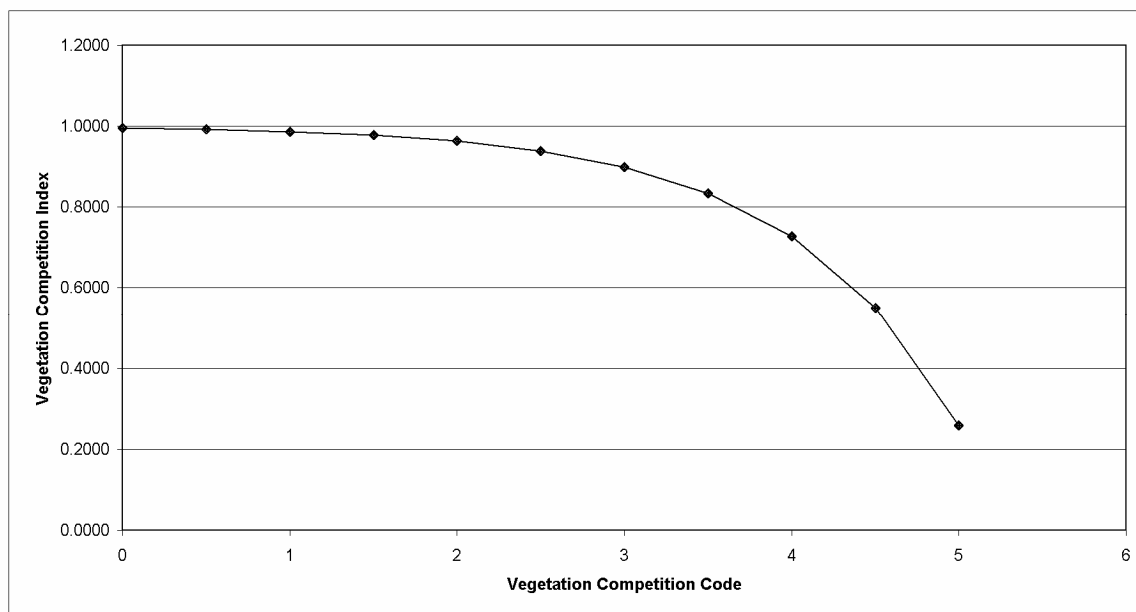


**Figure 21. The relationship between Beckingham's vegetation competition code and the vegetation competition index applied in the natural regeneration model.**

**The equation for this relationship is given in Eq. 3.**

$$\text{CompIndex} = 1 - (0.005 \cdot e^{(\text{CompCode})})$$  Eq. 2

Where     CompIndex is the competition index and

         CompCode is the competition code drawn from the ecosite classification.

$$\text{Seedlings} = \text{Seeds} \cdot \text{PocIndex} \cdot \text{SurvivalIndex} \cdot \text{DispersionIndex} \cdot \text{InvasionTime}$$  Eq. 3

Where     Seedlings is the number of seedlings that establish in a cell,

         Seeds is the number of seeds available in a source cell,

         PocIndex is the percent open cone index for a source cell,

         SurvivalIndex is the rate of survival for seedlings in a cell,

         DispersionIndex is the proportion of seeds that reached the target cell, and

InvasionTime is the assumed number of years for establishment.
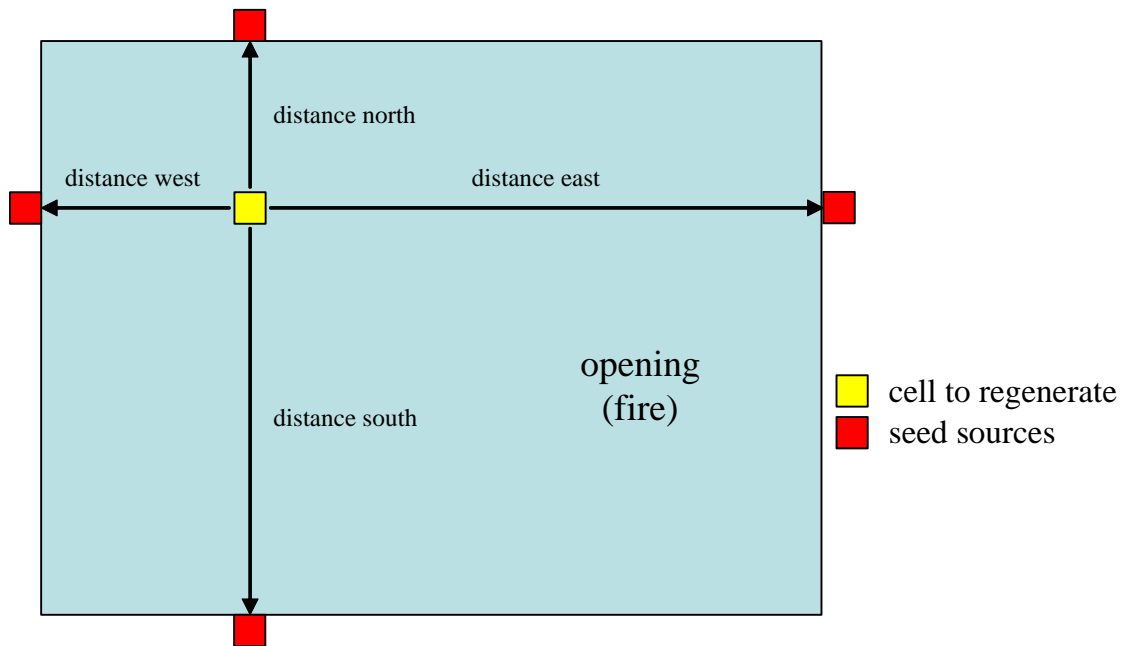


**Figure 22. Illustration of the functioning of *ex situ* regeneration within the natural regeneration model; the sub-models seeks out the nearest cardinal neighbours that contain seed trees.**

Once the number of surviving seeds is determined, the sub-model chooses the FORECAST run that has the most similar initial composition, and sets the cell on that trajectory. The method to carry out this process looks at all FORECAST runs with the same species composition, sets the cell to regenerate and the relevant FORECAST runs on a plane defined by the initial stem density, calculates the Euclidean distance from the cell to regenerate to all FORECAST runs, and selects the FORECAST run with the shortest distance to the cell (Figure 23). A systems diagram for the natural regeneration sub-model is provided in Figure 19.
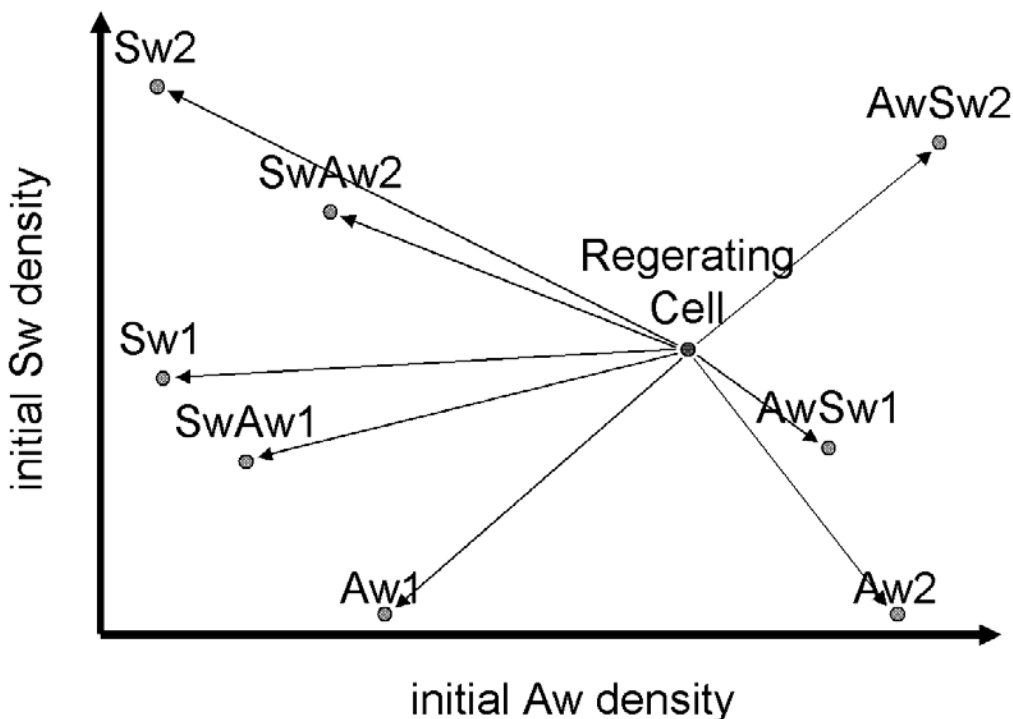
**Figure 23. Illustration of the process to assign a FORECAST run to a recently regenerated cell.**

**In a plane defined by the abundance of the stems in the initial composition, the cell to regenerate is compared to all FORECAST runs with similar composition (distance on the Euclidean plane indicated by arrows). In this example, the cell will be assigned FORECAST run AwSw1.**

## 2.4.11   The well sites sub-model

Based on a schedule of decadal well sites to establish, the well sites sub-model establishes the appropriate number of wells over the DFA.  In the version of the model used to generate the data presented in this report and discussed in the text that follows, the number of well sites was set to 17 annually for the DFA.  For the factorial experiment that is presented at the end of this report, two levels of oil and gas activity were applied: low (17 wells per year) and high (34 wells per year). Given that we expect coal-bed methane increase its footprint on the landscape over the coming years, we consider that the doubling of well sites is a conservative estimate of future oil and gas developments.  Well sites are set to have an area that is drawn from a uniform distribution, between 1 and 2 hectares.  If coal-bed methane should gain in importance on the landscape, this number should most likely be much higher, around 4 ha.  When a well site is established, the cell is set to non-forested and non-harvestable.

## 2.4.12   The pipelining sub-model

The pipelining sub-model establishes links between new wells and the existing network of wells and pipelines within the DFA.  It uses an algorithm that will yield a result similar to the

minimum spanning tree to determine the optimal manner in which to link a new well with the existing network of well sites. Essentially, the sub-model grows out from every existing cell in the pipeline and well site network simultaneously. When two fronts collide, the model verifies the fronts' information (the cells of the moving fronts carry information with them on their origin) to see if one of them belongs to an unattached well site. If one of them does, the model will link the origin of the two fronts with a pipeline, and record the fact that the new well site is no longer unattached, as illustrated in Figure 13.

### 2.4.13   The seismic line sub-model

Based on the analysis described above ("Analysis of oil & gas patterns on the DFA") seismic lines were laid down within the DFA boundaries on an annual time step. Seismic lines were set to have lengths drawn from a normal distribution with a mean of 1,000 m and a standard deviation 500, and clamped between 100 and 5,000 m. With each seismic line generated, the model subtracts the length of that line from the total length to establish that year. When a seismic line passes through a cell, it increments the number of seismic passes for that cell, and estimates the amount of volume that is removed by the pass. This is carried out by calculating the incremental amount of area occupied by this most recent seismic line (based on the relationships derived in section, 2.2.8 above), and by multiplying the proportion of the cell that this represents by the volume of that cell without seismic (drawn from a table). If the model is set to deduct seismic harvested volume from the AAC, it does so. Regardless of this setting though, when the growing stock sub-model determines the amount of volume in a cell, the volume is corrected by the amount of area occupied by seismic in that cell (this can be turned on and off in the model, but was always left on for the runs presented here). If the landscape model is set to decay the amount of seismic in a cell (again on an annual time step), then it is the succession sub-model that will reduce the extent of seismic in the cell (see the section on the succession sub-model for details).

## 2.5   Output data

The APLM produces a considerable amount of data, both in tabular form and in the form of rasters (or grids). Output in raster form currently includes the following:

- stand Age
- time since disturbance
- number of seismic passes
- stand Origin
- FORECAST run
- coniferous and deciduous merchantable volume
- salvageable volume

- well site and pipeline location

- BAP age and strata

- cumulative percent old-growth (as defined by Doyon and Duinker 1999)

- BAP index

The latter is a grid with 18,740 possible values, each pointing to a specific state under the BAP system of site classification, a state that includes descriptions for BAP strata and age, timber productivity rating, moisture, age class, and stand origin (whether of harvest or fire origin). This grid serves as the link between the APLM and the BAP toolbox (described in Doyon and Duinker 1999). The model also produces a set of tables, with one row for every year of simulation. These tables include:

- harvested volume and AAC information

- salvage harvesting reports

- wildfire records

- area by stand and BAP age classes

- area by BAP strata and age class (this table has 18 rows per year of simulation)

- volume by age class

- area by availability class (under minimum harvest age, salvageable, and available for harvest)

- area by landbase class (forested, non-forested, and harvestable)

- data on seismic abundance and occurrence

- data on well sites established

- detailed information on the regeneration sub-models (mostly for verification)

- detailed information on the transition of cells from one FORECAST run to another

## 2.6 Scenarios that were tested with the APLM

A set of 9 scenarios were tested with the model. The objective was to gain as much insight as possible about the cumulative impacts of disturbance agents (fire, harvesting, oil & gas, demographics) on the landscape, while maintaining a manageable set of outputs for analysis with

the BAP toolbox. The 9 scenarios retained for analysis are the following (letters in parentheses are the abbreviations that will be used in the remainder of the text):

- harvesting only (H)

- harvesting and fire (HF)

- harvesting and oil & gas (HO)

- harvesting, fire, and oil & gas (HFO)

- fire only (F)

- fire and climate change (FC)

- fire, harvesting, and climate change (HFC)

- fire, harvesting, oil & gas, and climate change (HFOC)

- fire, harvesting, oil & gas, demographic and climate change (HFOCD)

It should be noted that all scenarios involving fire without climate change applied the empirical fire model, described above. For the sake of calibration and comparison, a scenario was also run without climate change and with the mechanistic fire model.

The harvesting only scenario was first run in an iterative mode in order to identify the correction factor on the calculated AAC that would yield a sustained yield with no shortfalls over the course of the 200-yr simulation. This correction factor, or AAC multiplier, was found to be 0.79. It is, in essence, the correction required to pass the dip in the current age class distribution, in the stand age class of approximately 90 to 100 years.

It should also be mentioned that for the scenarios involving the empirical fire sub-model and the oil & gas sub-model together, the target area to burn was corrected annually for the area forested. That is to say that the target area to burn was recalculated from the target fire return interval and the remaining area forested after laying down well sites and pipelines. If this had not been carried out, the proportion of forest area burned on average annually would have increased as the area of forest decreased (since oil and gas shifts land from forested to non-forested).

Results of BAP analysis were analyzed with ANOVA, with the combination of disturbance agents (H, HF, HFO, etc.) used as the treatment factor level. Student-Neuman-Keuls a posteriori comparison test was applied to identify means that were significantly different from one another.

# 3. Results and Discussion

The results of the APLM simulations are presented here as a set of comparisons between the various cumulative impact scenarios and the harvesting only scenario.  This presentation was deemed of greatest interest since it highlights the implications of forest management that takes only harvesting activities into account.  Scenarios will be compared in terms of the following indicators:

**Stand age class and structural stage distribution**

As defined by Doyon (2000); these indicators describe the structure of the forest in terms of age and structural stage.

**Mean area-weighted landscape age:**

The average age of the landscape, obtained by adding the age of all forested cells in the landscape, and dividing by the number of forested cells; it yields a representative mean age for the landscape; generally in highly disturbed landscapes, the risk to biodiversity stems from the fact that the age of the landscape is driven lower by harvesting, fire, and other disturbances.

**Species composition**

The composition of the tree species that comprise the canopy of the stand.

**Volume harvested:**

The volume harvested by green wood harvesting, salvage harvesting, and clearing for seismic.

**Area non-forested:**

The area within the DFA that is not covered by forest; only oil and gas can modify the area non-forested within the APLM.

**Mean forest patch size:**

A patch is a area of forested land that is uniform with regards to composition (coniferous, deciduous, or mixedwood) and structural stage (open, developing, young, and old); this statistic is the mean size of all patches within the DFA; in a manner that is analogous to the situation with landscape age, the risk in a highly disturbed landscapes is that cumulative impacts fragment the landscape, so that in the simulations presented here, small forest patch sizes present a risk to biodiversity, and large forest patch sizes are, in this context, more desirable.

**Old patch area:**

The mean patch size for all patches composed of old forest; as with mean patch size, the more a landscape is disturbed, the more rare large patches of old forest become; thus, generally speaking, large old patch areas are better for biodiversity.

**Forest core area:**

This area is obtained by buffering (i.e., removing the edge on) forest patches, so that only the area of the patch that is unaffected by forest edge is taken into account (see Rudy (2000) for details), and by summing that area over the landscape; the interpretation of this indicator for biodiversity assessment is based on the assumption that certain species require forest that is unaffected by edge, and that in highly disturbed landscapes, forest core area can become limiting to biodiversity. Thus, generally speaking, more forest core area is favourable to biodiversity.

**Old forest core area:**

The total amount of core forest area that is composed of old forest, as classified according to the composition and age standards of Doyon (2000); once again, in disturbed landscapes, it is generally considered that more old forest core area is more beneficial to biodiversity.

**Mean edge contrast index:**

Edge contrast index is a value (between 0 and 1) that measures the abruptness of changes when travelling from one patch to its neighbour, and this indicator is the average value of edge contrast index for the entire landscape; generally speaking, excessively high mean edge contrast index values are detrimental to biodiversity.

**Contrast-weighted edge length:**

The sum of all edge lengths within the landscape, weighted by the edge contrast index between the two patches on either side of the edge; in the context of a highly disturbed landscape, large amounts of edge negatively impact biodiversity.

Unless otherwise indicated, the numeric results presented are the results from the first of 5 runs. Also, for graphical results (such as harvested volume over time), only data from the first of the 5 runs is presented. It will be specified in the text when numerical results refer to more than the first run.

# 3.1 Comparison of the harvesting only (H) and harvesting and fire (HF) scenarios

In the H scenario results, we can see that as time moves forward, the area from 0 to 100 years of age approaches normalization, while a considerable amount of area ages and, as such, migrates to the right of the age class distribution graph (Figure 24). This aging area corresponds to the area that was identified as non-harvestable under the TSA, and thus, is never harvested in the model. The age class distribution graph of the HF scenario (Figure 25), however, indicates that if wildfire is taken into account, the non-harvestable area will not age as it does under the H scenario. The age class distribution that is obtained resembles more closely that of the natural disturbance regime (Figure 26), since the non-harvestable area is exposed to the same fire regime as the rest of the forest. Thus, the first observation to come from this analysis is that the old growth forest that is expected to come from non-harvestable land will not be as abundant as expected, given an approach to forest management that does not take fire into account.
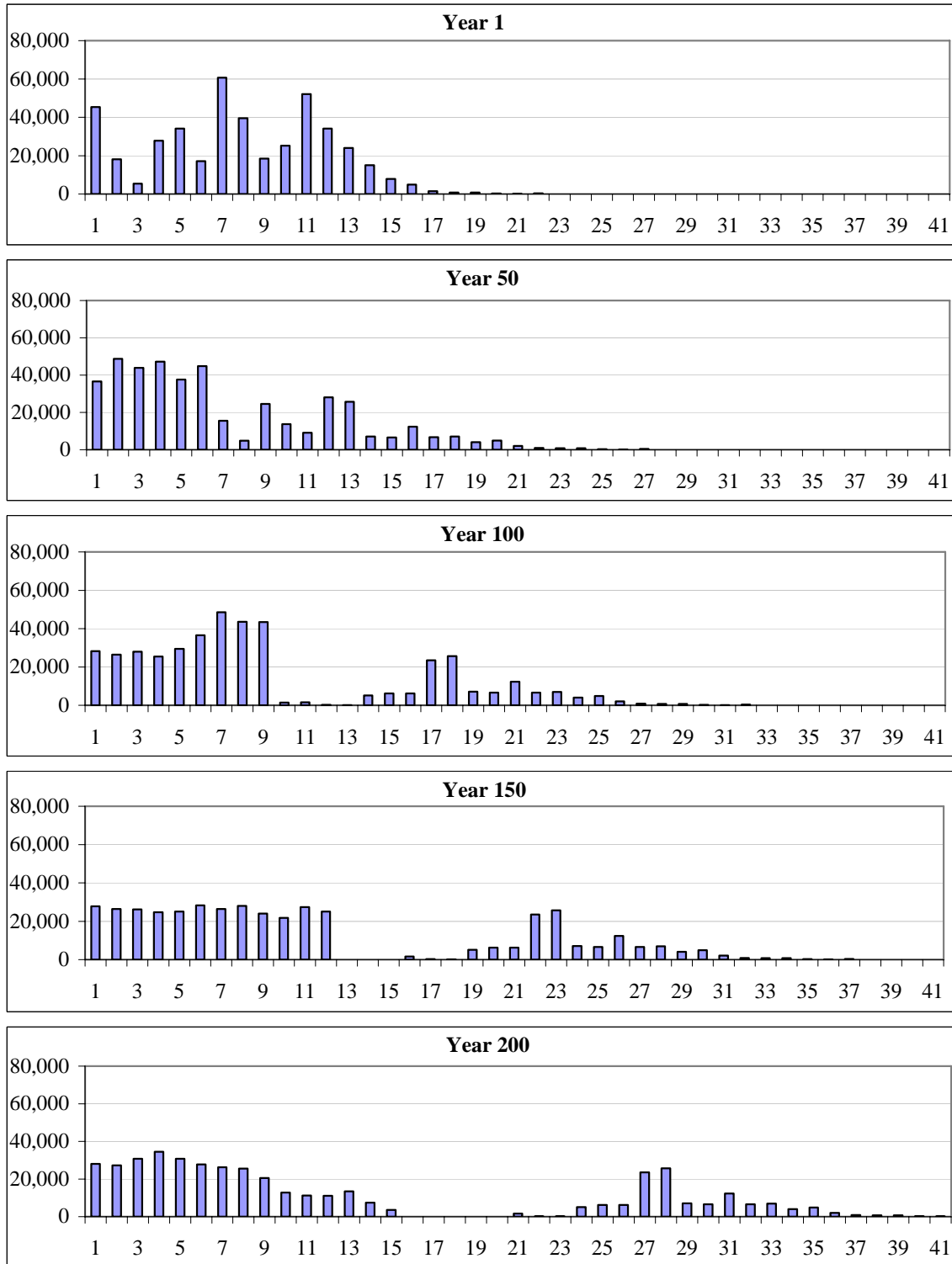
**Figure 24.  Age class distributions (with decades across x-axis, where 1 is for ages 0 to 10) at 50-year intervals for the harvesting only scenario; the non-harvestable portion of the landscape can be seen to migrate to the right of the graph.**
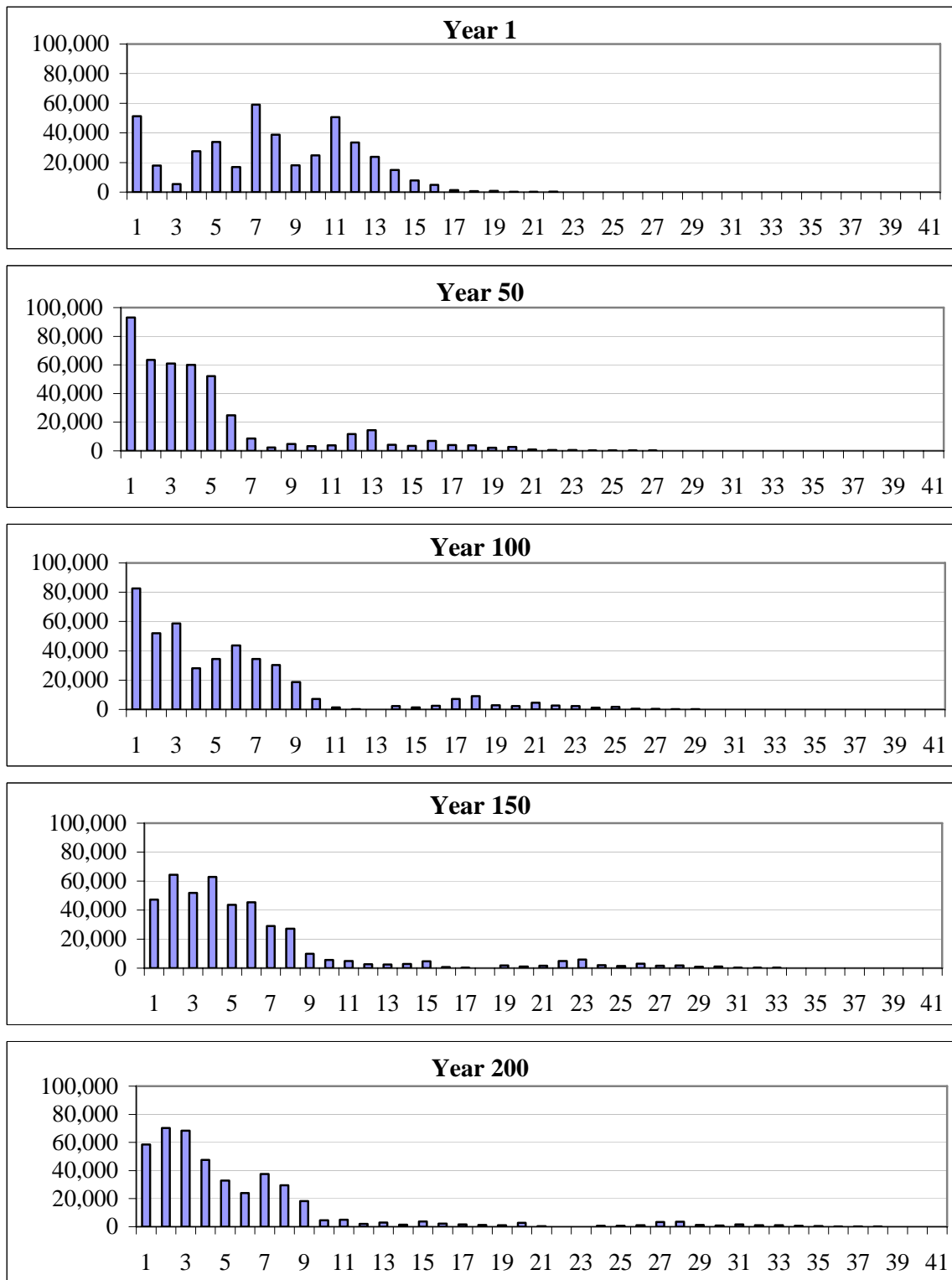
**Figure 25. Age class distributions at 50-year intervals for the harvesting and fire scenario.**
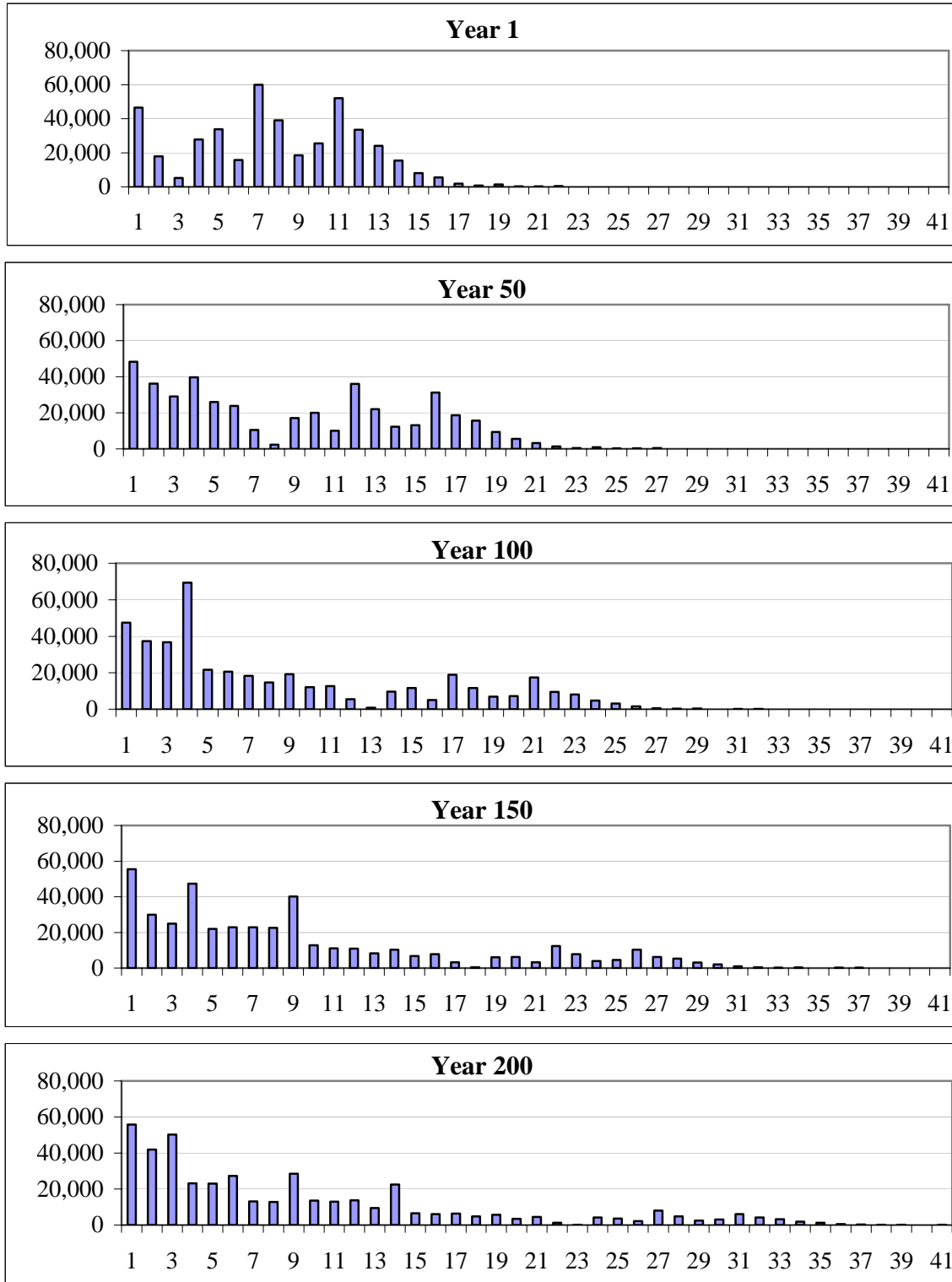
**Figure 26. Age class distributions at 50-year intervals for the fire only scenario.**

By examining timber supply under the H scenario (Figure 27), we can see that a stable supply of timber is obtained.  With the exception of 2 years of simulation with partial supply shortfalls,

which result from a scheduling of harvest blocks that differs from that obtained during the iterative process of harvest rate correction (see the Section 2.6 - Scenarios that were tested with the APLM), the volume harvested varies very little over the course of simulation. The AAC at the first year of harvest is approximately 550,000 cubic meters and gradually increases to 583,000 cubic meters (this 6% drift in the AAC results from the changing composition of the landscape; for details on AAC calculation, refer back to "The growing stock sub-model"). Meanwhile, under the HF scenario, the first shortfall is recorded in the 51st year, and shortfalls occur another 90 times over the following 149 years of simulation (Figure 28). On average, the HF scenario harvests 434,000 cubic meters, as compared to the baseline 578,000 cubic meters harvested (H scenario). The unstable nature of timber supply under this scenario suggests that, while mean volume harvested is useful for the comparison of scenarios, the impact of fire on the sustainable AAC would be greater than this indicator would suggest. Another round of simulations attempting to identify the AAC multiplier for the HF scenario would need to be run in order to find the sustainable yield under the wildfire assumption. A summary of mean volumes harvested is presented in Figure 46.
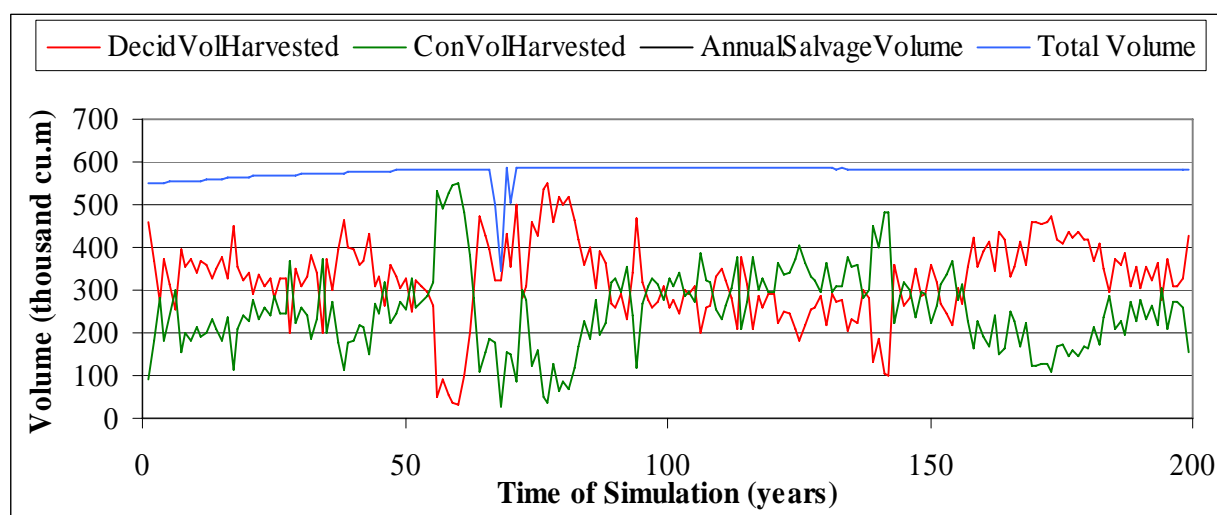


**Figure 27. Simulation model timber supply prediction under harvest scenario (H).**
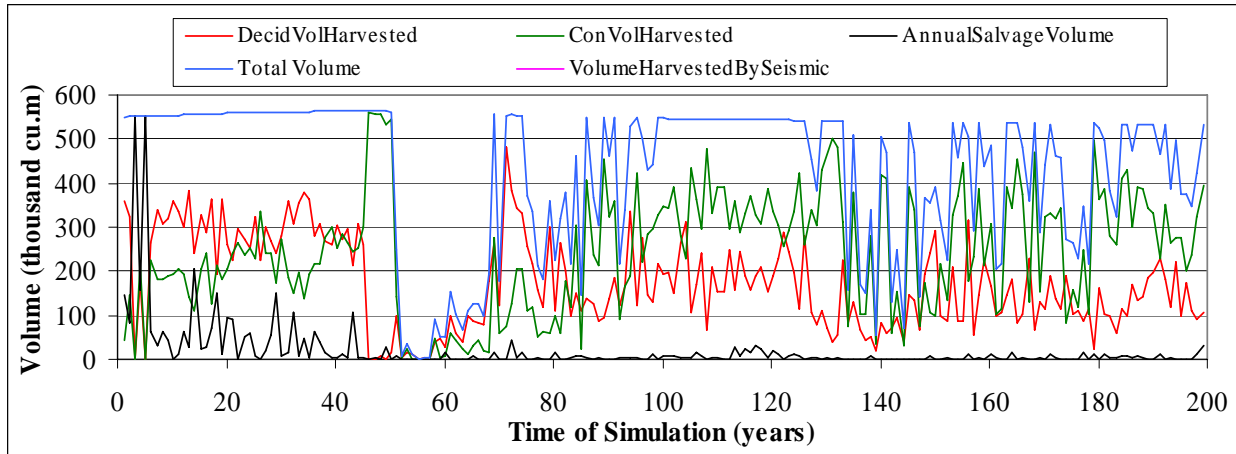
**Figure 28. Simulation model timber supply prediction under harvest and fire scenario (HF).**

Since the model can harvest volume from previously burnt forest, the data on salvage harvesting is of interest. Currently in forest management, the impacts of fire can be mitigated since it is possible to salvage much of the volume that has been burnt. However, the model demonstrates that important contributions by salvageable volume occur at the beginning of simulation only. As fire and harvesting continue to operate on the landscape, the amount of forest above minimum harvest age decreases (Figure 29). The result of this is that, on average, younger and younger forests burn, to the point where a significant portion of the area that is burnt annually is below minimum harvest age. This leads to a recovery of volume from salvageable area that decreases with time. Indeed, for the first 20 years, the model recovers on average from 10 to 140 cubic meters per ha of burned area (with an average of 27 cubic meters per ha), and by the end of the simulation, the model can rarely recover more than, on average, 5 cubic meters per ha of burned area (the average for the last 20 years is 1.3 cubic meters per ha). This will have important implications for this and future generations, as the quantity of wood that can be recovered as we normalize the forest will not be the same as salvage harvesting from forest that has not been normalized.
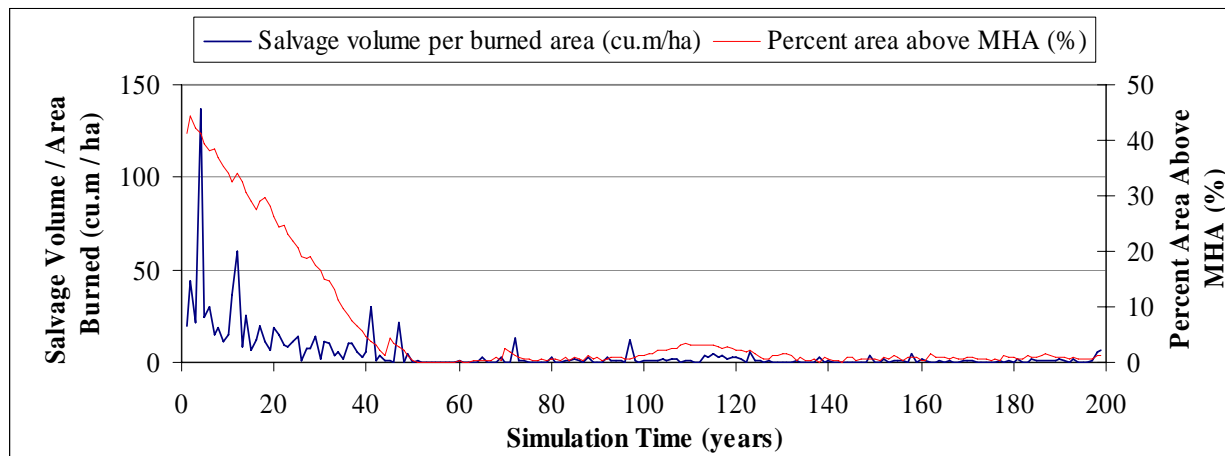
**Figure 29. Mean volume salvaged per unit area burned, and the proportion of the DFA that is above minimum harvest age (MHA).**

In terms of biodiversity, the impact of the interaction between harvesting and fire is clear; many of the BAP indicators applied to the model's output suggest more highly degraded biodiversity conditions under fire and harvesting than under harvesting alone or fire alone (the latter is the standard for the emulation of the natural disturbance regime). It is important to note here, however, that the high values of the BAP indicators under the harvesting only scenario result from the assumption that all non-harvestable forest (122 278 ha out of a total of a total of 433 559 ha of forested land) ages continuously over the course of simulation. This non-harvestable forested area contributes significantly to the apparently high levels of old forest and large patches.

For example, Figure 30 shows that harvesting-only leads to 239,000 ha of core area (all forest types combined) for the DFA (95,000 ha and 144,000 ha for W11 and W13, respectively), and that this amount decreases to 206,000 ha with fire and decreases yet again to 183,000 ha with fire and harvesting. Thus, under the unrealistic assumptions of the TSA, harvesting only leads to more forest core area, preferred by many species (Robinson et al. 1995), than either fire only or harvesting and fire. By comparing the F scenario (the natural disturbance regime standard) to the HF scenario, we find that there is a 11% drop in forest core area. Similar trends can be observed with other BAP indicators, such as the mean patch size of old forest (Figure 31), old forest core area (Figure 32), and contrast-weighted edge length (Figure 33). These results suggest an important fragmentation of habitat from the combined effects of harvesting and fire within the DFA, an effect which could only have been detected with spatial analysis of the combined impacts of fire and harvesting.
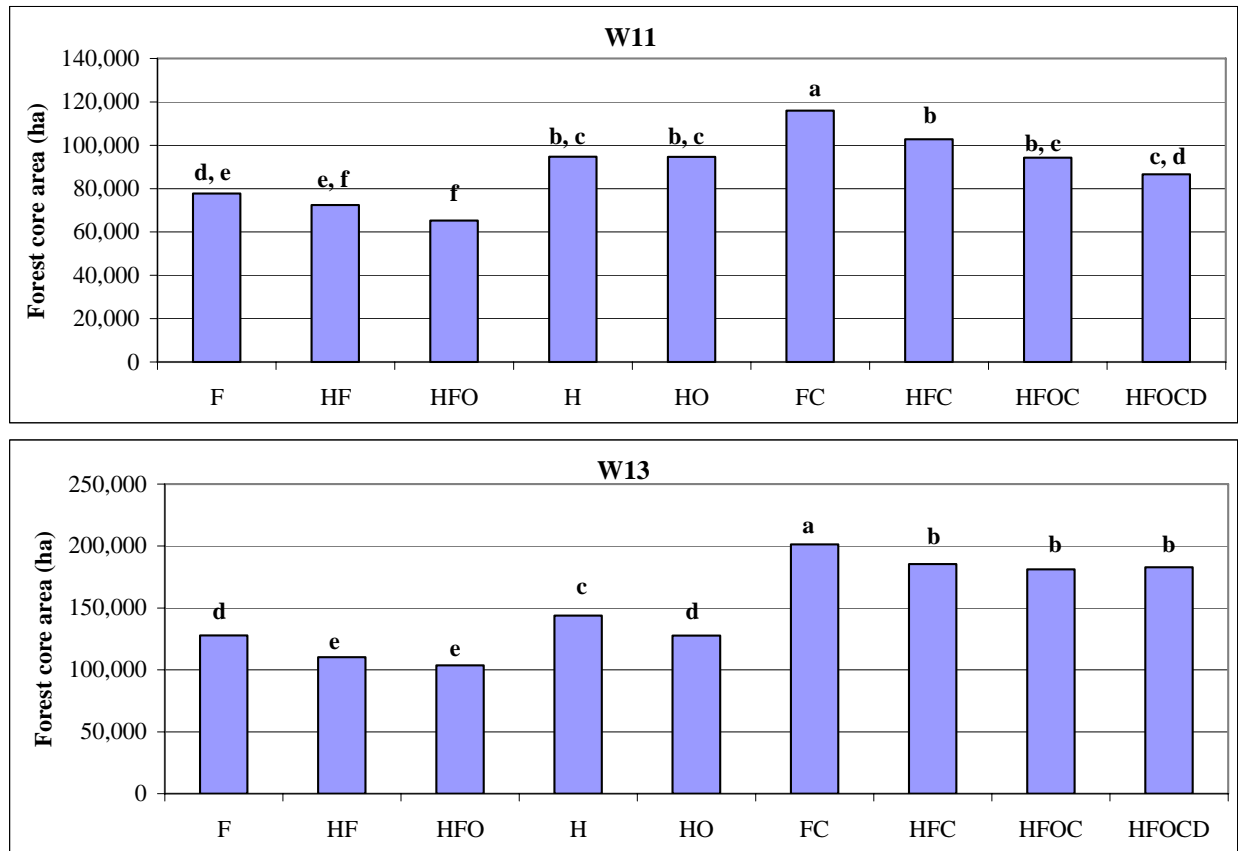
Histogram bars with the same letter are not significantly different at the 0.05 significance level.

**Figure 30. The total amount of core forest for the forest management area at the end of the 200-year simulation period, for each of the scenarios tested.**
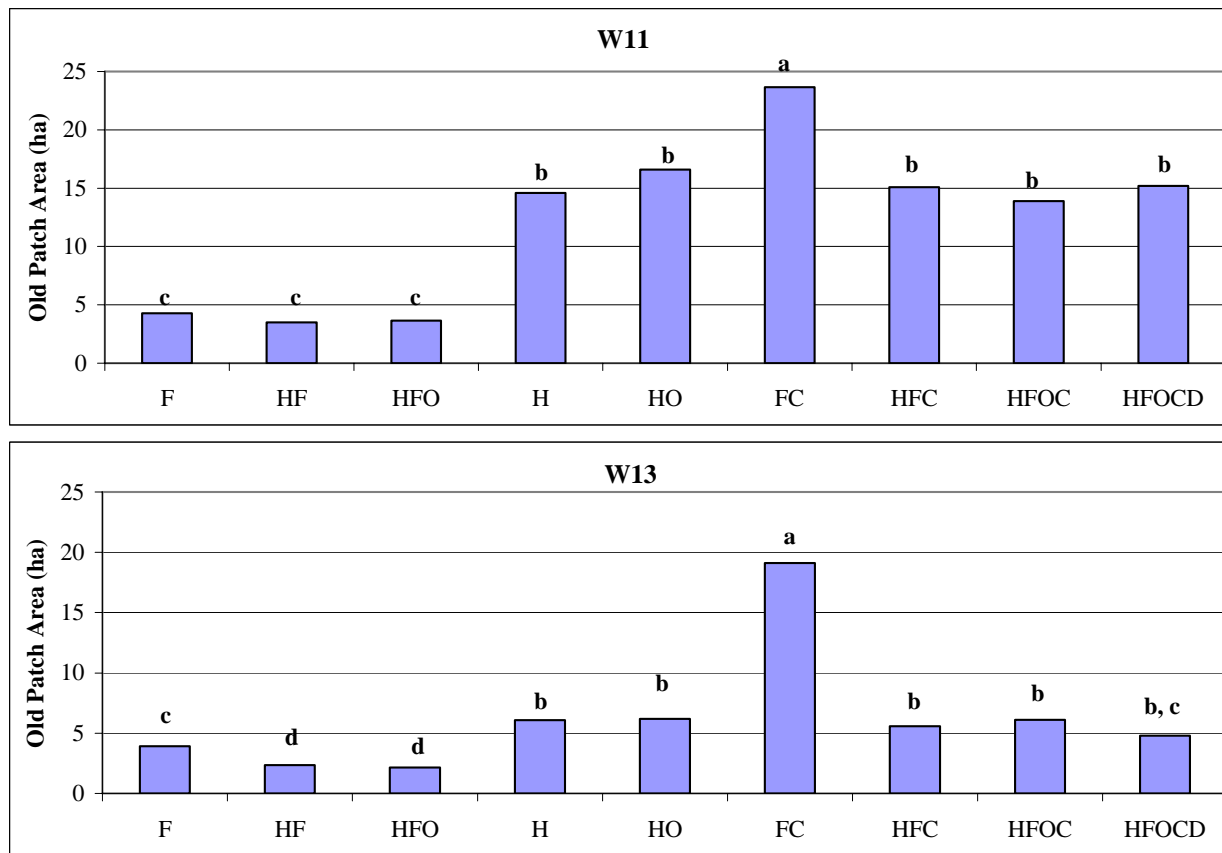
Histogram bars with the same letter are not significantly different at the 0.05 significance level.

**Figure 31. Mean patch sizes of old forest for the forest management area at the end of the 200-year simulation period, for each of the scenarios tested.**
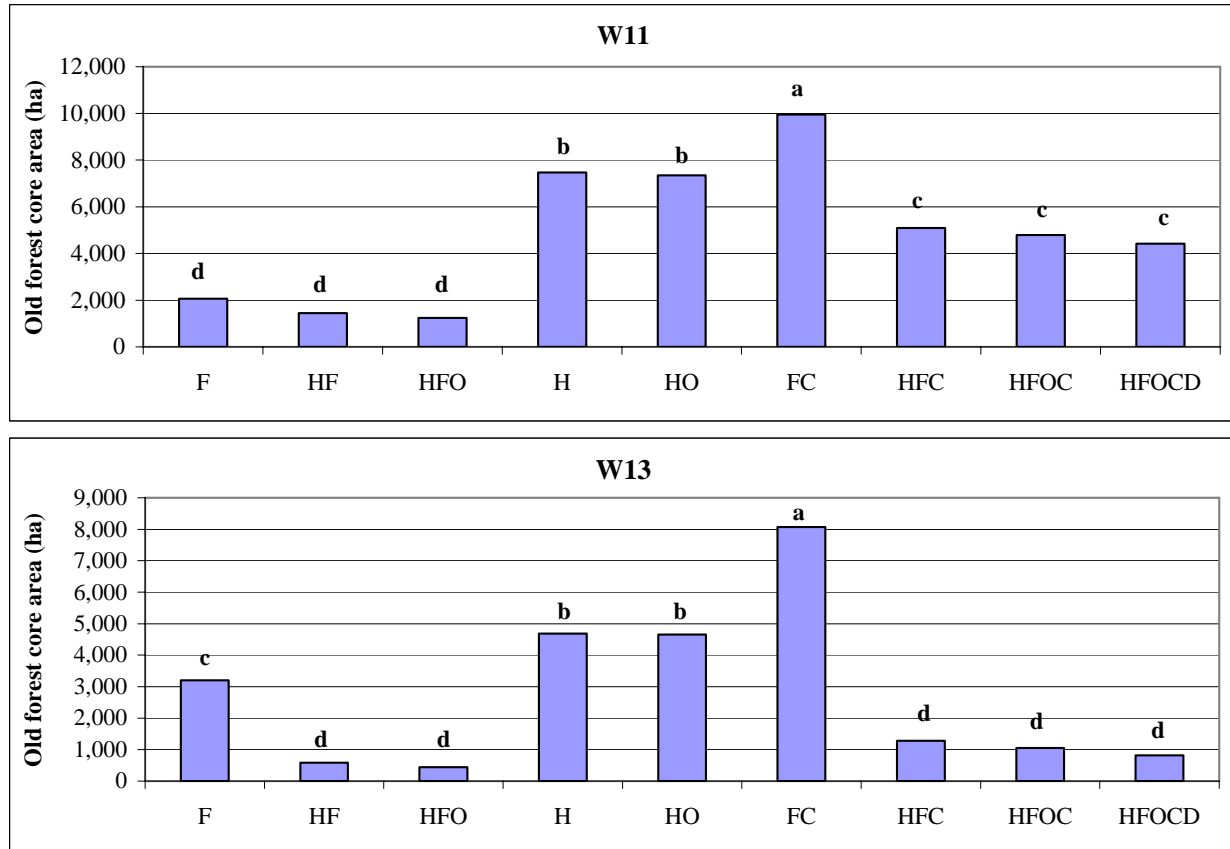
Histogram bars with the same letter are not significantly different at the 0.05 significance level.

**Figure 32. Total amount of core old forest for the forest management area at the end of the 200-simulation period, for each of the scenarios tested.**
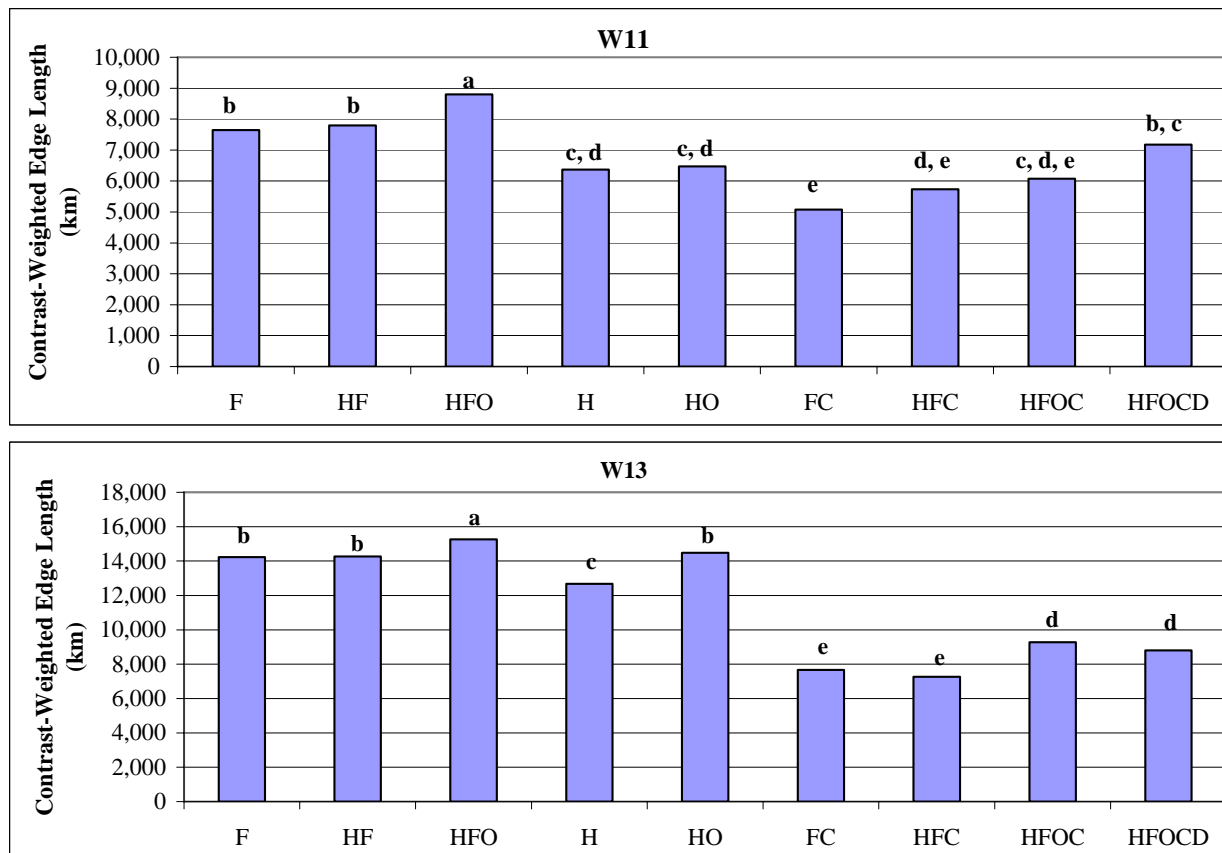
Histogram bars with the same letter are not significantly different at the 0.05 significance level.

**Figure 33. Contrast-weighted edge length for the forest management area, at the end of the 200-year simulation period, for each of the scenarios tested.**

## 3.2 Comparison of the harvest only (H) and harvesting and oil & gas scenario (HO)

Illustrations of the pattern of oil and gas activity are provided in Figure 34 and Figure 35.
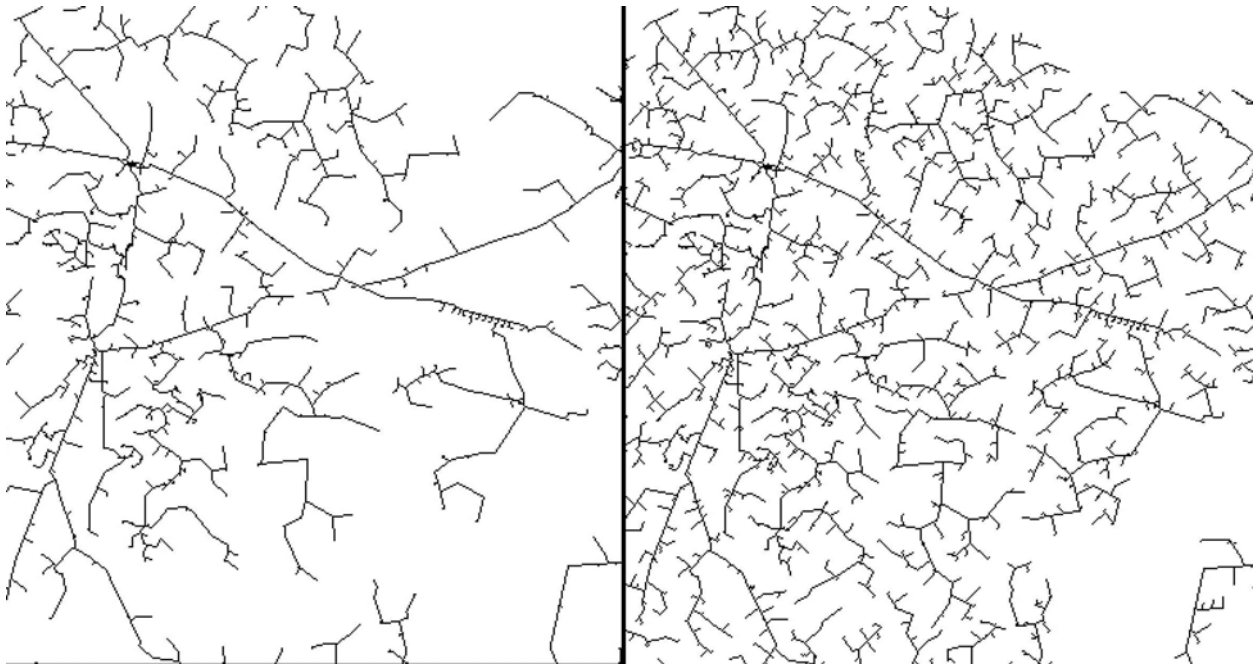
**Figure 34.** **Comparison of the initial pipeline network (left) and the pipeline network after 200 years of oil and gas development, for a section of the DFA (north-eastern quadrant of W13).**

The new wells can be seen to attach to existing spans of the pipeline network.
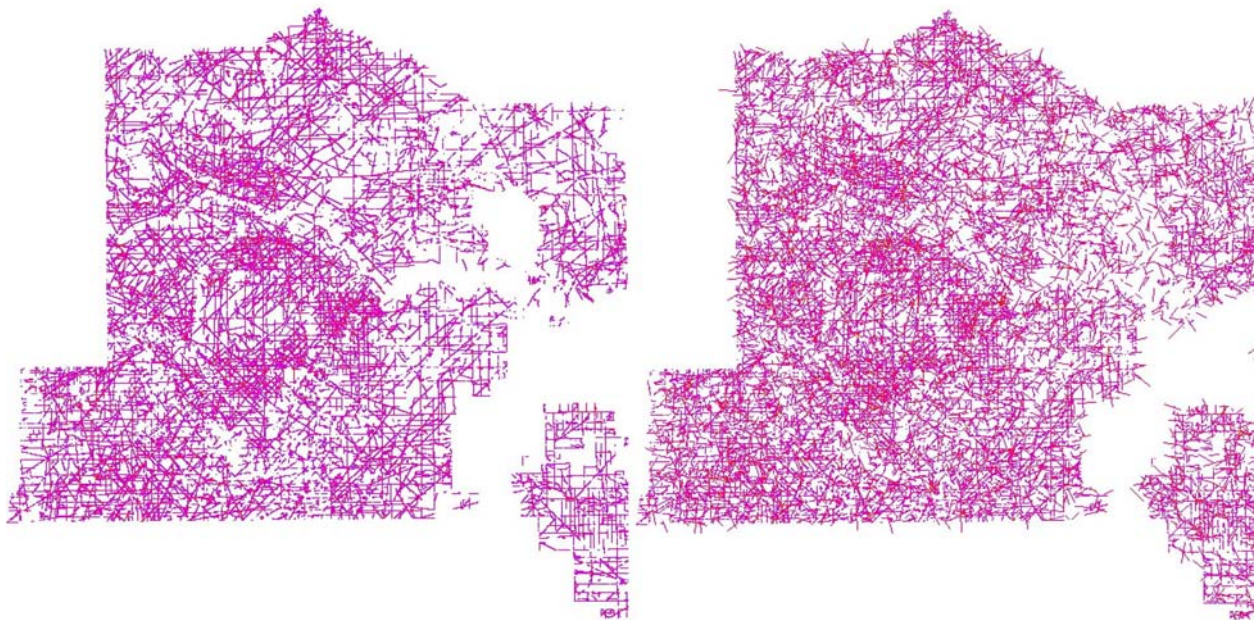


**Figure 35.** **Comparison of the area with seismic before (left) and after (right) 20 years of simulation in the APLM.**

**It should be noted that while the actual pattern of oil and gas (left) shows some amount of non-random clustering, the seismic that is superimposed onto this by the model (right) is completely random (though constrained to initiate within the DFA).**

The comparison of the H and HO scenarios yield some interesting insights into the impact of oil & gas impacts on the landscape. The most obvious impact that can be observed is the slow and continuous erosion of the forested land base. As can be seen in Figure 36 the non-forested area within the DFA increases from just over 45,000 ha to almost 62,000 ha, a 38% increase. The impact of this decrease in forested land can be observed in the gradually declining volume harvested in Figure 37. The annually harvested volume drifts from 550,000 cubic meters in the first year of simulation, to its composition-induced peak of 575,000 cubic meters at about year 75, and back down again by the end of the 200 year run; comparing this figure to Figure 27 highlights this loss in potential productivity. Also worth noting: given the assumption of 4 m wide seismic lines, seismic activity did not significantly contribute to the supply of timber.
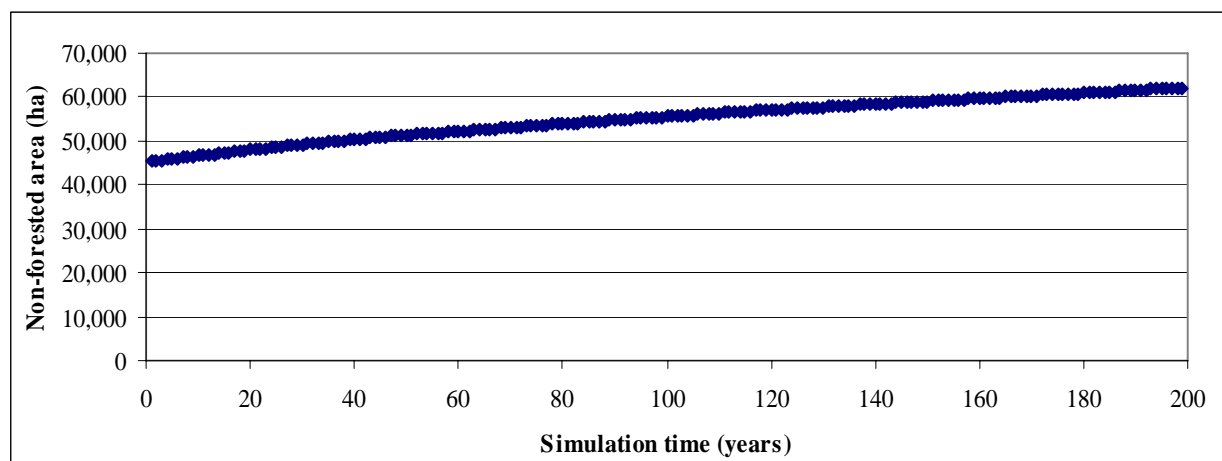


**Figure 36. Increase in the amount of non-forested land within the DFA, given oil & gas activity.**
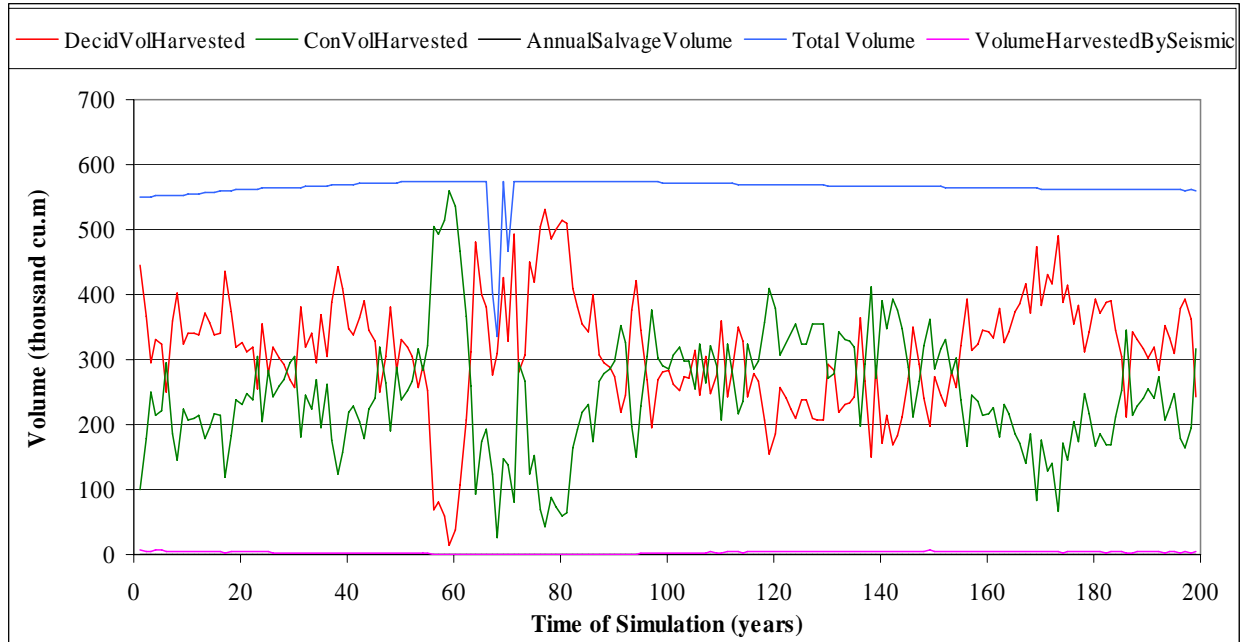
**Figure 37. Simulation model timber supply prediction under the harvesting and oil and gas scenario (HO).**

The BAP analysis of the outcomes of the H and HO scenarios more clearly illustrates some of the potential impacts of the combined impacts of harvesting and oil & gas activity. There is significantly more contrast-weighted edge under the HO than under the H scenario in W11 (Figure 33), and significantly smaller forest patches (Figure 38) and edge contrast (Figure 39) for W11 (the same trends can be observed for W13, but the differences are not significant). These indicators suggest that oil and gas activity has led to the fragmentation of the forested landscape. There is general agreement in the literature that fragmentation of the landscape, such as the fragmentation caused here by oil and gas, will have important implications for biodiversity in the future (Robinson et al. 1995, Harris 1988, Yahner 1988).
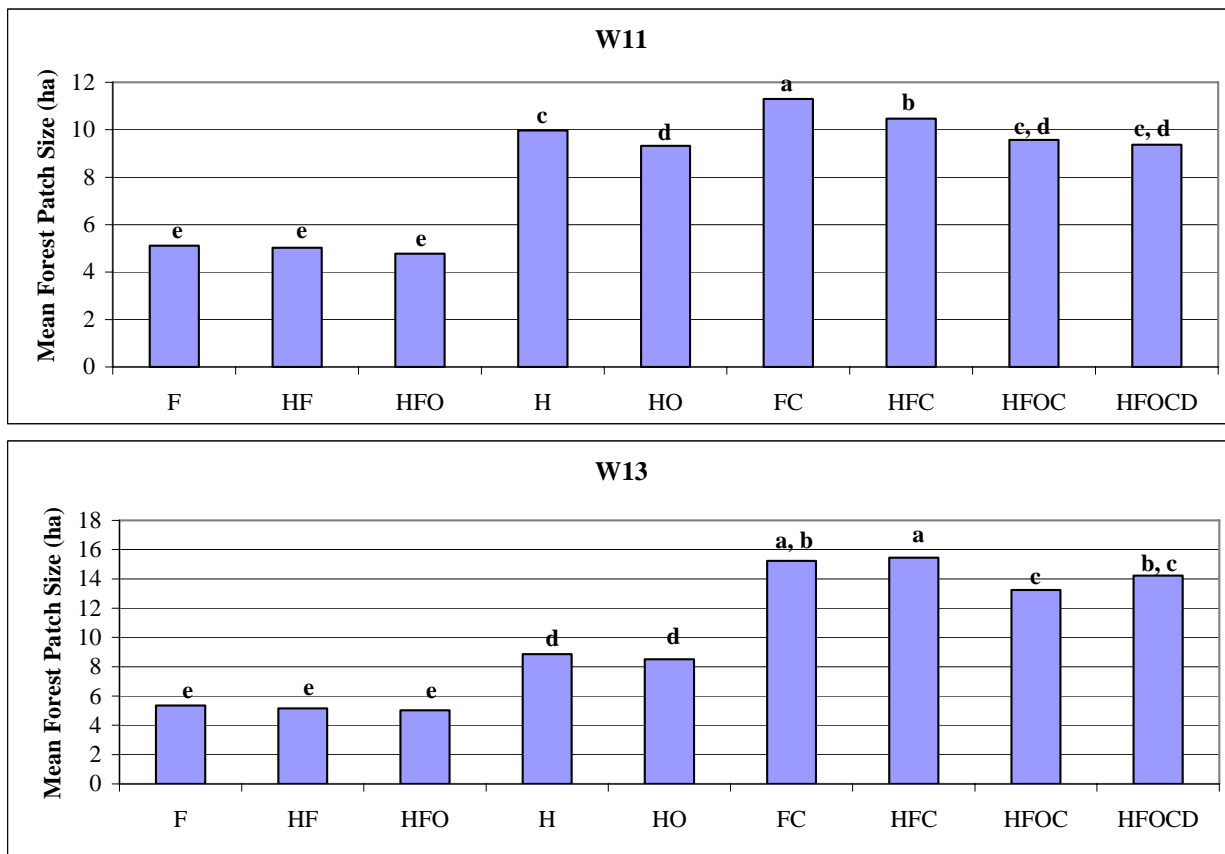
Histogram bars with the same letter are not significantly different at the 0.05 significance level.

**Figure 38. Mean patch sizes for all forest types for the forest management area, at the end of the 200-year simulation, for each of the scenarios tested.**
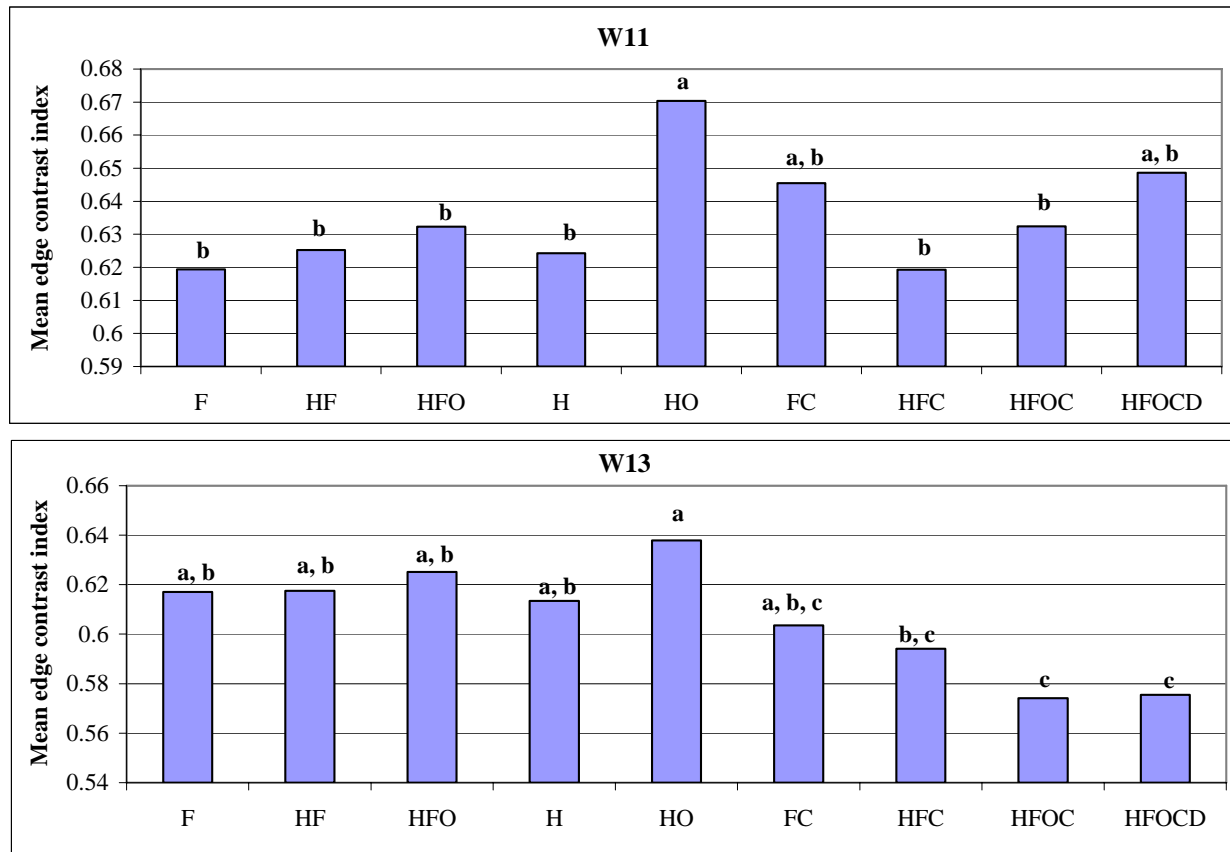
Histogram bars with the same letter are not significantly different at the 0.05 significance level.

**Figure 39. Mean edge contrast index for the forest management area, at the end of the 200-year simulation period, for each of the scenarios tested.**

Results from the HO scenario can only be seen as tentative. The most important reason for this is that the quality of the oil and gas data (data on the location, extent, and age of oil and gas features) that went into the oil and gas sub-model was inadequate, being limited to what could be obtained from the Alberta Vegetation Inventory (AVI) and Millar Western's own landuse update process. Attempts were made to gain access to additional information from government agencies and local oil and gas companies, but were unsuccessful. Data on oil & gas activity is available for purchase, but the costs and timelines were outside the scope of this project.

# 3.3 Comparison of the historical and climate change fire regimes

An initial test of the mechanistic fire model was run without any spatial constraints on fire spread; *i.e.*, fires were allowed to spread freely over an 8 hour period without any non-forested cells to hinder the spread of fire. Twelve hundred and eighty simulations were run with and without climate change (CC), over a range of fuel and weather conditions. Fuel conditions were drawn from FORECAST runs 1 to 40 of Duchesneau et al. (2007), thus incorporating all 40 FORECAST composition classes at age 40 and 80. Sixteen weather streams were pulled from the first year of the 30-year historical and CC adjusted fire weather streams (there were 16 townships with fire events that year). This test showed large differences between the behaviour of fire with and without CC. Results show that, over all 1,280 combinations of fuel and weather tested, fires burn 26% more area on average under CC than under historical weather conditions. Graphs of the distributions of fire event sizes are shown in Figure 40.
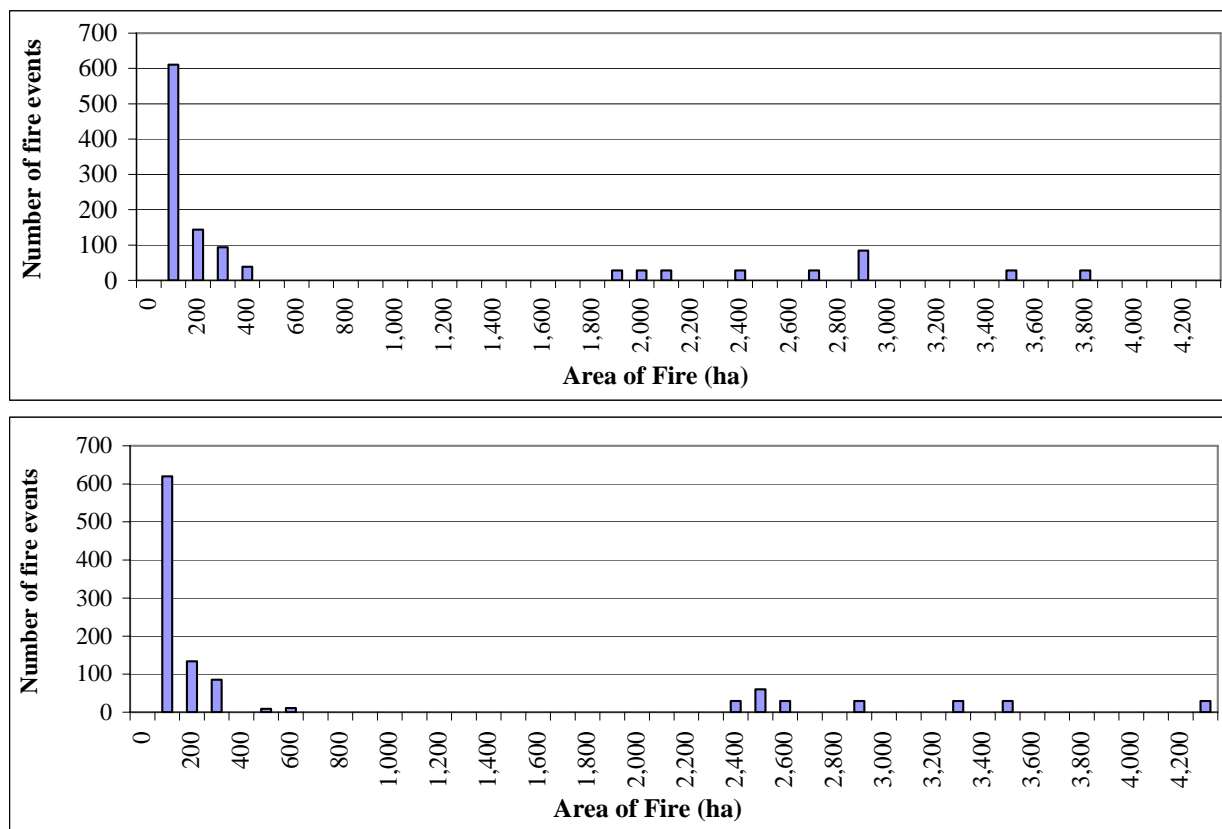


**Figure 40. Fire size distributions for the single fire tests run without (above) and with (below) climate change.**

The mechanistic fire model, having been calibrated for the landscape and the historical fire record (see section 2.4.1- The mechanistic fire sub-model), was set to burn over the DFA using the CC adjusted fire weather streams for the 200-year simulation period. Data was compiled and compared for the non CC and CC conditions. Results show considerably less of a difference

between the two than in the case of the spatially unconstrained burn, described in this section, above.  It would appear that while the spread rates are higher under conditions of CC, fires modeled over the DFA are limited in their expansion by the permeability of the landscape.  Over the course of the simulation, the CC scenario burned approximately 10% more area than the no CC conditions, for an average annual area burned of 5,443 ha, compared to 4,944 ha under non CC.  Under CC conditions, the largest fire that occurred was over 114,000 ha (Figure 41), while under non CC conditions the largest fire was just over 77,000 ha (Figure 42), an increase of almost 50%.
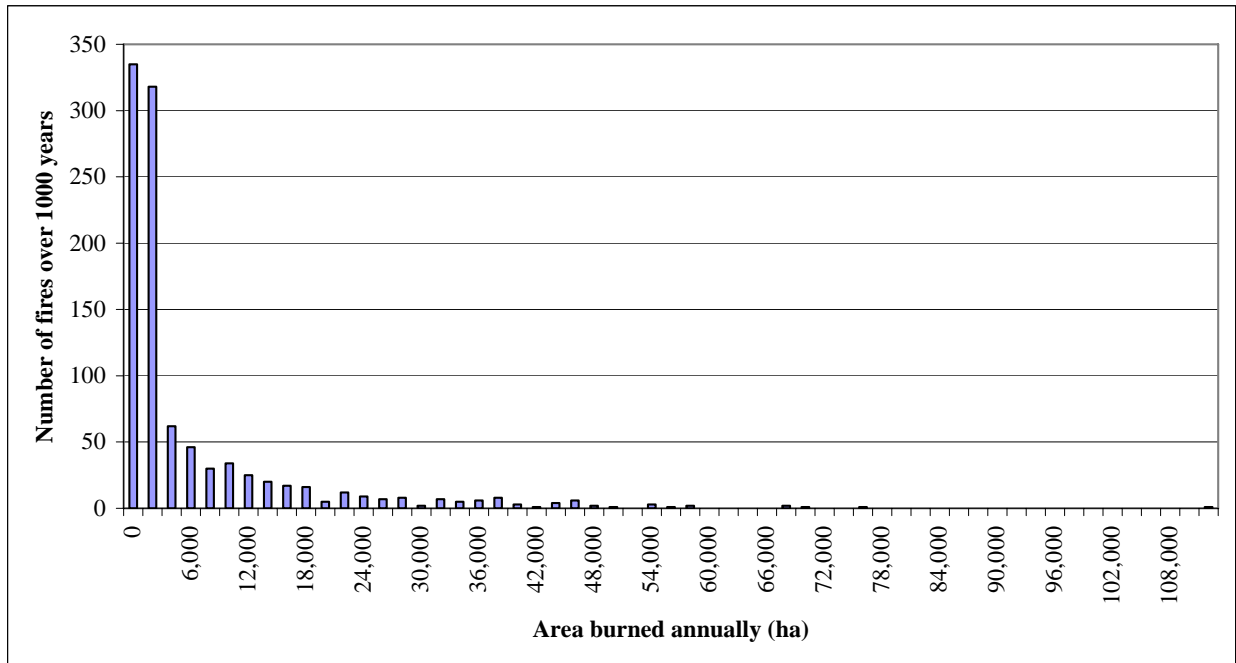


**Figure 41. Distribution of area burned annually for the 5 repetitions of the 200-year simulations, with climate change.**
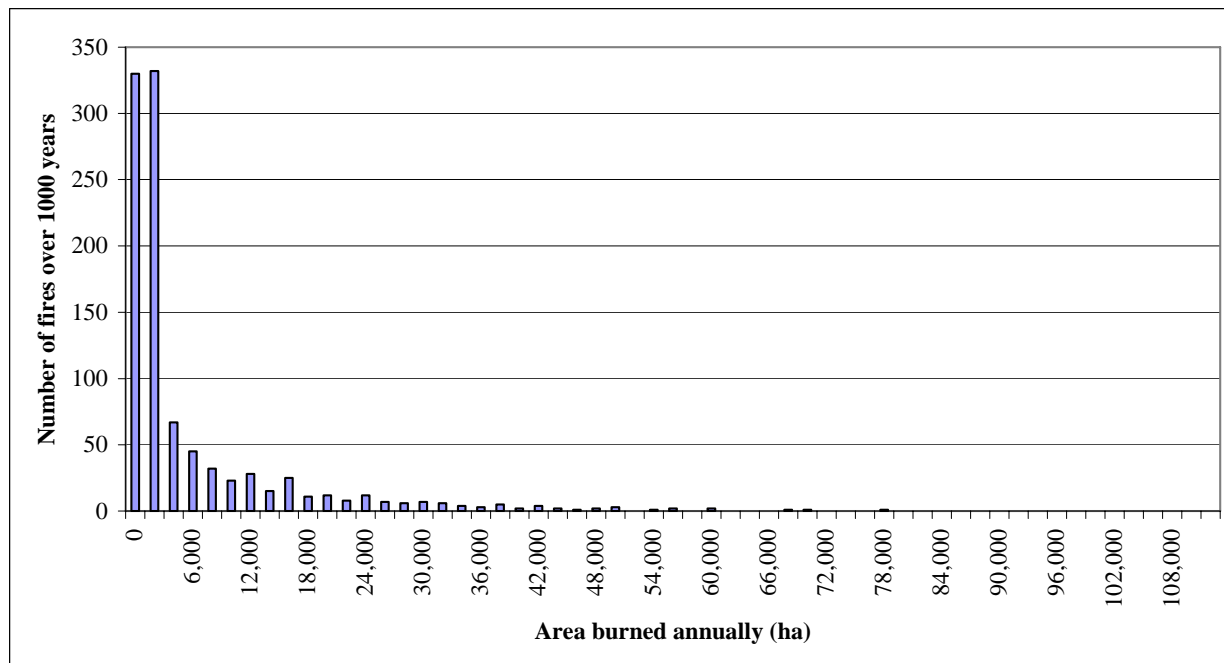
**Figure 42. Distribution of area burned annually for the 5 repetitions of the 200-year simulations, without climate change.**

A comparison of the empirical and mechanistic fire sub-models yields other observations of interest.  The mechanistic fire model burns in much larger patches and yields more inter-annual variability than the empirical fire model.  For the 5 runs of 200 years, we can observe that with the empirical sub-model, the largest area burned in a single year is almost 33,000 ha (Figure 43), while with the mechanistic sub-model, this value surpasses 77,000 ha (Figure 42).  Also, an analysis of the number of fire events per year, again over the 5 repetitions, indicates that with the empirical sub-model, there is a mean of 6.4 fires annually, while under the mechanistic sub-model only 1.3 fires are initiated annually (the former being the result of reproducing the fire event history for active townships, as described in the section "The mechanistic fire sub-model").  BAP analysis illustrates that there are significantly larger patches (Figure 38) and less contrast-weighted edge (Figure 33) under all scenarios applying the mechanistic fire model than scenarios applying the empirical fire model.  Also, since the mechanistic sub-model responds to elevation and wind direction as well as fuel type, the distribution of age classes over the landscape follows topography and is influenced by the dominant winds (here, from the west).
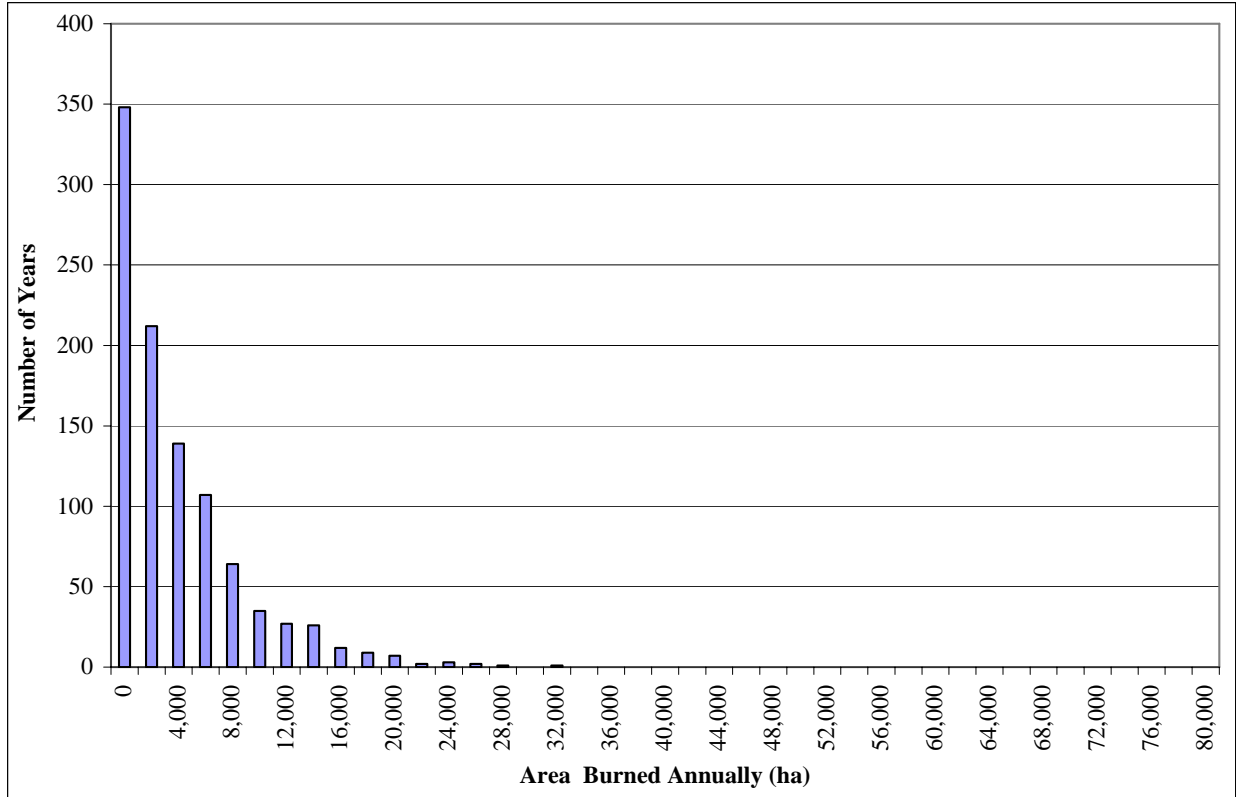
**Figure 43. Distribution of area burned annually with the empirical fire model.**
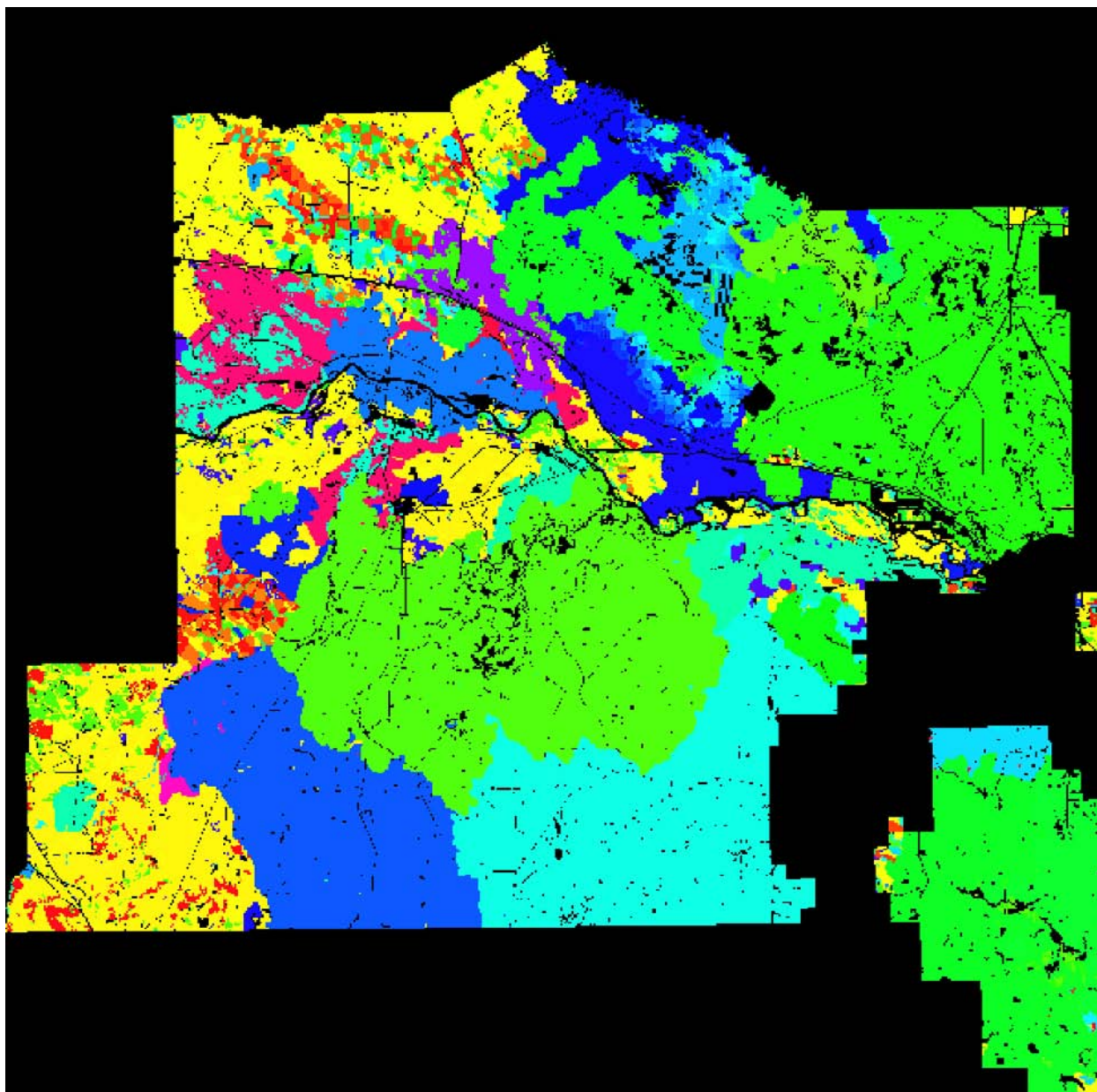
**Figure 44. Bap age for W13 under the mechanistic fire model, at the end of the 200 year simulation period, with the fire only scenario.**

The impact of forest fragmentation and initial composition on fire patch size can be observed in this figure, the Athabasca River acts as an impermeable boundary to fire, fire patches never spanning the river. Also, the patchy pattern in the upper left quadrant (Figure 44) corresponds closely to the pattern of recently harvested stands at the outset of simulation (Figure 45).
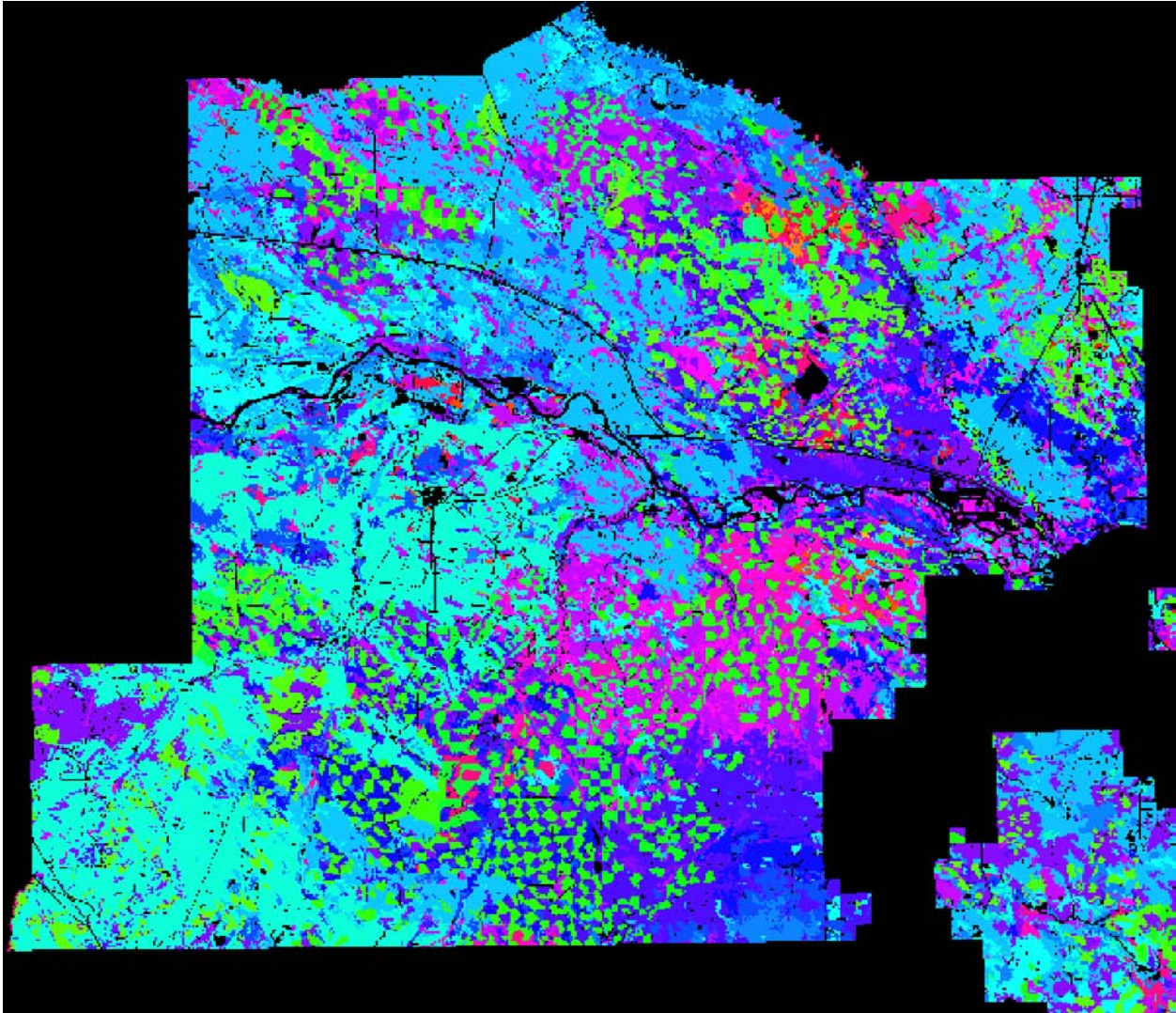
**Figure 45.  Initial BAP age.**

# 3.4  Interactions among fire, oil & gas, and harvesting

There is evidence to suggest that there is an interaction among fire, oil & gas, and harvesting. Indeed, BAP analysis indicates that, for W13, there is no significant difference in the amount of contrast-weighted edge length between the F, HF, and HO scenarios, which in itself suggests that these scenarios are comparable in terms of the amount of fragmentation they generate.  However, there is significantly more edge within the landscape when all three disturbance factors are active (Figure 33).  Analysis of mean edge contrast index (Figure 39), a global measure of contrast among the patches within the landscape, suggests that the differences in contrast-weighted edge length stem more from a difference in quantity of edge than from the contrast between patches. These trends are similar for W11.  It would seem that the creation of edge (that is, delineation between contrasting types of forest cover) by oil & gas activity becomes more pronounced when the landscape is under the combined pressures of fire and harvesting.

## 3.5   Comparison of fire and harvesting without (HF) and with (HFC) climate change

Under the climate change assumptions applied in the stand scale work (Duchesneau et al. 2007), forest ecosystems, on average, produced more merchantable volume.  The mean volumes at 85 years for the Group 1 simulations in FORECAST (the first 40 of 200 runs) under the no CC assumption is 121.2 cubic meters, while under CC assumptions, the average volume is 143.6 cubic meters, a difference of almost 20%.  However, as we model the interactions among CC, harvesting and fire, we can see that the APLM harvests, on average, significantly less volume annually under CC.  There is on average roughly 434,000 cubic meters harvested annually under the no CC assumption, and slightly less than 419,000 cubic meters under the CC scenario.  In terms of the reference harvest target, this translates into 92 shortfalls over the simulation time horizon for HF, and 111 for HFC.  This is in large part due to the increase in area burned (just under 4,900 ha annually for HF, and almost 6,500 ha under HFC).

It is worth noting here that the mechanistic fire model burns considerably more area when harvesting is active than when it is not active.  Under the FC scenario, there is an average of 5,443 ha burned annually, against almost 6,500 ha under the HFC scenario, as mentioned.  This must be the result of either: 1) the a re-arrangement of the fuels within the landscape by the harvesting sub-model such that the landscape is more permeable to fire; or 2) a shift in the composition of the landscape towards more flammable fuels (for the years immediately following harvesting, when stands are in the regenerating phase of development and dominated by herbaceous cover) under the HFC scenario.  Analysis of the data from the test of the mechanistic fire sub-model calibration indicates that the fuel types established shortly after harvesting (types 16 and 17) do indeed lead to higher spread rates than other fuel types.  To be certain, we would need to modify the model to (*i*) track the fuels that are encountered by the mechanistic fire model and (*ii*) the cause of extinction of fire events.

## 3.6   Comparison of fire, harvest, and oil & gas scenarios without (HFO) and with (HFOC) climate change

The addition of CC to the HFO scenario leads to dramatically different results.  Given the assumption of CC, the area that is burned annually is far greater under the FHOC scenario (at a mean value of 6,347 ha) than under the HFO scenario (with a mean of 4,743 ha), a 34% increase in area burned.  The result of this is, among other effects, that only 357,000 cubic meters are harvested annually on average, against the HFO scenario's 420,000 cubic meters, a 15% drop in harvested volume.  Once again, the addition of climate change effects significantly reduces, on average and over time, the mean amount of harvestable volume, despite productivity under CC that is on average greater than the productivity under the current climate (Duchesneau et al. 2007). This once again illustrates the value of integrating multiple disturbance agents. If we believe that CC is imminent, then we must take its projected effects into account.

It is worth noting that there is a slight drop in the area burned from the HFC to the HFOC.  As discussed in the section comparing fire with and without climate change, results suggest that the

disposition of non-forested area through the DFA limits the impact of wildfire. This is likely what is happening under the HFOC scenario, where there is more non-forested area than under the HFC scenario. This non-forested area appears to be acting as a barrier, especially since the non-forested that originates from oil & gas activity is linear rather than patchy, and thus more difficult to circumvent. Meanwhile, anecdotal evidence from the Swan Hills and Windfall Burn fires suggests that spring fires (that occur at a time when grasses are cured and more flammable) can travel quickly along grassy oil and gas right-of-ways. In order to replicate this behaviour, it would have been necessary to assign "open" fuel types to oil and gas features in the APLM and allow fires to spread along these non-forested features (at the moment, fires are only allowed to spread into forested cells).

# 3.7 Comparison of the HFOCD scenario with other scenarios

The scenario that led to the greatest area burned is clearly the HFOCD scenario. This scenario, with its climate change conditions and additional fire events (as described in Section 2.2.10 - Analysis of human population and fire data, and generation of new fire events, based on the work of Loreto and McCormack (2006)) led to an average area burned annually of over 7,000 ha annually, compared to the FC scenario and its average 5,443 ha burned annually. This represents an increase of almost 29% attributable to the impact of human populations on the incidence of fire. It is of interest to note that while the number of fire events almost tripled (Table 8), the area burned did not increase proportionally. This underlines, once again, the importance of spatial process-based modeling when seeking to project the implications of changes in the behaviour of disturbance agents. Thus, under the HFOCD scenario, there is the lowest mean annual harvest rate, and the greatest number of shortfalls. Under this scenario, the model harvested only 336,000 cubic meters annually on average. This represents a 42% drop in the average volume harvested, as compared to the harvesting only scenario. As mentioned previously, we observe a decrease in the average volume harvested despite the fact that the work of Duchesneau et al. (2007) suggests, on average, an increase in the productivity of ecosystems for the DFA. We present the annual volume harvested for all scenarios that involve harvesting for the sake of comparison (Figure 46).
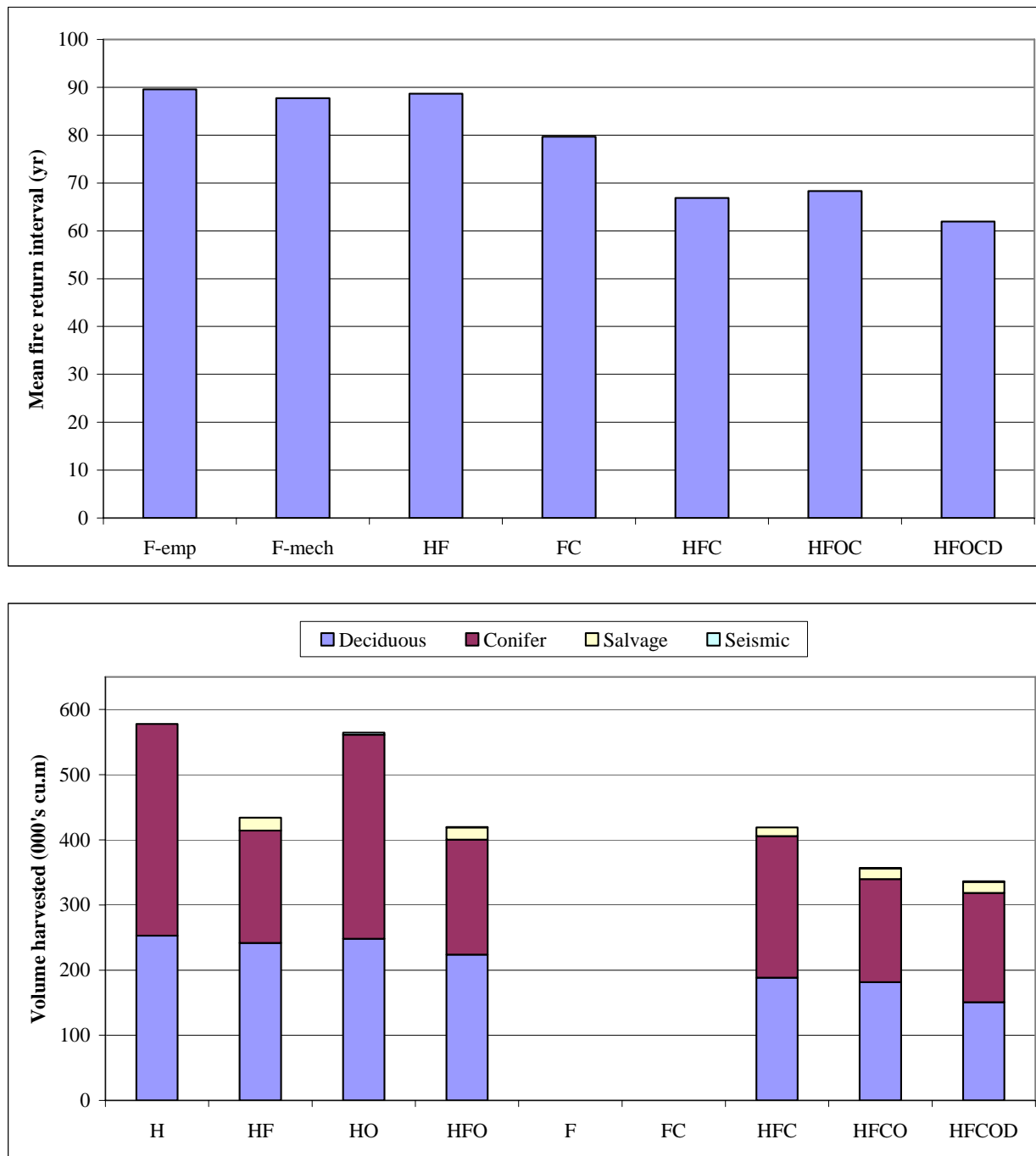
**Figure 46. Comparison of mean fire return interval (above) and mean volume harvested annually (below) for the various simulations.**

# 3.8 Independent contribution of each disturbance agent

A full-factorial simulation experiment was run in order to quantify the independent contribution of each disturbance agent on the simulated forest landscape. This type of analysis tests every

possible combination of the levels of each factor, in order to statistically derive the impact of each factor (here the disturbance agents) taken independently.  For this exercise, a doubling of oil and gas disturbance rates was included. Thus, simulations were run with and without harvesting, fire, and demographic and climate change (thus, 2 levels for each factor), and with oil and gas (2 levels) and without. This design yielded a total of 48 simulation runs, each run for 200 years from the same initial condition as that applied in the sequential cumulative impacts analysis, described above.  Table 10 presents all 48 runs and their associated indicator values. The results vary somewhat from those previously, since an entirely new set of runs was executed in order to generate this data.  Due to the volume of output data, BAP analysis was not run on these simulations' output.  The variables that were retained for analysis are the following:

- the amount of area with a BAP age greater than 100 years, at the end of simulation

- the fire return interval for the simulation

- mean volume harvested annually over the simulation

- the number of harvesting shortfalls (where the harvest target is not met) for the simulation

- the mean annual amount of volume salvaged per simulation

- the area forested at the end of simulation

- the mean annual volume harvested by seismic over the course of simulation

- the number of regeneration failures that occurred during the course of simulation.

The results from this full factorial experiment are presented in detail in Table 11.

**Table 10. Values of the indicator variables for all 48 of the runs carried out as part of the full factorial experiment [7].**

| Run | Fire | Harvest | OilAndGas | CC | Demographic | Area above 100 years (ha) | Fire Return Interval (years) | Volume Harvested (cubic m) | ShortFalls per Run (count) | Salvaged Volume (cubic m) | Area Forested (ha) | Volume from Seismic (cubic m) | Regen Failures (count) |
|---|---|---|---|---|---|---|---|---|---|---|---|---|---|
| 1 | 0 | 0 | 0 | 0 | 0 | 321764 | . | . | . | . | 433559 | . | . |
| 2 | 0 | 0 | 0 | 0 | 1 | 321764 | . | . | . | . | 433559 | . | . |
| 3 | 0 | 0 | 0 | 1 | 0 | 321764 | . | . | . | . | 433559 | . | . |
| 4 | 0 | 0 | 0 | 1 | 1 | 321764 | . | . | . | . | 433559 | . | . |
| 5 | 0 | 0 | 1 | 0 | 0 | 309061 | . | . | . | . | 416431 | 12405 | . |
| 6 | 0 | 0 | 1 | 0 | 1 | 309030 | . | . | . | . | 416452 | 12325 | . |
| 7 | 0 | 0 | 1 | 1 | 0 | 309116 | . | . | . | . | 416777 | 12359 | . |
| 8 | 0 | 0 | 1 | 1 | 1 | 309207 | . | . | . | . | 416678 | 12300 | . |
| 9 | 0 | 0 | 2 | 0 | 0 | 301183 | . | . | . | . | 405951 | 23241 | . |
| 10 | 0 | 0 | 2 | 0 | 1 | 301275 | . | . | . | . | 405943 | 23251 | . |
| 11 | 0 | 0 | 2 | 1 | 0 | 301110 | . | . | . | . | 405828 | 23286 | . |
| 12 | 0 | 0 | 2 | 1 | 1 | 301579 | . | . | . | . | 406001 | 23245 | . |
| 13 | 0 | 1 | 0 | 0 | 0 | 148178 | . | 578211 | 3 | . | 433559 | . | . |
| 14 | 0 | 1 | 0 | 0 | 1 | 149167 | . | 577742 | 3 | . | 433559 | . | . |
| 15 | 0 | 1 | 0 | 1 | 0 | 151127 | . | 582657 | 4 | . | 433559 | . | . |
| 16 | 0 | 1 | 0 | 1 | 1 | 151150 | . | 582223 | 4 | . | 433559 | . | . |
| 17 | 0 | 1 | 1 | 0 | 0 | 141272 | . | 564964 | 3 | . | 416684 | 3340 | . |
| 18 | 0 | 1 | 1 | 0 | 1 | 142076 | . | 565400 | 3 | . | 416723 | 3322 | . |
| 19 | 0 | 1 | 1 | 1 | 0 | 144360 | . | 568790 | 4 | . | 416639 | 3478 | . |
| 20 | 0 | 1 | 1 | 1 | 1 | 144458 | . | 568891 | 4 | . | 416456 | 3519 | . |
| 21 | 0 | 1 | 2 | 0 | 0 | 135981 | . | 554960 | 3 | . | 406157 | 6103 | . |
| 22 | 0 | 1 | 2 | 0 | 1 | 135996 | . | 555485 | 4 | . | 406263 | 6084 | . |
| 23 | 0 | 1 | 2 | 1 | 0 | 137737 | . | 559453 | 5 | . | 405945 | 6505 | . |
| 24 | 0 | 1 | 2 | 1 | 1 | 140029 | . | 559480 | 5 | . | 405945 | 6505 | . |
| 25 | 1 | 0 | 0 | 0 | 0 | 143746 | 84.3 | . | . | . | 433559 | . | 14298 |
| 26 | 1 | 0 | 0 | 0 | 1 | 141848 | 81.0 | . | . | . | 433559 | . | 3714 |
| 27 | 1 | 0 | 0 | 1 | 0 | 127118 | 67.1 | . | . | . | 433559 | . | 14558 |
| 28 | 1 | 0 | 0 | 1 | 1 | 118322 | 67.6 | . | . | . | 433559 | . | 18160 |
| 29 | 1 | 0 | 1 | 0 | 0 | 141700 | 98.0 | . | . | . | 416662 | 6855 | 6856 |
| 30 | 1 | 0 | 1 | 0 | 1 | 122936 | 79.3 | . | . | . | 416662 | 6031 | 5313 |
| 31 | 1 | 0 | 1 | 1 | 0 | 168430 | 87.5 | . | . | . | 416649 | 5958 | 4487 |
| 32 | 1 | 0 | 1 | 1 | 1 | 178579 | 97.6 | . | . | . | 416563 | 7301 | 2136 |
| 33 | 1 | 0 | 2 | 0 | 0 | 149671 | 108.7 | . | . | . | 405867 | 13057 | 3293 |
| 34 | 1 | 0 | 2 | 0 | 1 | 165265 | 95.8 | . | . | . | 405822 | 13538 | 1749 |
| 35 | 1 | 0 | 2 | 1 | 0 | 144738 | 87.9 | . | . | . | 405834 | 12290 | 4372 |
| 36 | 1 | 0 | 2 | 1 | 1 | 138806 | 82.4 | . | . | . | 405878 | 13135 | 3579 |
| 37 | 1 | 1 | 0 | 0 | 0 | 62045 | 74.8 | 399503 | 93 | 22413 | 433559 | . | 11590 |
| 38 | 1 | 1 | 0 | 0 | 1 | 51188 | 66.9 | 354210 | 123 | 14861 | 433559 | . | 11915 |
| 39 | 1 | 1 | 0 | 1 | 0 | 54135 | 68.6 | 345769 | 133 | 14645 | 433559 | . | 11014 |
| 40 | 1 | 1 | 0 | 1 | 1 | 57967 | 67.3 | 361873 | 124 | 19013 | 433559 | . | 12215 |
| 41 | 1 | 1 | 1 | 0 | 0 | 61960 | 89.2 | 403615 | 89 | 15465 | 416602 | 829 | 3511 |
| 42 | 1 | 1 | 1 | 0 | 1 | 54169 | 70.5 | 363444 | 115 | 15359 | 416358 | 728 | 9352 |
| 43 | 1 | 1 | 1 | 1 | 0 | 56614 | 62.6 | 349940 | 120 | 19987 | 416755 | 751 | 14583 |
| 44 | 1 | 1 | 1 | 1 | 1 | 46762 | 58.8 | 325822 | 126 | 23018 | 416548 | 635 | 20251 |
| 45 | 1 | 1 | 2 | 0 | 0 | 61753 | 79.3 | 345940 | 124 | 17961 | 406168 | 1546 | 8729 |
| 46 | 1 | 1 | 2 | 0 | 1 | 54429 | 72.0 | 336942 | 122 | 20559 | 405918 | 1448 | 9745 |
| 47 | 1 | 1 | 2 | 1 | 0 | 53465 | 79.6 | 371118 | 124 | 12582 | 405959 | 1595 | 9256 |
| 48 | 1 | 1 | 2 | 1 | 1 | 48588 | 67.9 | 346716 | 118 | 20084 | 405754 | 1339 | 9358 |

The data was analyzed as a standard ANOVA; the threshold probability applied to determine the significance of a factor or difference was 0.05. SNK (Student-Newman-Keuls) corrections were

---

[7] Values shown are the annual mean, a sum over all years, or the value after 200 years of simulation; see text for details. Levels for disturbance agents are 0 for off and 1 for on; for oil and gas 2 is double the base amount of oil and gas disturbance. Absence of data indicates that the indicator is not output for the run in question (e.g., area burned when fire is off).

applied to the *a posteriori* multiple comparison of means (SAS Institute 1999). A summary table of results is presented in Table 11.

**Table 11.  Full factorial summary**

| | Level | Area above 100 years (ha) | Fire Return Interval (years) | Volume Harvested (cubic m) | ShortFalls per Run (count) | Salvaged Volume (cubic m) | Area Forested (ha) | Volume from Seismic (cubic m) | Regen Failures (count) |
|---|---|---|---|---|---|---|---|---|---|
| Fire | Off | **227090** | n.a. | **568188** | **3.75** | n.a. | 418723 | **11329** | n.a. |
| | On | **100176** | 78.95 | **358741** | **117.58** | 17996 | 418686 | **5440** | 8918 |
| Harvesting | Off | **227907** | 86.44 | n.a. | n.a. | n.a. | 418686 | **13786** | **6876** |
| | On | **99359** | 71.45 | 463464 | 60.67 | 17996 | 418723 | **2983** | **10960** |
| Oil And Gas | Off | 165190 | **72.21** | 472773 | 60.88 | 17733 | **433559** | n.a. | **12183** |
| | Single | 164983 | **80.46** | 463858 | 58.00 | 18457 | **416602** | **5758** | **8311** |
| | Double | 160725 | **84.19** | 453762 | 63.13 | 17797 | **405952** | **11011** | **6260** |
| Climate Chan | Off | 163644 | **83.31** | 466701 | 57.08 | 17770 | 418714 | 8381 | 7505 |
| | On | 163622 | **74.59** | 460228 | 64.25 | 18221 | 418695 | 8388 | 10331 |
| Demographic | Off | 164501 | **82.29** | 468743 | 58.75 | 17175 | 418724 | 8350 | 8879 |
| | On | 162765 | **75.61** | 458186 | 62.58 | 18816 | 418685 | 8419 | 8957 |

Result of the factorial experiment, showing summary values of key indicators from APLM output, for each level of the disturbance agents. Means shown in bold identify the indicators on which the disturbance agent had a significant impact. Certain results, such as fire return interval when fire is off, were not applicable (indicated by "n.a."). A table showing the percent change in the indicator variables that result from the disturbance agent being turned on is shown in Table 12.

**Table 12.  Full factorial percent summary. The percent change which results from a disturbance agent being turned on for simulation with the APLM[8].**

| | Level | Area above 100 years (ha) | Fire Return Interval (years) | Volume Harvested (cubic m) | ShortFalls per Run (count) | Salvaged Volume (cubic m) | Area Forested (ha) | Volume from Seismic (cubic m) | Regen Failures (count) |
|---|---|---|---|---|---|---|---|---|---|
| Fire | On | **-55.89** | n.a. | **-36.86** | 3035.55 | n.a. | -0.01 | **-51.98** | n.a. |
| Harvesting | On | **-56.40** | **-17.34** | n.a. | n.a. | n.a. | 0.01 | **-78.36** | 59.39 |
| Oil And Gas | Single | -0.13 | **11.43** | -1.89 | -4.72 | 4.09 | **-3.91** | n.a. | -31.78 |
| | Double | -2.58 | **4.64** | -2.18 | 8.84 | -3.58 | **-2.56** | 91.21 | -24.68 |
| Climate Change | On | -0.01 | **-10.47** | -1.39 | 12.55 | 2.54 | 0.00 | 0.07 | 37.64 |
| Demographic Change | On | -1.06 | **-8.12** | -2.25 | 6.52 | 9.55 | -0.01 | 0.83 | 0.88 |

---

[8] All values given are percent change relative to the agent being turned off, with the exception of the doubling of oil and gas activity, which is expressed as a percent of the single rate of oil and gas activity. Values in bold indicate a significant effect of the agent on the indicator variable.

### 3.8.1    Impacts on age class structure

Results indicate that fire and harvesting have comparable impacts on the amount of forested area with BAP ages greater than 100 years.  This is to be expected since fire return interval (roughly 80-90 years) and rotation period (Table 6) are roughly the same in this area, and so harvesting and fire have a similar effect on the age class distribution. The mean rotation period for the DFA is somewhat longer that the mean fire return interval, but since harvesting in the model targets older stands first, harvesting has an impact on older age classes that is as important as fire with a shorter fire return interval.

### 3.8.2    Impacts on fire return interval

While harvesting, climate change, and demographic change shortened the fire return interval (by increasing the mean area burned annually), oil and gas activity lengthened the fire return interval (Table 12). Harvesting had the greatest impact; as has been discussed previously, harvesting increases the prevalence of the open fuel types in the model (even if only for a number of years), and these fuel types are considerably more flammable than other fuel types.  Climate change is the second most important factor that decreases this indicator, decreasing the fire return interval by more than 10 percent. Finally, demographic change, because it increases the number of anthropogenic fires annually, decreases the fire return interval by over 8 percent.  An unexpected result from the modeling work is the lengthening of the fire return interval by the oil and gas activity. Indeed, since we have applied a mechanistic fire model to these simulations, and since this model is sensitive to fragmentation of the landscape (fire spread is halted by the absence of fuel in immediately adjacent cells), it is in the end no surprise that by fragmenting the landscape with well sites and pipelines, the oil and gas sub-model reduces the mean area burned annually. It should be noted that in these results, the effect is not cumulative as a doubling of oil and gas activity can be seen to increase the fire return interval by only another 4.6%, and in fact, both the single and double rate of oil and gas are significantly different from no oil and gas, but the two oil and gas levels are not significantly different from each other.

### 3.8.3    Impacts on harvesting indicators

The indicators related to harvesting show that fire, of all the disturbance agents tested, has the greatest impact on harvested volume.  Indeed, volume harvested and the volume that is harvested by seismic decrease significantly (by almost 40% and over 50%, respectively) and the number of shortfalls in supply increase significantly (by a multiple of 30) when fire is turned on in the simulations.  Results thus indicate that, on average, there are 117 out of 200 years when the harvest target cannot be reached.  This, clearly, has important implications for the forest industry. It should also be noted that harvesting decreases the amount of volume that is harvested by seismic activity (given constant seismic activity), since the volume of wood that is harvested by seismic is no longer above minimum harvest age. Fire also has a similar impact on the volume harvested by seismic.  The volume that is harvested by seismic almost doubles when oil and gas doubles, but this effect is strictly due to the increased seismic activity (since the length of seismic laid down in a year is proportional to the number of wells that is laid down.

## 3.8.4    Impacts on indicators of forest health

Given the structure of the APLM, oil and gas is the only process that can influence the area forested in the model. Under the simple rate of oil and gas activity, the area forested decreases by almost 4%, while under the double rate the forest area decreases by another 2.6%. The most interesting result for this class of indicator is the impact of harvesting and oil and gas on the mean number of regeneration failures annually. The results suggest that, through its impact on the age class structure, harvesting increases significantly the number of regeneration failures that occur annually after fires. Since there is a minimum age to produce seed (25 years for the runs presented here), and since natural regeneration often relies on the dispersal of seeds into a burnt area from neighbouring cells, by driving the age of stands below 25 years in stands adjacent to burnt stands, harvesting has a significant impact on natural regeneration. Oil and gas has the opposite effect. The results indicate that oil and gas, through its fragmenting of the landscape, decreases the number of regeneration failures, on average. This is most likely results from the fact that oil and gas limits the area of fires and harvest blocks, so that regenerating stands are often closer to seed sources than without oil and gas active on the landscape. While strong (an increase of almost 40%), the effect of climate change on the number of regeneration failures is not significant. This results from the high variability among runs with climate change, and from the interactions among climate change and the other disturbance agents, which have been described in the sections above (on the cumulative impacts).

# 4. Conclusion

It is clear from the results that have been presented in this report that forest management planning must take into account key ecosystem drivers in order to earnestly attempt and achieve sustainability.  This work has demonstrated that forest management planning, as it is currently carried out, leads to an over-estimation of the wood volumes that can be harvested over time and, through this action, to a deterioration of the forest resource, in terms of its ability to provide forest products as well as in terms of the maintenance of biodiversity.  We suggest that the interaction among wildfire, oil and gas, and demographic change, along with industrial forestry, are of paramount importance in shaping the forest resource for future generations.  As well, a simple implementation of climate change impacts has shown that climate change has the potential to seriously compound the impacts of ecosystem drivers on the forests of Alberta.  It is imperative that these factors become an integral part of the forest planning process.

Many would argue that an integration of such factors can be carried out in response to observed disturbances and changes; that is, that harvest targets can be recalculated after the occurrence of large fires or severe insect outbreaks. There are two principal reasons not to perpetuate such an impromptu approach to forest planning. First, given the stochasticity inherent in these forested ecosystems (through the impacts of fire and insects, for example), very large disturbances may occur far enough into the future so as to allow decades of over-harvesting before the reality of the disturbance regime becomes impossible to ignore.  Such a situation has been observed in the Gaspésie region of Quebec, where supposedly-sustainable harvest rates had been calculated and applied for decades.  Spruce budworm outbreaks, which had been well documented and known to be cyclic, had been left out of forest planning until it was too late.  Overnight, the annual allowable cut for the region was cut by 20%, many jobs were lost, and the region has been slow to recover.  Second, infrastructure for the forest industry is costly, skilled labour will emigrate if not gainfully employed, and forest-dependant communities require stability in order to flourish. When large catastrophic forest disturbances occur, communities and their forest sector industries are caught between the rock of ecological reality and the hard place of poor planning: either the harvest rate must be dramatically dropped, which can lead to mill closings and massive layoffs,

or the harvest rate is maintained notwithstanding and the resource and all that it provides are completely dilapidated. Such a situation occurred with the centuries-old northern cod fishery off Newfoundland. Government was not willing to make the politically unpopular decision to decrease fishing quotas, although scientists had claimed for decades that the harvest rates were unsustainable, and over-fishing continued until stocks were completely and utterly exhausted. To date, this example of poor natural resource planning has led to over 40,000 layoffs and 15 years of social upheaval and hardship for the people of Newfoundland.

Up until recently, tools to carry out this type of integration were not available. Planning foresters were limited to forest inventories and aspatial planning tools to carry out their work. However, the situation has changed dramatically over the past decade. The technology and, as this report has demonstrated, the knowledge exists to allow the integration of many of the most important ecosystem drivers that influence the forest. Clearly there is still considerable uncertainty regarding climate change, the impacts of demographics on the fire regime, and other components of the forest ecosystem. However, it is our conviction that disregarding these key elements because of uncertainty would be reckless in itself. There are methods to deal with such uncertainty, such as the methods proposed by Armstrong (1999). Uncertainty can be quantified and the impact of this uncertainty on key indicators following various scenarios can be modeled. By looking at the outcome, risk-benefit analysis can be carried out and a judgement made regarding the most desirable scenario to adopt. The point is the following: there is most certainly more risk involved in ignoring key ecosystem drivers (fire, climate change, etc.) than in integrating them and embracing the uncertainty that accompanied them.

The work presented here, while exploring a number of issues that are not currently addressed by forest management, covers only a few of the potential impacts that may influence the Whitecourt forest management area over time. For example, insect outbreaks, such as the recent arrival of the mountain pine beetle, and their possible interactions with climate change have not been addressed. The displacement of native species by exotic invasive species has also not been addressed; and the same holds for the introduction of new pathogens. So, while the results suggest important changes to the forest landscape as a result of climate change, the changes presented here may represent only a small portion of the sources of disturbance that will shape the forests of tomorrow.

## 4.1 Recommendations for Forest Management and Forest Policy

Projections of AAC over time must take wildfire into account. While most will argue that losses to wildfire can be taken into account *a posteriori*, the reality is that once a mill has been established in a community, the forest industry expects to obtain a return on its investments (investments on the mill itself, but also on equipment owned by contractors), and mill employees expect to keep their jobs. The harsh reality is that the concerns of ecologists becomes of secondary importance when the livelihoods of people are at risk. It is the responsibility of the provincial government to integrate stochasticity and the key ecosystem drivers into the forest planning system, both on a large scale and over the long run.

While there is uncertainty surrounding the potential impacts of climate change, the magnitude of the impacts shown in this study suggest that greater attention should be paid to the implications of climate change for forestry.

When estimating the volumes that are expected to be recovered through salvage harvesting, long-term shifts in the age class distribution must be taken into account.

SRD, as the institution mandated to oversee the management of the forest on behalf of the citizens of Alberta, must gain access to detailed data on the impacts of the oil & gas industry on Alberta forests, and make this data available to the forest industry so that it can better manage its DFA's.

## 4.2 Recommendations for Future Research

The work presented here suggests that there is an interaction among climate change, fire, and harvesting so that there is a greater amount of area burned under fire, harvesting, and CC than under fire and CC alone. Future work should aim to clarify these interactions. In particular, the link between CC and the length of the fire season should be examined more closely. In this study, the fire season was taken to be static over time, whereas observation and theoretical considerations suggest that the fire season is most likely lengthening. This has most likely resulted in an underestimation of the impacts of CC on the fire regime.

Stopping rules for the mechanistic fire model based on an understanding of the behaviour of wildfires will help to make the simulation of fires more realistic. Also, the role of grasses along oil and gas features and their impact on the fire regime should be investigated, both through modeling and through field research.

The transitions of stands from one composition to another after disturbance are of great significance, since these transitions control the composition of the forest over time. In building the model, information on the dispersal of seeds of all species modelled was not available. Information on the impact of climate (and the derived CMI index) on the germination and survival of seeds and seedlings was also not available for the study area. Research on these subjects would greatly benefit this type of work.

At the time this report was prepared, information on the regeneration of stands following the establishment of seismic lines was sparse. Anecdotal evidence suggests that factors, such as ATV traffic, can interfere with regeneration, and that some sites that have been disturbed by seismic appear to remain un-regenerated for very long periods.

Work on the impact of stochastic processes, such as fire, and processes that are difficult to predict, such as oil & gas activity and climate change, should be approached from a probabilistic perspective. As described by Armstrong (1999), when the object of management is a stochastic system, one can never project outcomes with absolute certainty, and so it becomes necessary to define the outcomes in probabilistic terms, and in terms of acceptable and unacceptable risk. Future work should look at the probability distribution of modeling outcomes, so that risk may be weighed against potential gains.

# 5.  Acknowledgements

- Cordy Tymstra and Kurt Frederik and SRD

- Andrew Fall of Gowlland Technologies

- Pascal Rochon and Régis Pouliot at IQAFF

# 6. References

Alberta Agriculture. 2006. Interpolation of Climate Station Data. http://www1.agric.gov.ab.ca/$department/deptdocs.nsf/all/sag6305#description

Armstrong, G.W. 1999. A stochastic characterisation of the natural disturbance regime of the boreal mixedwood forest with implications for sustainable forest management. Can. J. For. Res. 29: 424-433.

Botkin, D.B., Janak, J.F. and Wallis, J.R. 1972. Some ecological consequences of a computer model of forest growth. J. Ecol. 60: 849-873.

Bradshaw et al. 2000. The effects of climate change on the distribution and management of Picea abies in southern Scandinavia. Can. J. For. Res. 30: 1992-1998.

Calogeropoulos, C., Greene, D.F., Messier, C., and Brais, S. 2003. Refining tree recruitment models. Can. J. For. Res. 33: 41-46.

Charron, I. and Greene, D.F. 2002. Post-fire seedbeds and tree establishment in the southern mixedwood boreal forest. Can. J. For. Res. 32: 1607-1615.

Cramer 1996. In: Global Change and Arctic Terrestrial Ecosystems. pp. 312-329. Springer, New York.

Doyon, F. 2000. BAP Report #3: Habitat classification. Institut québécois d'Aménagement de la Forêt feuillue: St-André Avellin, QC. 11 pages.

Duchesneau, R., Yamasaki, S.H., and Doyon, F. 2006. Impacts of Climate Change at the Stand Level. Report from the Climate Change Landscape Projection Group. 2007-2016 Detailed Forest Management Plan. Millar Western Forest Products. Edmonton, Alberta. 57 pages.

FCFDG (Forestry Canada Fire Danger Group). 1992. Development and Structure of the Canadian Forest Fire Behaviour Prediction System. Inf. Rep. ST-X-3. Ottawa: Forestry Canada.

Feunekes, U. 1991. Error analysis in fire simulation models. MSc. Thesis. Dept. of Forest Resources, University of New Brunswick. 74 pages.

Gauthier, S., Bergeron, Y., Simon, J.-P. 1996. Effects of fire regime on the serotiny level of jack pine. J. Ecol. 84: 539-548.

Government of British Columbia. 2007. Mixedwood Growth Model Support / Publications. Research Branch. http://www.for.gov.bc.ca/hre/gymodels/MGM/support.htm

Gracia, C.A., Tello, E., Sabaté, S., Bellot, J., 1999. Gotilwa: An Integrated Model of Water. Dynamics and Forest Growth". En Rodà, F., Retana, J., Gracia, C., y Bellot, J. (Eds.), Ecology of Mediterranean Evergreen Oak Forest, Berlín, Ed. Springer-Verlag, Series Ecological Studies 137, pp. 163-178.

Greene, D.F. 2000. Sexual recruitment of trees in strip cuts in eastern Canada. Can. J. For. Res. 30: 1256-1263.

Greene, D.F. and Johnson, E.A. 1994. Estimating the mean annual seed production of trees. Ecology. 75: 642-647.

Greene, D.F. and Johnson, E.A. 1996. Wind dispersal of seeds from a forest into a clearing. Ecology. 77: 595-609.

Greene, D.F. and Johnson, E.A. 1999. Modelling recruitment of Populus tremuloides, Pinus banksiana, and Picea mariana following fire in the mixedwood boreal forest. Can. J. For. Res. 29: 462-473.

Greene, D.F. and Johnson, E.A. 1998. Seed mass and early survivorship of tree species in upland clearings and shelterwoods. Can. J. For. Res. 28: 1307-1316.

Harris, L.D. 1988. Edge effects and conservation of biotic diversity. Conservation Biology. 2:330-332.

He et al. 2002. Study of landscape change under forest harvesting and climate warming-induced fire disturbance. For. Ecol. Manage. 155: 257-270.

Hogg, E.H. 1994. Climate and the southern limit of the western Canadian boreal forest. Canadian Journal of Forest Research 24: 1835-1845.

Hogg, E.H. 1997. Temporal scaling of moisture and the forest-grassland boundary in western Canada. Agricultural and Forest Meteorology 84: 115-122.

Hogg, E.H. and Schwarz, A.G. 1997. Regeneration of planted conifers across climatic moisture gradients on the Canadian prairies: implications for distribution and climate change. J. Biogeo. 24: 527-534.

Hogg, E.H., J.P. Brandt and B. Kochtubajda. 2002. Growth and dieback of aspen forests in northwestern Alberta, Canada, in relation to climate and insects. Can. J. For. Res. 32: 823-832.

IPCC (Intergovernmental Panel on Climate Change). 2001. Climate Change 2001: Impacts, Adaptation and Vulnerability. McCarthy, J. J., Canziani, O. F., Leary, N. A., Dokken, D. J., and White, K. S. Eds. Cambridge, UK, Cambridge University Press.

Kimmins, J.P., Mailly, D., and Seely, B. 1999. Modelling forest ecosystem net primary production: the hybrid simulation approach used in FORECAST. Ecol. Modelling. 122: 195-224.

Korol et al. 1996. Testing a Mechanistic Model for Predicting Stand and Tree Growth. For. Sci. 42: 139-153.

Lasch, P., Lindner, M., Ebert, B., Flechsig, M., Gerstengarbe, F.-W., Suckow, F. and Werner, P.C., 1999. Regional impact analysis of climate change on natural and managed forests in the Federal State of Brandenburg, Germany. Environmental Modelling and Assessment, 4, 273-286.

Lasch, P., Lindner, M., Erhard, M., Suckow, F., Wenzel, A., 2002. Regional impact assessment on forest structure and functions under climate change: the Brandenburd case study. For. Ecol. Manage. 162, 73-86.

Li, C., Flannigan, M.D., and Corns, I.G.W. 2000. Influence of potential climate change on forest landscape dynamics of west-central Alberta. Can. J. For. Res. 30: 1905-1912.

Loreto, R. and McCormack, T. 2006. Population Projections and Impacts. Report from the Population Landscape Projection Group. 2007-2016 Detailed Forest Management Plan. Millar Western Forest Products. Edmonton, Alberta. 97 pages.

Muir, P.S. and Lotan, J.E. 1985. Disturbance history and serotiny of Pinus contorta in western Montana. Ecology. 66: 1658-1668.

Neilson et al. 1998. In: The Regional Impacts of Climate Change. Cambridge University Press, Cambridge, UK.

Plummer, D., D. Caya, H. Côté, A. Frigon, S. Biner, M. Giguère, D. Paquin, R. Harvey and R. De Elía, 2006: Climate and climate change over North America as simulated by the Canadian Regional Climate Model. J. Climate, 19 (13): 3112-3132

Prentice IC, Sykes MT, Cramer W (1993) A simulation model for the transient effects of climate change on forest landscapes. Ecol. Model. 65: 51-70.

Radeloff, V.C., Mladenoff, D.J., Guries, R.P., Boyce, M.S. 2003. Spatial patterns of cone serotiny in Pinus banksiana in relation to fire disturbance. For. Ecol. Manage. 189: 133-141.

Robinson, S.K., Thompson, F.R., Donovan, T.M., Whitehead, D.R., and Faaborg, J. 1995. Regional forest fragmentation and the nesting success of migratory birds. Science. 267: 1987-1989.

Rudy, A. 2000. BAP Report #8: BAP Program Documentation. KBM Forestry Consultants Inc.: Thunder Bay, ON. 65 pages.

SAS Institute. 1999. SAS OnlineDoc®, Version 8, Cary, NC: SAS Institute Inc.

Schwalm and Ek 2001. Climate change and site: relevant mechanisms and modeling techniques. For. Ecol. Manage. 150: 241-257.

Schwartz, M. W., Iverson, L. R. and Prasad, A.M. 2001. Predicting the potential future distribution of four tree species in Ohio, USA, using current habitat availability and climatic forcing. Ecosystems. 4: 568-581.

Shugart, H.H., West, D.C., 1977. Development of an Appalachian deciduous forest succession model and its application to assessment of the impact of the chestnut blight. J. Environ. Manage. 5, 161–179.

Stocks, B.J., B.D. Lawson, M.E. Alexander, C.E. Van Wagner, R.S. McAlpine, T.J. Lynham, and D.E. Dubé. 1989. The Candian forest fire danger rating system: an overview. For. Chron. 65, 450-457.

VEMAP Members, Vegetation/ecosystem modeling and analysis project: Comparing biogeography models in a continental-scale study of terrestrial ecosystem responses to climate change and CO2 doubling, Glob. Biogeochem. Cycles, 9, 407-437, 1995.

Watson et al. 1996. In: Contribution of Working Group II to the Second Assessment Report of the Intergovernmental Panel on Climate Change. Cambridge University Press, Cambridge.

Wotton, Taylor, and Alexander. 2000. The Canadian Forest Fire Danger Rating System: Changes, Fixes, and an Evaluation Dataset. CFS.

Yahner, R. H. 1988. Changes in wildlife communities near edges. Conservation Biology. 2: 333-339.

------

G:\MWFP\Projects\P485_DFMP\Doc\zApp019_Cumulative_Impact_Mod_Rpt\Document\App019_CumulativeImpactsMod_20071026.doc